2021

Versican/collagen Interactions In Tissue Structure And Mechanics

Dongning Chen
University of Pennsylvania

Versican/collagen Interactions In Tissue Structure And Mechanics

Abstract

ABSTRACT

VERSICAN/COLLAGEN INTERACTIONS IN TISSUE STRUCTURE AND MECHANICSDongning Chen
Rebecca G. Wells Type I collagen is the most abundant structural protein in the extracellular matrix (ECM), forming a dynamic 3D fibrous network that is highly regulated by other ECM components including proteoglycans (PGs) and glycosaminoglycans (GAGs). Matrix PGs, especially the small leucine rich PG (SLRP) subgroup, have been well studied as collagen binding proteins and regulators of fibrillogenesis. However, the impact of the hyalectan subgroup of PGs, particularly versican, on collagen behaviors is not well understood. There is a particular need for understanding the role of versican in the collagen network because of its universal distribution in tissues and its altered expression during collagen-related fibrotic disorders. My aim was to study collagen/versican interactions and to investigate the role of versican in modulating collagen structural and mechanical behaviors. I used solid phase binding assays and the Collagen Toolkit to identify binding sites, and I carried out in vitro turbidity assays combined with fibroblast-derived matrices (FDM) to study fibrillogenesis. Collagen fiber organization was visualized using scanning electron microscopy (SEM), and cell-mediated collagen realignments and contractions were assessed by collagen plug and engineered microtissue assays. Shear rheometry was carried out on collagen gels and liver tissues to evaluate the impact of versican on tissue mechanics. I determined that versican and its V3 isoform bind collagen via the versican G3 domain and collagen R-G-Hydrophobic-O motif, independent of versican GAG residues. Compared to SLRPs and the structurally similar hyalectan aggrecan, versican shows unique effects on multiple collagen behaviors: 1) versican upregulates collagen gelation and promotes the deposition of collagen-rich matrix with aligned fibers; 2) the presence of versican improves fibril fusion into large bundles and forms a looser network; 3) versican improves cell-mediated collagen compaction, alignment and microtissue contraction; 4) versican contributes to collagen gel mechanics by decreasing stiffness and attenuating strain stiffening. In tissues, versican and its GAGs also play a role by downregulating compression stiffening. Thus, versican is a unique regulator of various collagen behaviors and therefore has potential therapeutic value in collagen-related fibroproliferative diseases such as inflammation, fibrosis and cancer.

Degree Type

Dissertation

Degree Name

Doctor of Philosophy (PhD)

Graduate Group

Bioengineering

First Advisor

Jason A. Burdick

VERSICAN/COLLAGEN INTERACTIONS IN TISSUE STRUCTURE AND MECHANICS

Dongning Chen

A DISSERTATION

in

Bioengineering

Presented to the Faculties of the University of Pennsylvania

in

Partial Fulfillment of the Requirements for the

Degree of Doctor of Philosophy

2021

Supervisor of Dissertation	Graduate Group Chairperson
_____	_____
Dr. Rebecca G. Wells	Dr. Yale E. Cohen
Professor of Medicine	Professor of Otorhinolaryngology

Dissertation Committee

Dr. Jason A. Burdick, Professor of Bioengineering, University of Pennsylvania

Dr. Paul A. Janmey, Professor of Physiology, University of Pennsylvania

Dr. David M. Chenoweth, Professor of Chemistry, University of Pennsylvania

Dr. Lin Han, Associate Professor of Biomedical Engineering, Drexel University

ACKNOWLEDGMENTS

I would like to thank all the help and support from my supervisor, committee members, colleagues, family, and friends. My doctoral thesis would not have been done without all the contributions from them. First, I would like to thank my supervisor, Dr. Rebecca Wells, for her patient guidance, advice, and kindness. I want to express my great appreciation to her for dedicate mentoring, invaluable training, warm support, and encouragement in my experiments, career development and everyday life throughout my entire master and PhD years. I also would like to thank my committee members, Dr. Jason Burdick, Dr. Paul Janmey, Dr. David Chenoweth, and Dr. Lin Han, for their invaluable advice, support, and insight for my project. Second, I greatly appreciate all the efforts from my lab members for their generous help and for the memorable and enjoyable research experience with them. I would like to especially recognize Dr. LiKang Chin, Dr. Yu Du and Dr. Jessica Llewellyn for all their experimental and technical support. I also want to thank Yuri Veklich at Cell & Developmental Biology Microscopy Core for helping with scanning electron microscopy and Dr. Biao Zuo at Electron Microscopy Resource Laboratory for helping with immune electron microscopy.

I would also like to thank all the collaborators of my lab. I want to show my gratitude to the Shenoy lab for computational modeling support, the Han lab from Drexel University for helping me with versican isolation and giving me native aggrecan as a gift, and the Chen lab from Boston University for technical support on engineered microtissue assay and traction force microscopy.

Finally, I want to show great appreciation to my family and friends for their unconditional support and encouragement.

ABSTRACT

VERSICAN/COLLAGEN INTERACTIONS IN TISSUE STRUCTURE AND MECHANICS

Dongning Chen

Rebecca G. Wells

Type I collagen is the most abundant structural protein in the extracellular matrix (ECM), forming a dynamic 3D fibrous network that is highly regulated by other ECM components including proteoglycans (PGs) and glycosaminoglycans (GAGs). Matrix PGs, especially the small leucine rich PG (SLRP) subgroup, have been well studied as collagen binding proteins and regulators of fibrillogenesis. However, the impact of the hyalectan subgroup of PGs, particularly versican, on collagen behaviors is not well understood. There is a particular need for understanding the role of versican in the collagen network because of its universal distribution in tissues and its altered expression during collagen-related fibrotic disorders. My aim was to study collagen/versican interactions and to investigate the role of versican in modulating collagen structural and mechanical behaviors. I used solid phase binding assays and the Collagen Toolkit to identify binding sites, and I carried out in vitro turbidity assays combined with fibroblast-derived matrices (FDM) to study fibrillogenesis. Collagen fiber organization was visualized using scanning electron microscopy (SEM), and cell-mediated collagen realignments and contractions were assessed by collagen plug and engineered microtissue assays. Shear rheometry was carried out on collagen gels and liver tissues to evaluate the impact of versican on tissue mechanics. I determined that versican and its V3 isoform bind collagen via the versican G3 domain and collagen R-G-Hydrophobic-O motif, independent of versican GAG residues. Compared to SLRPs and the structurally similar hyalectan aggrecan, versican shows unique effects on multiple collagen behaviors: 1) versican upregulates collagen gelation and promotes the deposition of collagen-rich matrix with aligned fibers; 2) the presence of versican improves fibril fusion into large bundles and forms a looser network; 3) versican improves cell-mediated collagen compaction, alignment and microtissue contraction; 4) versican contributes to collagen gel mechanics by decreasing stiffness

and attenuating strain stiffening. In tissues, versican and its GAGs also play a role by downregulating compression stiffening. Thus, versican is a unique regulator of various collagen behaviors and therefore has potential therapeutic value in collagen-related fibroproliferative diseases such as inflammation, fibrosis and cancer.

TABLE OF CONTENTS

LIST OF TABLES

LIST OF ILLUSTRATIONS

CHAPTER 1 INTRODUCTION

The compositional, structural, and mechanical complexity of the extracellular matrix (ECM) is important for maintaining appropriate cell and tissue functions. ECM consists of a three-dimensional (3D) fibrous network in the form of crosslinked fibers primarily type I and other fibrillar collagens. There are other important ECM components, including glycoproteins, proteoglycans (PGs) and glycosaminoglycans (GAGs), which play key roles in controlling and modulating ECM structural and mechanical properties as well as biological functions. The heterogeneity of ECM composition and fibrous network organization contributes to tissue specificity, and abnormal ECM deposition, organization and mechanics have been observed in various pathological disorders.

Type I collagen, which is the most abundant member of the collagen superfamily, is a triple helical ECM structural protein with two α1 and one α2 chains. Each α chain is composed of repeating glycine-X-Y peptides, where X and Y are proline (28%) and hydroxyproline (38%) (Gordon and Hahn 2010). The organization of collagen, which forms a fibrous network, is essential for regulating ECM properties, especially structure and mechanics. Basically, there are 4 levels of collagen organization that have been defined: (1) triple helix collagen monomer (length=280 nm and diameter=1.5 nm (Bozec and Horton 2005)); (2) collagen fibril (diameter=25-400 nm, length=1 μm (Gelse, Pöschl, and Aigner 2003)(Buehler 2006)); (3) collagen fiber (diameter=200-500 nm, up to a micron (Shen et al. 2008), but the difference between fibers and bundles is not clearly defined) and (4) networks, bundles or sheets, which are very important for maintaining appropriate cell and tissue behaviors during development and homeostasis but are poorly defined. All four levels of collagen structures are precisely controlled by numerous factiors including cells and collagen binding proteins and are crucial for stabilizing physiological tissue properties and functions. Reorganization of collagen structure and the collagen fibrous network

has been found during embryonic development and tissue remodeling, and remarkedly abnormal alterations have been observed in pathological process especially the collagen-related fibrotic disorders such as fibrosis, inflammation and cancer metastasis.

1.1 COLLAGEN FIBRILLOGENESIS

Type I collagen is a heterotrimer of two α1 and one α2 chain. COL1A1 and COL1A2, the α chain genes for type I collagen (type I collagen will be referred to as collagen without additional labels in this thesis), are transcribed into their corresponding mRNAs which are then translated into procollagen α1 and α2 chains and synthesized on ribosomes along the rough endoplasmic reticulum. The pro-α1 and α2 chains are folded from C-propeptide to N-propeptide to form left-handed helical polypeptides and then these α chains join together to form the right-handed triple helix (procollagen monomer) (Yamauchi and Sricholpech 2012)(Doege and Fessler 1986). Procollagen peptide chain biosynthesis can be regulated at the translational level. For example, published work indicates that two cis-acting sequences (5' stem-loop and C-rich region in the 3' untranslated region) are involved in α1(I) mRNA stabilization and translation which can lead to increased collagen deposition from hepatic stellate cells (HSCs) (Stefanovic 2005).

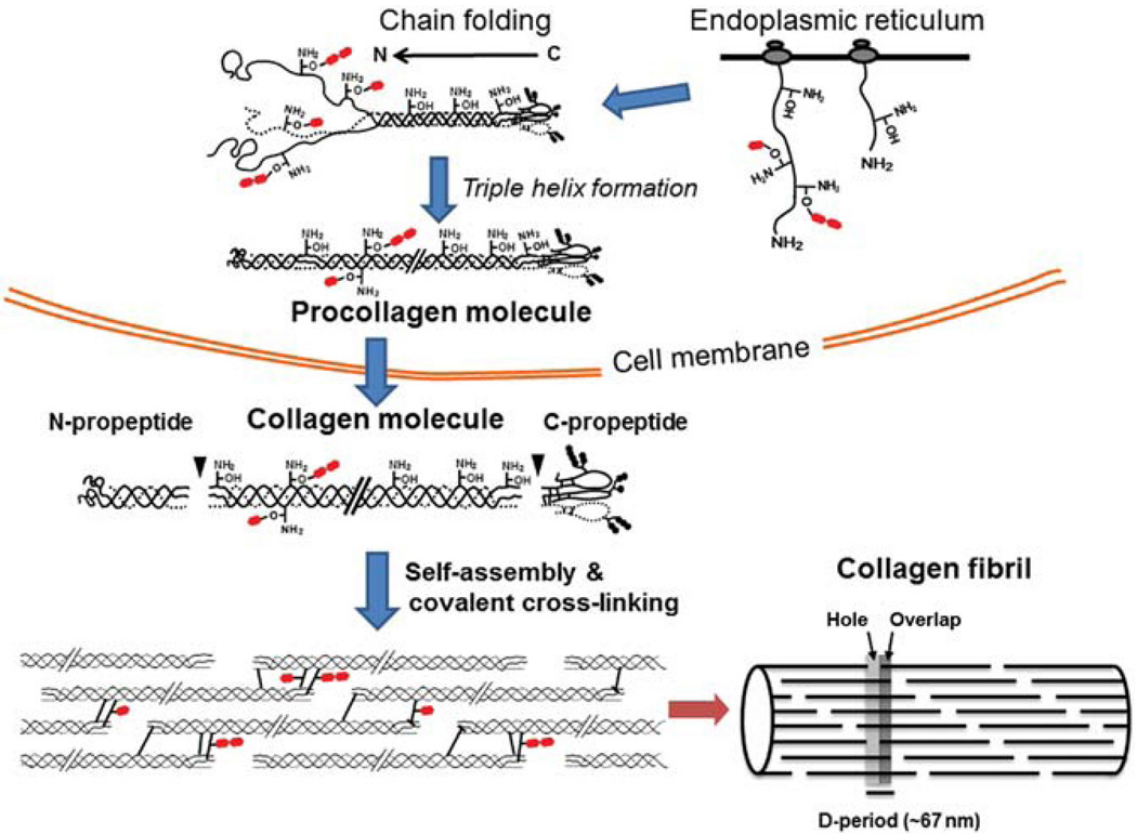

Figure 1.1 Collagen biosynthesis and fibrillogenesis (designed by M. Yamauchi and M. Sricholpech (Yamauchi and Sricholpech 2012) and reprinted with permission)

For fibrillar collagen (type I is mainly discussed here), the N- and C-propeptides are cleaved by ECM enzymes such as a disintegrin and metalloproteinase with thrombospondin motifs (ADAMTS), bone morphogenetic protein 1 (BMP1) and tolloid-like protein 1 (TLL-1) (Humphries et al. 2008) to expose N- and C-telopeptides, which trigger spontaneous collagen fibril formation (Figure 1.1). In addition, the post-translational modifications of collagen are crucial for stabilizing collagen fibril assembly. Lysine modifications, happening both intra and extracellularly, are examples of collagen modifications for which lysine residues are hydroxylated into hydroxylysine selectively inside cells and lysine and hydroxylysine residues in the telopeptides are oxidated by lysyl oxidase (LOX) in the ECM to form aldehydes for collagen crosslinking (Yamauchi and

Sricholpech 2012). The crosslinks between telopeptidyl aldehydes and lysine or hydroxylysine in the helical region are responsible for spontaneous self-assembly into fibrils (Prockop et al. 1979)(Kadler et al. 1996). However, there are two models (the Kadler and Birk models) of the in vivo process of collagen fibrillogenesis. The Kadler model suggests that the cleavage of the propeptide happens intracellularly and that fibril assembly can happen both intra and extracellularly (Canty and Kadler 2005), while the Birk model postulates that the cleavage of propeptides occurs extracellularly and is based on data that the N- and C-proteinase are found in the culture medium (Birk and Trelstad 1986). Although these proteinases are found in media, they may be functional for cleaving collagen propeptides inside cells and may be secreted from cells along with collagen. Thus, it is important to further understand the synthesis and secretion of these proteinases in detail, focusing especially on whether they are activated intra or extracellularly, which will shed light on the actual fibrillogenesis process in vivo. During fibrillogenesis (mainly studied in vitro), there is a lag phase during which tropocollagen monomers nucleate (into trimers) and then a rapid growth phase during which lateral growth occurs by the addition of monomers longitudinally with fibrils fusion into larger fibers (Farber et al. 1986)(Dewavrin et al. 2014). The highly ordered fibrillar collagen structure shows a 67 nm D-periodicity when imaged via atomic force microscopy (AFM) or electron microscopy (EM) (Baselt, Revel, and Baldeschwieler 1993)(Hulmes et al. 1981). Compared to higher levels of collagen organization, the mechanism of fibril formation has been well studied, with a particular focus on factors such as temperature, pH and other ECM components that regulate collagen fibrillogenesis both in vitro and in vivo. The effects of physical factors, such as pH and ionic strength, on in vitro fibrillogenesis have been investigated using a turbidity assay, illustrating that both the rate and fibril formation plateau increase with increasing pH in the range of 6-9 (Y. Li et al. 2009) and decrease with increasing ionic strength (Yan et al. 2012). For in vivo fibrillogenesis, the most crucial factors appear to be the presence of collagen binding partners such as collagen V (Birk 2001), fibronectin (Dzamba et al. 1993), GAGs (Stuart and Panitch 2008) and PGs (S. Chen et al.

2014); their temporal and spatial expression during embryonic development can alter fibril formation (as well as fibrous network organization) in different ways .

Collagen V can facilitate collagen I fibrillogenesis, but it is not required (Kadler, Hill, and Canty-Laird 2008). The helical region of collagen V can co-assemble with collagen I to form heterotypic fibrils, and the N-terminal domains (consisting of highly charged sulfate groups) of collagen V, which are located in the gap region between highly-ordered collagen I monomers and exposed horizontally to the fibril surface; a large number of the N-terminal domains at the surface can limit the lateral growth (adding fibrils is not favored) (Birk 2001). In vivo, the corneal stroma in collagen V-conditional null mice shows an increased collagen fibril diameter, abnormal fibril assembly, disrupted lamellar structure and decreased corneal transparency (Sun et al. 2011). Fibronectin, a ECM glycoprotein that forms focal adhesions with integrins at the cell membrane, accelerates in vitro collagen fibrillogenesis (Speranza, Valentini, and Calligaro 1987). It can directly interact with collagen (Balian, Click, and Bornstein 1980)(Owens and Baralle 1986), form a collagen-fibronectin fibrillar structures and has a specific regulation during collagen deposition(McDonald, Kelley, and Broekelmann 1982). Both collagen I and fibronectin can bind integrins (for example, α5β1 for fibronectin and α2β1 for collagen I), but the role of the combined-presence and interactions between collagen-fibronectin-integrin complexes in mediating collagen fibrillogenesis are still under investigation. Fibronectin polymerization and collagen fibril assembly have shown to have the same mechanistic elements in that integrins and the cytoskeleton are required (S. Li et al. 2003). Other ECM proteins also play key roles in regulating collagen fibrillogenesis especially PGs, and the PG/collagen interaction and its functional relevance in multiple collagen behaviors, including fibrillogenesis, reorganization/realignment and mechanics, will be discussed in detail in this work.

1.2 FIBRILLOGENESIS ASSAYS

Beginning in the 1950s, researchers started using transmission electron microscopy (TEM) to study the morphology of collagen fibrils and investigate regulators of fibril formation. For example, P. Vanamee and K. R. Porter first used TEM to investigate the effect of salt and pH on fibril morphology and the characteristic banding structure (Vanamee and Porter 1951). TEM mainly focuses on visualizing the morphology of mature fibrils but the entire process of fibrillogenesis cannot be investigated. Starting in 1960, G. C. Wood and M. K. Keech published a series of papers reporting the use of an in vitro turbidity assay (also known as a spectrophotometric assay and an in vitro fibrillogenesis assay) for studying the kinetics of collagen fibrillogenesis in vitro (Wood and Keech 1960)(Keech 1961). G. C. Wood also used this assay to investigate the effects of chondroitin sulfate (CS) and polyanions on fibrillogenesis (Wood 1960). The kinetic curves of the turbidity assay generated by tracking the absorbance changes during collagen gelation using a plate reader are typically sigmoidal with a lag phase representing collagen nucleation and a growth phase representing the lateral growth of fibrils (Figure 1.2). This technique has been widely used in a large number of studies focusing on various types of factors and regulators of collagen fibrillogenesis, such as temperature (Achilli and Mantovani 2010), collagen concentration (Raspanti et al. 2007), GAGs (Stuart and Panitch 2008), PGs (Vynios et al. 2001)(Reese, Underwood, and Weiss 2013), cartilage oligomeric matrix protein (COMP) (Halász et al. 2007) and fibronectin (Speranza, Valentini, and Calligaro 1987). Although the findings from these publications highlighted some of the diverse and distinct roles of modulators of collagen fibrillogenesis, there is a limitation that this technique cannot overcome. The absorbance readout only indicates the turbidity changes of the collagen solution, but it cannot provide detailed information about the actual morphological and structural features of collagen fibrils such as fibril diameter and length as well as fibril quantities. Turbidity is mainly determined by the molecular weight and light scattering factors of different aggregates (fibrils) (Silver and Birk 1983). Thus, a combination of TEM and the turbidity assay has been commonly used for fibrillogenesis studies, providing information about both kinetic and morphological changes during fibril formation. In the

last twenty years, the development of time-lapse confocal reflection microscopy (CRM) has made it possible to research the changes in fibril morphology and the kinetics of fibril growth during almost the entire fibrillogenesis process (Brightman et al. 2000). Numerous biopolymers including collagen have a special intrinsic optical feature that they can reflect light and this reflection can be detected by a confocal microscope for imaging and quantitative analysis. The kinetic curves tracking the pixel intensity of CRM during gelation share similar patterns as the absorbance curves generated by the traditional turbidity assay and CRM-based findings on fibril morphology strongly support that there is a lag phase for nucleation and a growth phase for fibril lateral growth (Brightman et al. 2000)(Zhu and Kaufman 2014). CRM, however, cannot capture collagen monomers or even early formed small aggregates during nucleation; thus, confocal fluorescence microscopy (CFM) of fluorescently-labeled collagen has often been used to investigate the early stages of gelation although it also has limitations in that labeling itself has a negative effect on fibril formation (Y. Yang, Leone, and Kaufman 2009). Rheology has been used as a complementary assay to evaluate both the mechanics and kinetics of fibrillogenesis. It has been combined with CRM to study the effect of hyaluronic acid (HA) on collagen fibrillogenesis, especially the structural and mechanical alterations of the collagen network during gelation (Y. Yang and Kaufman 2009). AFM has also been used to investigate collagen assembly. For example, the orientation and structural patterning of collagen assembly can be guided by mechanical force applied using AFM tips and the collagen fibers deposited on a surface can be imaged using AFM scanning (Jiang et al. 2004). The impact of small leucine rich proteoglycans (SLRPs, such as decorin and lumican) on fibrillogenesis has been quantitatively investigated by using AFM to scan surfaces coated with collagen/SLRPs mixtures (at different ratios) showing that the increasing addition of decorin and lumican downregulates fibril diameter and increase interfibrillar space (Stamov et al. 2013).

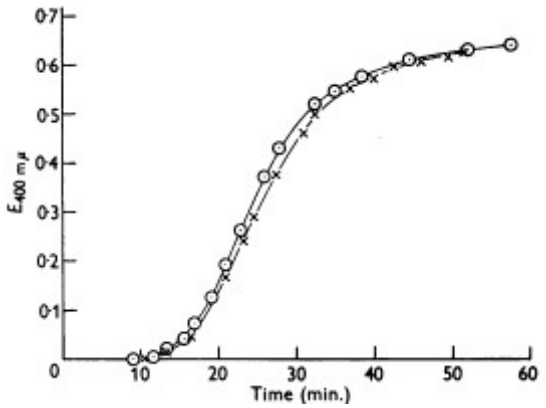

Figure 1.2 The kinetic curves generated by the in vitro turbidity assay (collagen gelation in two successive, identical experiments) published by G. Wood and M. Keech (Wood and Keech 1960) and reprinted with permission.

1.3 COLLAGEN FIBROUS NETWORK ORGANIZATION

Collagen fibrous networks are networks formed by highly ordered and packed semiflexible collagen fibers which are organized by covalent crosslinking of fibers as well as non-covalent weak electrostatic interactions among charged or glycosylated residues. Fibrous networks are essential 3D scaffolds for strengthening the ECM and are highly controlled and dynamically mediated, supporting normal biological, structural and mechanical properties of tissues. The regulatory mechanisms of collagen fiber formation, network formation, and in particular higher-level organization of networks are not well understood and require further investigation. Generally, nearby fibrils can entangle and twist into large fibers after collagen self-assembly into fibrils (Zhu and Kaufman 2014). The organization of collagen fibrous networks is a crucial mediator of the mechanics of collagenous matrices. In vitro gelation of collagen at different temperatures results in different collagen networks with different size fibers and pores and these networks show distinct mechanical properties including stiffness and strain stiffening behaviors (Jansen et al. 2018). It has also been shown that the shear storage modulus (G') of a collagen gel can be

predicted from its structural parameters such as fiber diameter and pore size, which are mediated by network connections via covalent crosslinks and non-covalent weak interactions between fibers (Y. Yang, Leone, and Kaufman 2009). For example, the addition of CS to collagen gels, which causes increased fiber bundling and pore size, leads to decreased G', while the addition of HA, which decreases the pore size, leads to increased stiffness (Y. Yang et al. 2011). In addition, the crosslinks within a collagen fibrous network also determine its mechanics. Glutaraldehyde-mediated crosslinking increases collagen gel stiffness via reorganizing and condensing fibrous networks (Raub et al. 2007). In vivo, the formation of fibers and the lateral fusion of fibers into higher order structures of bundles, sheets and networks are tissue specific. The appropriate collagen organization at the third and fourth levels is extremely important for biological and physiological functions (Figure 1.3), especially in tissues such as tendon and cornea with highly ordered collagen organization. The well-oriented and highly-organized collagen fibrils in corneal stroma are fundamental for its transparency. A typical lamellar structure has been observed in corneal stroma (Jester et al. 2010) and the different orientation and arrangement of collagen fibers in anterior and mid/posterior stroma are responsible for bearing stress from osmotic pressure in the eyeball (Meek and Boote 2004). Tendon, which bears large tensile loads, has highly oriented and packed collagen fibers and bundles arranging along the tensile direction (Maria De Souza et al. 2006).

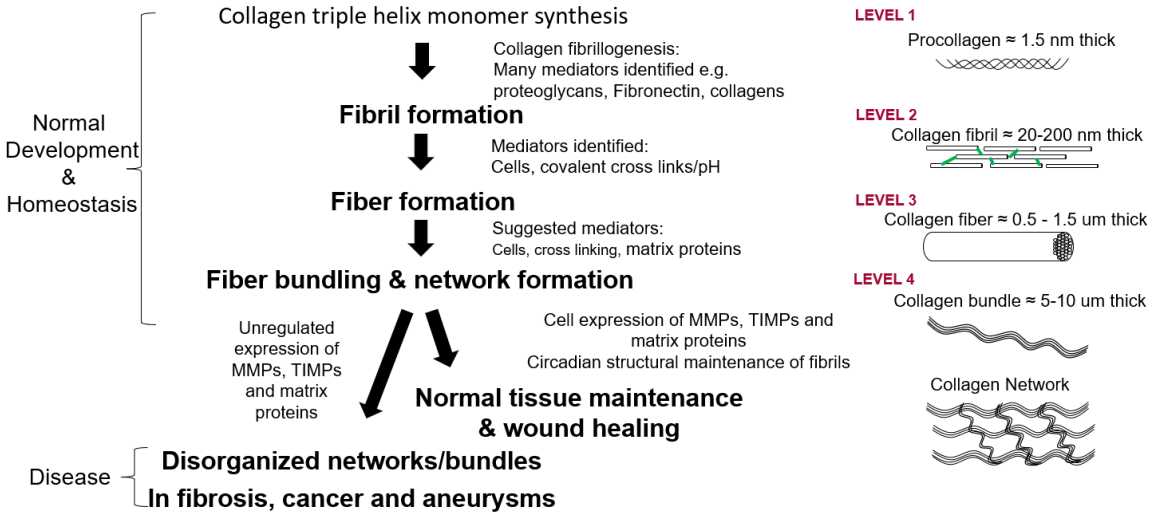

Figure 1.3 The four levels of collagen organization (designed by J. Llewellyn)

Native tissues consist of ECM networks formed by collagen fibrous scaffolds and cells embedded within these networks. Cells can modulate the organization of collagen fibrous networks in multiple ways including applying contractile forces via mechanotransduction and secreting collagen-related regulators (or binding proteins). Reciprocal cell-ECM crosstalk plays an important role in mediating tissue development, homeostasis and remodeling and irregular cell-ECM interactions have been observed in pathological states. On the one hand, cells can recognize mechanical signals from the ECM and convert them into downstream signaling pathways via mechanosensing through cell-membrane proteins (such as integrins for focal adhesion) which have specific effects on cell functions including migration and differentiation (Y. Chen et al. 2017). On the other hand, contractile cells can apply force to collagen fibrous networks and alter their organization by stretching, contracting and re-aligning collagen fibers (Abhilash et al. 2014). Long-range force transmission, as a phenomena representing cell-ECM crosstalk, is generated by contractile cells and the distance it acts over ranges from 250-1000 μm (Wang et al. 2015). This cell-mediated collagen reorganization results in highly compacted and

aligned collagen fibers and increased stiffness in the aligned area. Importantly, a fibrous network with cross-linked collagen fibers is required for these long range cell-cell interactions (Ma et al. 2013). Externally applied mechanical forces and cell contractile forces also play similar roles in collagen reorganization by stretching and aligning fibers (Vader et al. 2009). In native tissues, dramatic alterations in collagen fibrous network organization can trigger and lead to the progression of fibrogenesis and fibroproliferative diseases (Herrera, Henke, and Bitterman 2018). Taking hepatic fibrosis as an example, bridging (septal) fibrosis, which shows a remarkable reorganization of collagen fibrous networks and is mediated by activated fibroblasts, consists of highly condensed and aligned thick fibers and has been regarded as a precursor of tissue stiffening and severe chronic fibrosis such as cirrhosis (Maria De Souza et al. 2006). Interestingly and similarly, early tissue stiffening during pulmonary fibrosis is mainly due to altered organization of collagen fibrous networks via upregulated LOX-mediated crosslinking instead of the accumulation of ECM (increased collagen content), which further highlights the importance of understanding the mechanism of collagen network organization (Jones et al. 2018).

1.4 MATRIX PROTEOGLYCAN SUBFAMILIES AND THEIR FUNCTIONS AS COLLAGEN REGULATORS

PGs are highly glycosylated matrix proteins of covalently-bound GAG side chains attached to a core protein. Because of the highly negatively charged GAGs, PGs can attract water, cause swelling, occupy large volume and enable tissues to resist compression (Yanagishita 1993). There are two main subgroups of matrix (interstitial) PGs, SLPGs and the hyalectan family of large chondroitin sulfate proteoglycans (CSPGs), which both have important regulatory functions for various collagen behaviors. SLRPs, including decorin, lumican, fibromodulin, biglycan and others, have core proteins of about 50-60 kDa with 1-4 GAG chains (Figure 1.4). They have been studied for decades as collagen regulators mainly due to their significant effects on fibrillogenesis both in vivo and in vitro. The mechanism of collagen/SLRPs interactions and their relevance to

collagen behaviors in vivo, particularly fibrillogenesis during development, have been well studied. The temporal and spatial expression of SLRPs is precisely controlled during development and is important to support the regular physiological properties of specific tissues that require highly organized collagen fibrous networks for their biological functions. For example, biglycan and lumican participate in the formation of the lamellar collagen structure in cornea which is crucial for corneal transparency (S. Chen et al. 2014), and decorin, fibromodulin and lumican play a role in tendon development, modulating fiber morphology, diameter and arrangement as well as interfibrillar space (Ezura et al. 2000)(G. Zhang et al. 2006). In vitro fibrillogenesis (turbidity) assays suggest that decorin, lumican and biglycan downregulate collagen gelation with a decreased fibril formation plateau and that their core proteins play distinct roles compared to intact SLRPs (with GAG side chains) (Rada, Cornuet, and Hassell 1993)(Reese, Underwood, and Weiss 2013). By using AFM to scan a mica disc coated with collagen/SLRP mixtures, researchers have found that the addition of decorin and lumican to collagen leads to collagen networks with enlarged interfibrillar spaces and decreased fibril diameters (Stamov et al. 2013). Importantly, the binding sites between collagen and SLRPs have been identified through a combination of 3D crystal structures and solid phase binding assays. SLRPs have typical leucine-rich protein domains that form a horseshoe shaped structure (Orgel et al. 2009) and interact with collagen via these leucine rich repeats (LRRs). Decorin, for example, interacts with charged residues in the d band of the collagen α1 chain via the charged residues on its concave (inner) surface, which allows decorin to function as a structural spacer between collagen monomers during fibrillogenesis (Weber, Harrison, and Iozzo 1996). In more detail, researchers confirmed that fibromodulin and lumican compete for binding collagen as they interact with collagen at similar sequences on LRRs (Svensson, Närlid, and Oldberg 2000)(Kalamajski and Oldberg 2009), while another research showed that fibromodulin and decorin bind to collagen at different sequences on LLRs (Hedbom and Heinegard 1993). Both findings provide strong support for concluding that lumican and decorin interact with collagen differently. In addition, the core proteins of different SLRPs have different quantities of LRRs and the horseshoe structures have

different concave diameters (Scott 1996), which can further affect their roles in regulating collagen fibrillogenesis and arrangement structurally. Different SLRPs also have different numbers, types and locations of GAG side chains: decorin has one CS or dermatan sulfate (DS) side chain located close to its N-terminus, biglycan has two CS or DS located close to its N-terminus, while lumican has 4 keratan sulfate (KS) chains on its leucine-rich domain (Y. Zhang et al. 2013)(Appunni et al. 2019). The variations in their GAG side chains can induce distinct alterations on collagen fibrillogenesis (Stuart and Panitch 2008). Thus, different SLRPs including decorin and lumican, although belonging to the same subfamily and sharing similar core protein structures, differentially regulate multiple collagen behaviors.

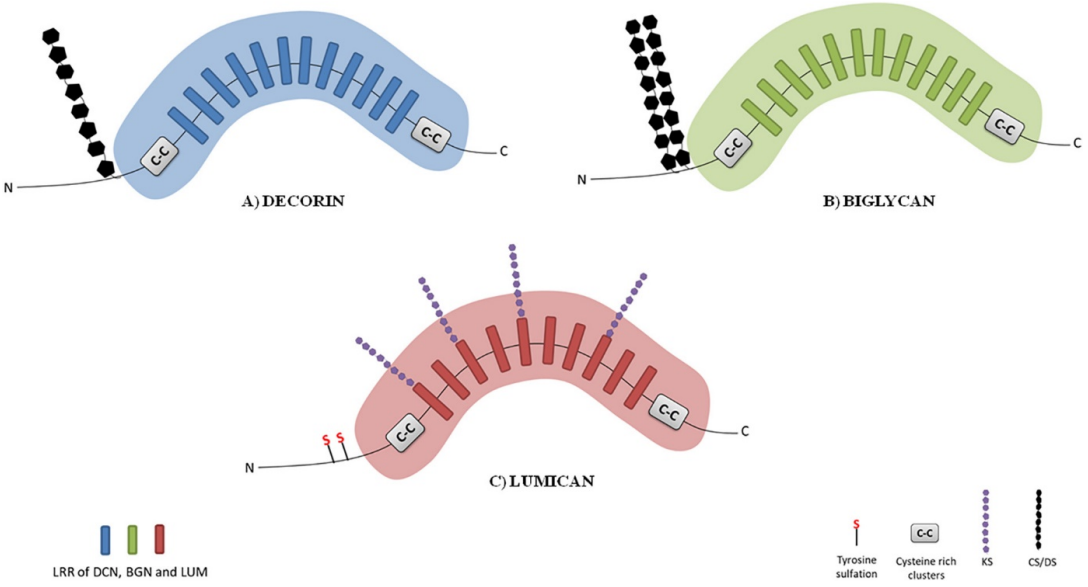

Figure 1.4 The structure of decorin, biglycan and lumican (published by S. Appunni, et al. (Appunni et al. 2019) and reprinted with permission)

The hyalectan family, named for the HA binding abilities of its members, consists of versican, aggrecan, neurocan and brevican (Iozzo and Schaefer 2015). Compared with SLRPs, these large CSPGs have a significantly larger mass of negatively charged GAG side chains with total molecular weights of 1-2.5 MDa. They can bind HA to form larger bio-complex aggregates that retain water, increase osmotic pressure and occupy large spaces in the ECM (Wight 2002)(Kiani et al. 2002). Aggrecan is predominantly found in cartilage and neurocan and brevican are mainly expressed in the central nervous system. However, versican is universally distributed and demonstrates versatile biological functions. It demonstrates altered expression and turnover in ECM-related disorders such as fibrosis and metastasis. Unlike SLRPs, which have been deeply investigated as collagen binding proteins and regulators of fibrillogenesis, the mechanisms of collagen/CSPGs interactions and the roles of large CSPGs in modulating fibrillogenesis remain unclear. Taking aggrecan as an example, a microplate solid-phase binding assay has indicated that aggrecan interacts with collagen through its KS binding domain (Hedlund et al. 1999) and the turbidity assay has found that aggrecan has no impact on in vitro collagen gelation (Vynios et al. 2001). On the other hand, although a solid-phase binding assay was reported to show a direct interaction between versican and rat type I collagen (Yamagata et al. 1986), the physical nature and mechanism of the interaction between versican and collagen have not been well defined and the binding sites have not been identified. Additionally, the CS side chains, numbering up to 23 for the largest versican V0 isoform while over 100 for aggrecan, have complicated and controversial effects on regulating collagen fibrillogenesis. Work by Bierbaum et al. (Bierbaum et al. 2006) and Öbrink et al. (Öbrink 1973) has shown that the addition of CS accelerates in vitro collagen gelation while Mathews et al. (Mathews and Decker 1968) have reported opposing findings. Overall, there is a particular need to clarify the role of versican in regulating collagen behaviors given its widespread distribution, unknown collagen-binding mechanism and precisely regulated expression during collagen-related fibroproliferative disorders.

1.5 VERSICAN AND ITS BIOLOGICAL FUNCTIONS

Versican, as a hyalectan family member, has a typical N-terminal G1 domain that can bind HA (in combination with link protein) to form large aggregates in the ECM and also has a C-terminal G3 domain that can interact with integrin, tenascin and fibronectin (Wight, Kang, and Merrilees 2014). Unlike aggrecan which has a KS binding domain adjacent to the G1 domain that functions as a collagen binding site, versican only has CS GAG side chains. Thus, the interaction between collagen and versican cannot be predicted from its structural similarity to aggrecan. There are 5 different versican isoforms. V0-V3 are commonly found in tissues and their structures are shown in Figure 1.5: V0 has both α- and β-GAG domains (17-23 CS chains), V1 has the β-GAG domain (12-15 CS chains), V2 has the α-GAG domain (5-8 CS chains), V3 has no GAG domain (Wight 2002) and newly-found V4 from breast cancer has part of the β-GAG domain (Kischel et al. 2010).

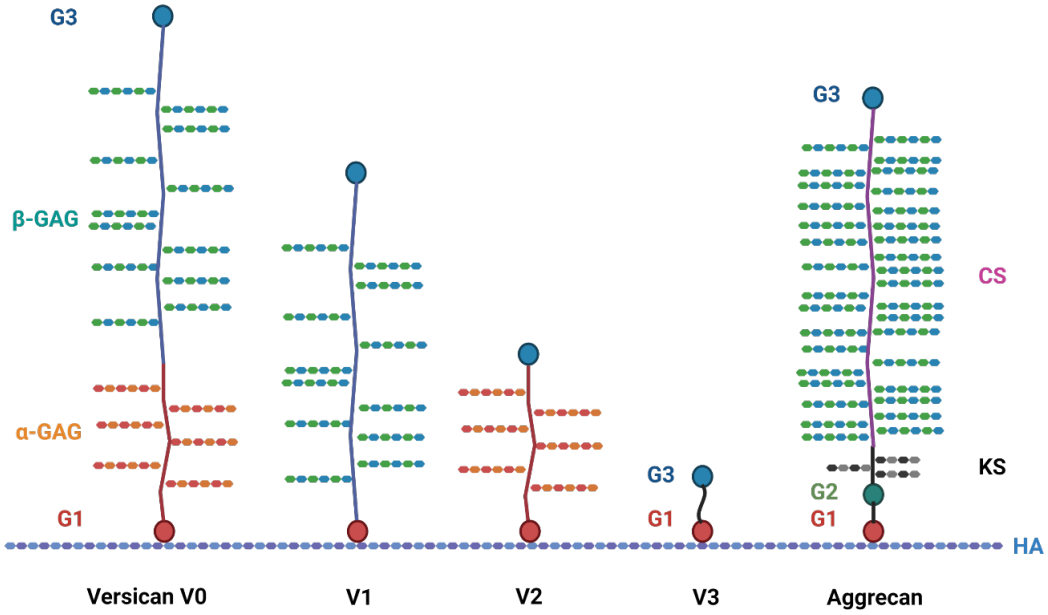

Figure 1.5 The structure of different versican isoforms and aggrecan (created with BioRender.com)

Most researches on versican are focused on its versatile roles in regulating cell behaviors such as adhesion, proliferation and migration (Wight 2002) and on its altered gene expression and ECM deposition during pathological states. Versican, especially its different isoforms and domains, has also been widely studied for its diverse and controversial biological regulation of cell responses and tissue functions. Conflicting findings have shown that versican can mediate adhesion: the G1 domain inhibits 3T3 fibroblast adhesion (B. L. Yang et al. 1999) while the G3 domain interacts with β-integrin to promote astrocytoma cell adhesion (Y. Wu et al. 2002). Another published work studying the V1 isoform (containing G1, G3 and β-GAG domain) has found that V1 increases fibroblast adhesion and decreases migration (J. M. Carthy et al. 2015). In addition, versican shows an inhibitory effect on neural cell migration and axonal growth in the peripheral nervous system (Landolt et al. 1995) with both G1 and the versican GAG side chains playing important regulatory roles. Different versican isoforms also have distinct effects in modulating cell proliferation and apoptosis: V1 can upregulate fibroblast proliferation and inhibit cell death while V2 shows opposing effects (Sheng et al. 2005). However, the distinct mechanisms of these versican-related isoform- and domain-specific regulations of cell behaviors have not been well explained. In collagen-related fibroproliferative diseases such as cancer, inflammation and fibrosis, versican generally shows increased deposition and participates in disease progression. For example, versican promotes tumorigenesis, increases cancer cell proliferation, upregulates angiogenesis and induces tumor invasion and metastasis (Du, Yang, and Yee 2013)(Ricciardelli et al. 2009). Versican has also been confirmed as an early regulator during pulmonary and hepatic fibrosis; it remains increased during the entire fibrogenesis and shows decreased expression during recovery (Venkatesan et al. 2000)(Bukong et al. 2016). Versican also plays a role in embryonic development with a precisely modulated pattern of

expression. In a mouse model, versican expression reaches a peak at E13.5 and then decreases during development and remains at a low level in the adult. When comparing the expression of different isoforms during development, V0 and V1 are predominantly expressed while the deposition of V2 and V3 remains low in embryonic head and lung (Snyder et al. 2015); isoform distribution has not been well studied in other tissues. Although versican has shown a well-controlled expression during embryonic development and an abnormally altered expression during various collagen-related fibroproliferative malignancies, the effects of versican on regulating collagen behaviors including fibrillogenesis, fiber organization and tissue mechanics have been understudied and significant knowledge gaps remain.

CHAPTER 2 VERSICAN BINDS COLLAGEN VIA ITS G3 DOMAIN AND COLOCALIZES WITH COLLAGEN FIBERS

J. Llewellyn contributed to the dissection of mouse bile ducts.

B. Zuo, from the Electron Microscopy Resource Laboratory (Department of Biochemistry & Biophysics), helped with bile duct sample processing and staining and immune electron microscopy imaging.

The Collagen Toolkit II and its sequence information were provided by R. W. Farndale at Cambcol, Cambridge, UK.

2.1 INTRODUCTION

Collagen is the most important structural protein in the ECM, representing about 25-35% of total proteins and is responsible for maintaining ECM structural and functional integrity (Ricard-Blum 2011). Among all types of collagens, type I collagen is the most abundant (more than 90%) and most ubiquitous member. Collagen I have two α1 and one α2 chains containing repeats of the specific amino acid sequence glycine-X-Y and is organized in left-handed helices. The three α chains rotate into a right-handed triple helix stabilized by hydrogen bonds between interchain glycine and by electrostatic interactions between adjacent α chains (Ramachandran and Chandrasekharan 1968)(Persikov et al. 2005). After being secreted from cells and undergoing the cleavage of N- and C-terminal propeptides, collagen (used to refer to collagen type I when not otherwise specified in this thesis) monomers can self-assemble into fibrils and entangle into fibers or large bundles. Because of its high content, wide distribution and fibrillar organization, collagen's interactions with various ECM components, cell membrane proteins/receptors and growth factors have been well studied and the collagen-binding sites have been mapped for key interactors such as integrins, fibronectin and SLRPs (Emsley et al. 2000)(Kalamajski and Oldberg 2010).

Collagen binding partners, which participate in cell-ECM crosstalk, have been investigated in depth. Cell-ECM interactions are achieved by the binding between collagen and cell-membrane receptor integrins such as α1β1 and α2β1 (Jokinen et al. 2004). Integrins serve as linkers between cells and the matrix in this reciprocal cell-collagen (ECM) communication: cells can sense the mechanical cues from collagen fibrous networks via integrins and collagen fibrous networks can be re-organized and aligned by cellular contractile force applied via integrins. By using collagen mimetic peptides in a solid phase binding assay, researchers have found that α1β1 and α2β1 integrins interact competitively with GER and GER-like motifs and have mapped the typical binding sequences on collagen for integrins to be GFOGER (central binding region) and GLOGER (N-terminal binding region) (Knight et al. 2000)(Xu et al. 2000). Additionally, fibronectin, an ECM glycoprotein, can function as a 'link' protein that binds both collagen and integrin to stabilize and facilitate cell-collagen interactions. Through the use of proteolytically-cleaved collagen peptides, the fibronectin binding site was found to be located at residues 757-791 of α1(I), which overlap with the collagenase cleavage site between residues 775 and 776 (Kleinman et al. 1978). Similar techniques have been applied to study the binding mechanism between collagen and other ECM proteins including SLRPs.

Matrix PGs, also known as interstitial PGs, which are highly glycosylated with negatively-charged GAG side chains, are important ECM proteins that can interact with collagen and regulate collagen fibrillogenesis. There are two main subfamilies of matrix PGs: SLRPs (less than 100 kDa) and large CSPGs (the hyalectan family, over 1 MDa). SLRPs, including decorin, lumican, fibromodulin and others, have been appreciated for decades as important collagen-binding proteins and crucial regulators of structural and functional collagen network maturation during development (Kalamajski and Oldberg 2010). Importantly, the structural interactions and binding sites between collagen and SLRPs have been well studied compared to large CSPGs. SLRPs

interact with collagen via their LRRs and have specific impacts on fibrillogenesis because of their horseshoe-like structures (Scott 1996). For example, by mapping the charged residues on the concave surface of decorin and the d band of collagen α1(I), a space-filling representation of a decorin/collagen binding model was generated showing that the collagen monomer fits into the inner cavity formed by horseshoe structure of decorin LRRs (Weber, Harrison, and Iozzo 1996). However, another structural binding model (the fibril surface model) proposes that decorin interacts with adjacent collagen monomers via its N- and C-terminal arms, instead of LRRs, to alter the arrangement of collagen monomers (Scott 1996)(Orgel et al. 2009). Importantly, different SLRPs have different numbers of LRRs that make the size of the horseshoe structure variable: decorin has 10 LRRs which are a combined size of about 5-6 nm, while lumican has 11 LRRs and fibromodulin has 12 LRRs (more than 6 nm) (Scott 1996). Different SLRPs have distinct roles in arranging collagen fiber organization. By using radiolabeled SLRPs in a collagen binding assay, SLRPs binding sites on collagen were further assessed and it was found that fibromodulin and lumican bind to the same sites on collagen but that these are distinct from the decorin binding site (Hedbom and Heinegard 1993)(Svensson, Närlid, and Oldberg 2000). This assay using radiolabeled SLRPs to bind fibrillar collagen uses other non-labeled SLRPs as potential inhibitors to study competitive collagen binding among various SLRPs. To further understand the homologous collagen binding site of fibromodulin and lumican, fragments containing different LRRs from each SLRP were expressed by bacteria; the solid phase binding assay using the LRR fragments of opposing SLRPs as inhibitors confirmed that fibromodulin and lumican interact collagen via the same LRR 5-7 (Kalamajski and Oldberg 2009). A controversial result using this method suggested that fibromodulin LRR 11 has a higher binding affinity than LRR 5-7 and that mutating Glu-353 and Lys-355 destroys its collagen binding ability (Kalamajski and Oldberg 2007). The recent development of the Collagen II and III Toolkit libraries (containing 56 and 57 triple helical synthetic collagen mimetic peptides, respectively) by the University of Cambridge (Cambcol) has made it possible and convenient to identify collagen binding sites for numerous proteins including integrins, fibromodulin and matrix metalloproteinases (MMP) (Farndale 2019).

With this tool, fibromodulin has been found to interact with Toolkit peptides II/III-44, III-5 and III-53; II/III-44 are known as the MMP cleavage sites and III-5/53 with a similar KGHR sequence are involved with helical crosslinking (Kalamajski et al. 2016). In addition to the in vitro binding assays, immune electron microscopy (IEM) has also been used to study the colocalization of collagen fibers and their binding partners in vivo and it has been shown that decorin colocalizes with collagen fibers in fetal human dermis and aggrecan colocalizes partially with collagen II fibers in cartilage (Fleischmajer et al. 1991)(Hedlund et al. 1999).

With the solution of SLRP crystal structures, synthesis of SLRP fragments and the development of the Collagen Toolkit library, the interactions between collagen and SLRPs have been well studied and the binding sites have been mapped. However, the interactions between collagen and large CSPGs (the hyalectan family) have been neglected in these studies. The hyalectan family is a group of large matrix PGs with CS side chains which can interact with HA (thus, the derivation of the name hyalectan) to form large bottlebrush like bio-aggregates. Both of the hyalectans versican and aggrecan play key roles in modulating ECM structural, mechanical and functional features via their various interacting partners including HA, tenascin and fibulin (Y. J. Wu et al. 2005)(Aspberg 2012). Many more studies have been carried out for aggrecan/collagen interactions given its important biological and mechanical functions in cartilage, while less is known about versican/collagen interactions in spite of versican's universal distribution throughout various tissues. For aggrecan, a solid phase binding assay has shown that aggrecan interacts with both type I and II collagen via its KS domain and that it colocalizes with type II collagen fibers in vivo (Hedlund et al. 1999). For versican, there is one report in the literature of solid-phase binding data indicating its binding to rat type I collagen (Yamagata et al. 1986). Given that versican participates in various collagen-related fibroproliferative diseases (Theocharis 2008), it is important to identify the actual interaction between versican and collagen and map their binding sites.

In this chapter, I investigate the localization of versican in collagenous tissues using IEM, which can show both versican localization and collagen fibers. To study the mechanism of collagen-versican interactions in vitro, a solid phase binding assay is carried out using native versican as well as the recombinant V3 isoform and G1 and G3 domains. To identify the versican binding sites on collagen, the Collagen Toolkit, a library of synthetic collagen memetic peptides, is used.

2.2 METHODS

2.2.1 Reagents and antibodies

Rat tail type I collagen (with intact telopeptides) was from Corning (Corning, NY, USA). Versican was isolated from bovine liver (Plaas and Sandy 1993). Cesium chloride, aggrecan (A1960), decorin (D8428), hyaluronan biotin sodium salt, chondroitinase ABC (ChABC) from Proteus vulgaris, bovine serum albumin, casein blocking buffer and Tween-20 were from Sigma (St. Louis, MO, USA). Sodium hyaluronate (200 kDa) was from Lifecore (Chaska, MN, USA). Versican extraction buffer contained guanidine hydrochloride (Sigma), sodium acetate (Sigma) and protease complete tablets (Roche, Basel, Switzerland). Recombinant human lumican and versican isoform V3 proteins were from R&D Systems (Minneapolis, MN, USA). Recombinant human versican G1 and G3 domains (ab152303 and ab236178) were from Abcam (Cambridge, UK). Biotinylated versican G1 domain was from Echelon Biosciences (Salt Lake City, UT, USA). High sensitivity streptavidin-HRP and 1-step Ultra TMB-ELISA were from Thermo Fisher Scientific (Waltham, MA, USA). The Collagen Toolkit II was from Cambcol Laboratories (Ely, UK).

Anti-versican antibody 12C5 was from DSHB (Development Studies Hybridoma Bank, Iowa city, IA, USA), anti-aggrecan BC-3, anti-collagen I antibody (biotin, ab24821) and HRP anti-6X His antibody (MA1-21315-HRP) were from Thermo Fisher Scientific, and anti-versican (β-GAG

domain, Ab1033), anti-decorin antibody ab175404 and anti-versican antibody (β-GAG domain, Ab1033) were from Sigma. Donkey Anti-Rabbit IgG H&L (12nm Gold) preadsorbed (ab105295) was from Abcam.

2.2.2 Immune electron microscopy

Neonatal day 3 and adult mouse bile ducts were fixed with 4% paraformaldehyde/0.1% glutaraldehyde in 0.1 M sodium cacodylate buffer (pH 7.4) overnight at 4°C. Fixed samples were submitted to the Electron Microscopy Resource Laboratory (Department of Biochemistry & Biophysics, University of Pennsylvania, Philadelphia, PA, USA) for processing and staining. After subsequent rinsing in buffer and diH_2O, samples were dehydrated with a graded ethanol series and then infiltrated and embedded in LRWhite. After cutting, thin sections were stained with anti-versican antibody (β-GAG domain, ab1033) at 1:10 dilution overnight at 4°C. After rinsing 3 times, sections were incubated with secondary anti-rabbit antibody (12 nm gold particles (ab105295)) at 1:50 overnight at 4°C. After rinsing, sections were stained with phosphotungstic acid (PTA) and uranyl acetate (UA). Sections were imaged with a JEOL 1010 electron microscope fitted with a Hamamatsu digital camera and AMT Advantage NanoSprint500 software, and IEM images were taken randomly on each sample. Collagen fibers with gold particles attached were captured at 75,000× and the number of gold particles per fiber area was quantified (all 55 IEM images from one neonatal sample and 38 images from one adult sample were analyzed).

To confirm that there was no non-specific binding of antibodies, a control experiment was carried out using IEM to study plain collagen and collagen-versican matrices. Rat tail type I collagen was diluted to a final concentration of 1.5 mg/mL (in PBS) using 10× PBS and diH_2O and the pH was adjusted to 7.4 using 1 N NaOH. For some collagen gels, versican was added to a final concentration 0.1 mg/mL. 200 µL gel solution was added to a 1.5 mL tube and was incubated at

37°C for gelation. The gels were gently detached from the tube by pipetting and were washed with PBS 3 times. After fixing with 10% formalin for 10 min, the gels were rinsed and permeated with 0.1% Triton-X. After rinsing, the gels were incubated with antibodies as described previously for bile duct samples. After rinsing, sections were stained with PTA and UA. Sections were imaged with a JEOL 1010 electron microscope fitted with a Hamamatsu digital camera and AMT Advantage NanoSprint500 software, and IEM images were taken randomly on each sample.

2.2.3 Versican isolation

Native versican was extracted from bovine liver using a modification of a published protocol (Plaas and Sandy 1993). Briefly, bovine liver tissue was mechanically disrupted and digested with extraction buffer (pH=7.2) containing 4 M guanidine hydrochloride, 100 mM sodium acetate and protease Complete tablets at 4°C for 72h. The supernatant of the extraction buffer was obtained by spinning down tissue residues at 16,000×g for 1h. Cesium chloride was added to the supernatant solution until the density reached 1.59 g/mL and it was then centrifuged at 100,000×g for 24h. 1 mL fractions were pipetted carefully from the top surface to the bottom and the density of each fraction was measured. Fractions with a density above 1.54 g/mL were dialyzed against 1 M sodium chloride for 24h and against diH_2O for 24h. Samples were reconcentrated using a 100 kDa centrifugal filter (Millipore Sigma, Burlington, MA, USA). The compositions of extracted samples were analyzed by dot blotting using anti-versican, -aggrecan and -decorin antibodies.

2.2.4 Solid phase binding assay

The solid phase binding assay was designed based on Enzyme-linked immunosorbent assay (ELISA) methods. To study the interaction between collagen and versican, a 96-well plate was coated with isolated versican or recombinant V3 isoform at 0.25 µg/ml. The plate was then

blocked with 3% BSA in TTBS (TBS supplemented with 0.05% Tween-20) or casein blocking buffer at room temperature (RT) for 3h. After it was rinsed 3 times, type I collagen was diluted to 0.1, 0.5, 1.0, 2.5 and 5 μg/ml (in 1% BSA/PBS binding buffer) and added to the plate for overnight incubation at RT. After 3 rinses, biotinylated anti-collagen antibody was added to each well at 1:1000 (with 1% BSA/TBS) and incubated at 37°C for 1h. After 3 rinses, Streptavidin-HRP was added at 1:4000 and incubated at RT for 30 min. After 5-7 rinses, TMB was added until color became apparent (about 10 min) and 2 N sulfuric acid was added to stop the reaction. The absorbance was read at 450 nm. To assess the interactions of the versican core protein, isolated versican was digested with 250 mU ChABC (per mg substrate in 50mM sodium acetate pH=8) at 37°C overnight and then dialyzed with diH_2O to remove CS. To study the binding site on V3, recombinant G1 and G3 domains were compared using the solid phase assay described above. The interaction between collagen and G1 was also studied using biotinylated G1: the 96-well plate was coated with collagen at 10 and 100 μg/mL and biotinylated G1 was added at 0.1, 0.5, 1, 5 and 10 μg/mL for binding. A competition experiment was designed to study the role of HA in collagen/versican interactions and the role of collagen in HA/versican interactions. A plate was coated with 0.25 μg/mL V3 and bound with 1 μg/mL collagen mixed with increasing content of HA (0.1, 0.5, 1, 5, 10 ng/mL) or the plate was coated with 0.25 μg/mL V3 and bound with 10 ng/ml biotin-HA with increasing content of collagen (0.1, 0.5, 1.0, 2.5 and 5 μg/mL). To study the effect of pH on the interaction between collagen and versican, the pH of 1% BSA/TBS buffer was adjusted to 6, 7.4 and 8. To study the effect of ionic strength on the interaction between collagen and versican, sodium chloride was added to 1% BSA/TBS buffer to reach a concentration of 0.05, 0.1, 0.15, 0.2, 0.25, 0.3, 0.35, 0.4, 0.45, 0.5, 0.55 and 0.6M (Hedlund et al. 1999).

2.2.5 Collagen Toolkit binding assay

The Collagen Toolkit II, a library of synthetic collagen mimetic peptides, was synthesized by Cambcol and was coated and lyophilized on a 96-well plate. Additional empty wells on the plate

were coated with full-length collagen (rat tail type I). The plate was blocked with casein blocking buffer at RT for 3h and recombinant V3 isoform or G3 domain was added at 10 µg/mL and incubated at 4°C overnight. After rinsing, the bound V3 or G3 was detected using anti-His antibody (HRP conjugated, diluted at 1:1000). After rinsing, TMB was added until color appeared (about 10 min) and 2 N sulfuric acid was added to stop the reaction. The absorbance was read at 450 nm.

2.3 RESULTS

2.3.1 Versican colocalizes with collagen fibers both in vivo and in vitro

As published previously by our group using immunostaining, the expression of versican decreases during bile duct development (Khandekar et al. 2020), I compared the localization and deposition of versican in neonatal and adult bile duct using IEM. The extra-hepatic bile duct is a tube-like structure formed by cholangiocytes and surrounded by a collagen-, PG- and HA-rich matrix. The nano gold particles (the black dots on IEM figures, seen Figure 2.1A, B) illustrated the localization of versican via primary versican β-GAG antibody and 12 nm gold conjugated secondary antibody staining. Collagen fibers in the adult bile duct were more mature with a highly organized and aligned pattern and large fiber bundles. Unlike in the adult bile duct, collagen fibers in the neonatal bile duct were sparse, wavy and thin. Versican colocalized with collagen fibers in both neonatal and adult bile ducts and its deposition decreased during development (Figure 2.1C). IEM was also applied to plain collagen (as a control) and collagen-versican co-gels. Collagen fibers in collagen gels visualized by IEM were not as well-organized as native fibers in vivo, but versican was still found to colocalize with collagen fibers. As there are no black dots in Figure 2.1E, I confirmed that the antibodies I used did not have non-specific binding to collagen itself.

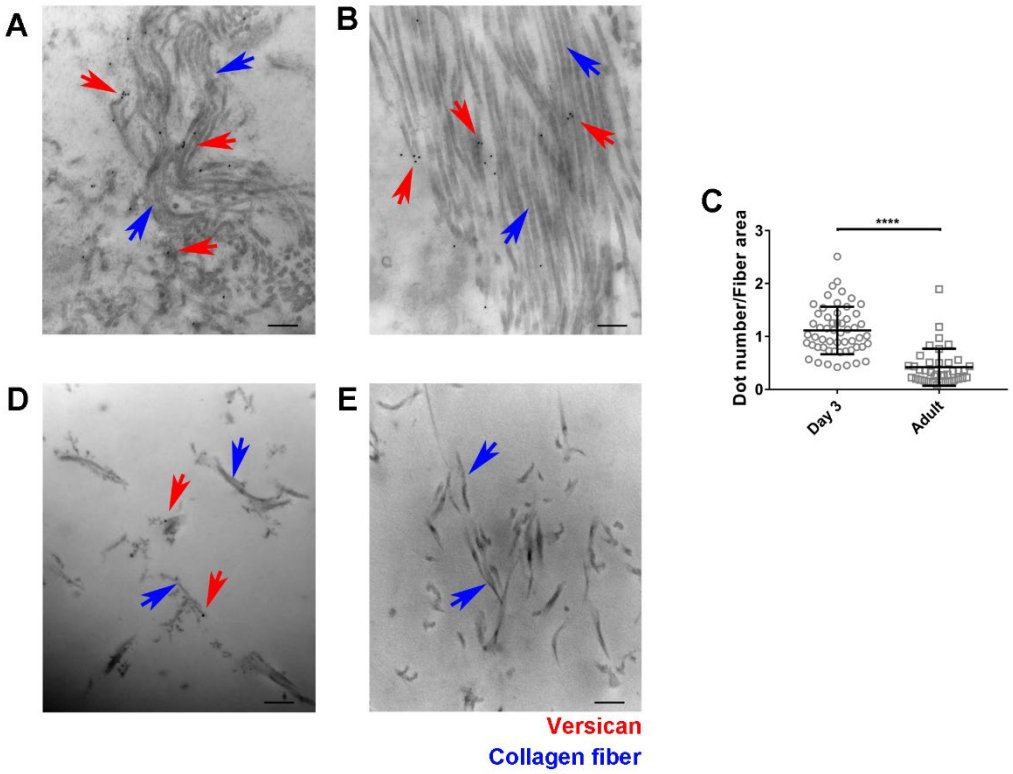

Figure 2.1 Versican colocalizes with collagen fibers in the extrahepatic bile duct and in vitro, as shown by immune-gold labeling. (A, B) Representative IEM figures showing the colocalization of versican on collagen fibers in mouse bile duct samples: (A) neonatal day 3, (B) adult. (C) Quantification of versican colocalized with collagen fibers was calculated by the number of gold particles per total fiber area (all 55 IEM images from one neonatal sample and 38 images from one adult sample were analyzed). (D, E) Representative IEM figures showing that there is the colocalization of versican and collagen fibers in collagen-versican gel but not in pure collagen gel (as a control). One experiment was done for each condition with three technical repeats for bile duct samples and two technical repeats for gel samples. Red arrows point at gold dots binding to versican and blue arrows point at collagen fibers. Scale bar = 200 nm, direct magnification = 75,000×. Data represent mean ± SD, ****P<0.0001.

2.3.2 Versican isolation and analysis

Native versican was isolated from bovine liver and purified with ultracentrifugation. After assessing its purity by dot blotting, I found that isolated versican samples were contaminated with aggrecan and decorin (Figure 2.2). In this case, the following approaches described in this thesis had both aggrecan and decorin as negative controls and had pure recombinant V3 isoform as a positive control.

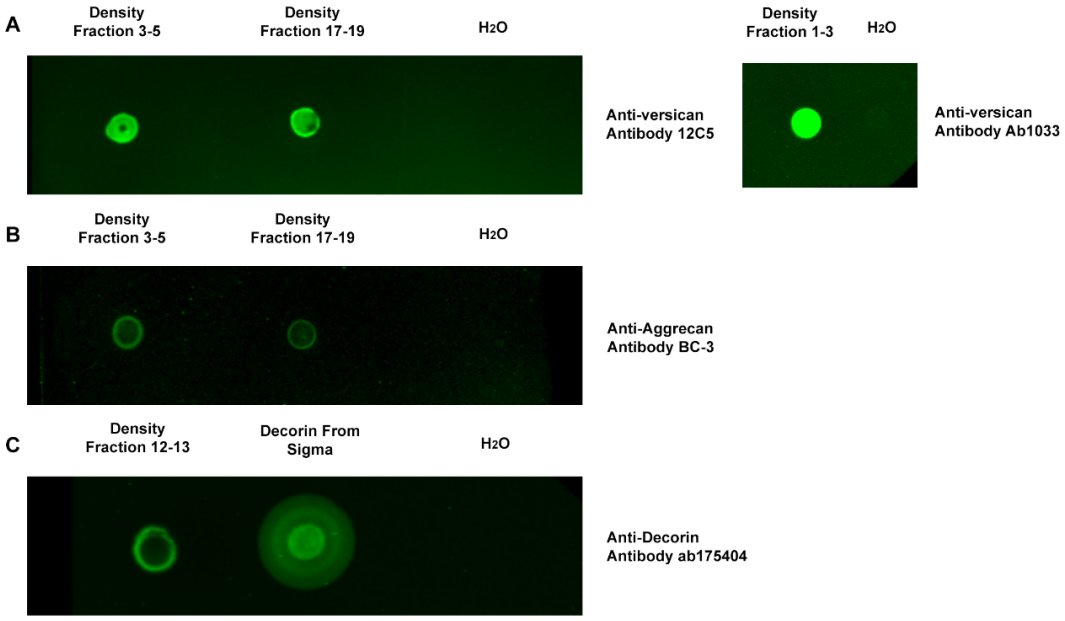

Figure 2.2 The purity of isolated versican from bovine liver. (A) Dot blotting of representative density fractions stained with anti versican G1 (12C5) and anti veriscan βGAG (Ab1033) antibodies confirmed the presence of versican (mostly V0 and V1 isoforms). (B, C) Dot blotting with aggrecan and decorin antibodies also demonstrated minor contamination of the versican sample with aggrecan (B) and decorin (approximately 0.37 mg/mL decorin in 4.68 mg/ml extracted sample) (C).

2.3.3 Versican and its V3 isoform bind to collagen

To investigate the interaction between collagen and versican, a solid phase binding assay was used. A 96-well plate was coated with isolated versican and recombinant V3 isoforms (contains G1 and G3 domain lacking GAG-binding domains). The amount of collagen bound to versican-coated wells increased with increasing addition of collagen and showed saturable binding (Figure 2.3A). When the plate was coated with increasing concentrations of versican, I also observed an increased binding of collagen (Figure 2.3A). The same trend was found for V3-coated plates, as shown in Figure 2.3B, although the plateau was higher compared to versican coating. To validate this solid phase binding assay, versican, V3, decorin, lumican and aggrecan were compared and similar saturable binding patterns were observed (Figure 2.3C). The binding of collagen to V3, decorin and lumican was higher compared to its binding to versican and aggrecan (Figure 2.3C). After digesting isolated versican with chondroitinase ABC to remove GAG residues (no GAG was detected using the Blyscan assay after digestion and data were not shown here), I found that it was mainly the versican core protein that participated in its collagen interactions (Figure 2.3D). To analysis binding affinity, I analyzed the data using the Scatchard equation: $\Delta A/C = \Delta A_{max}/K_d - \Delta A/K_d$ (ΔA is measured value of absorbance and C is collagen concentration). By plotting $\Delta A/C$ versus C, the dissociation constant (K_d) and maximum absorbance (A_{max}) were calculated from the slope and X-intercept of the linear fitting of the Scatchard plot and R^2 showed the quality of linear fitting (Figure 2.3E-G). The interaction between collagen and V3 was stronger with a lower K_d (without significant difference, Figure 2.3H) compared to isolated versican and its core protein, and the maximum amount of collagen binding to V3 and the versican core protein were significantly higher than binding to intact versican (Figure 2.3I).

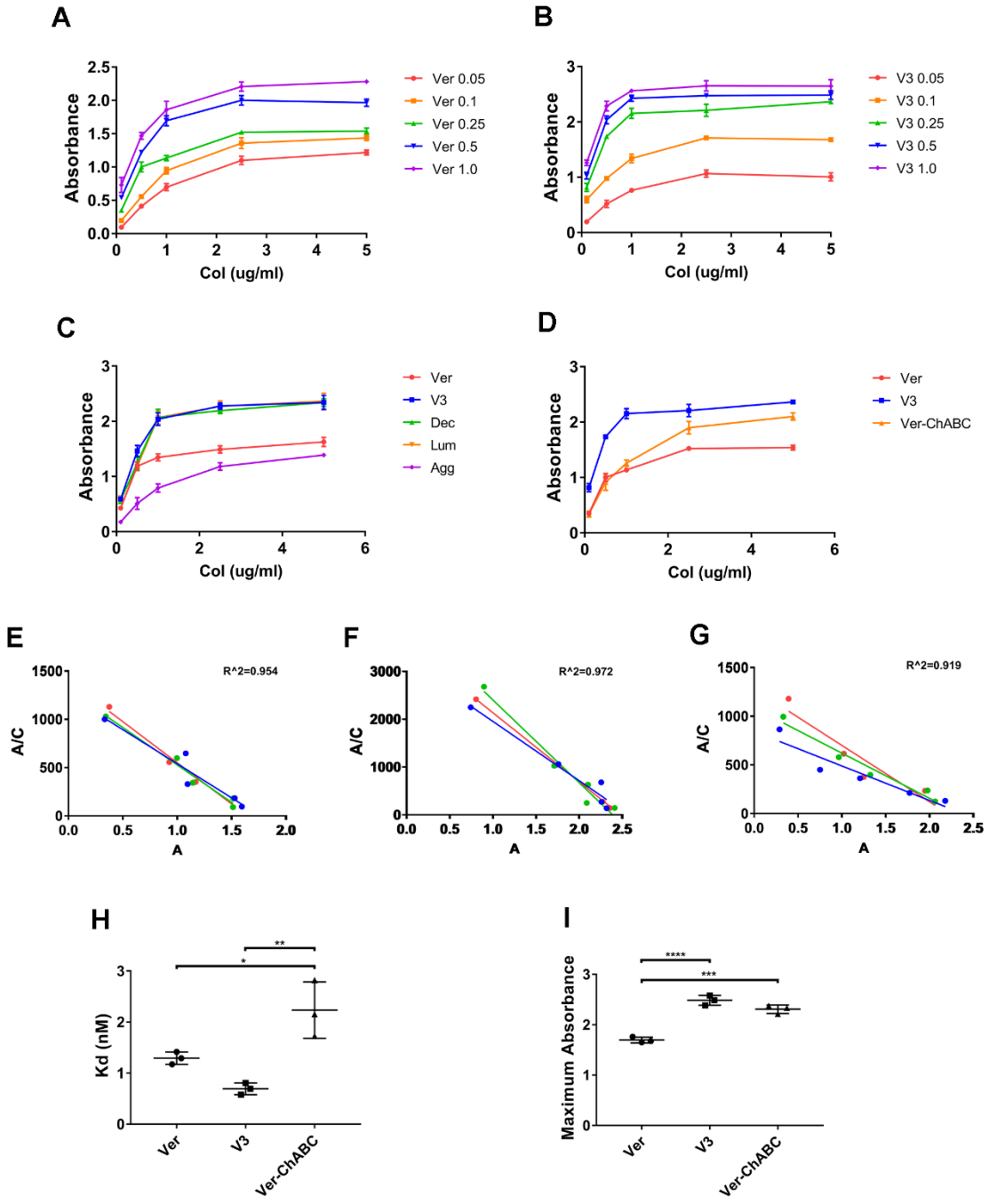

Figure 2.3 Versican and its V3 isoform bind collagen. (A, B) A 96-well plate was coated with isolated versican (Ver) or recombinant V3 isoform (V3) at 0.05, 0.1, 0.25, 0.5 and 1 µg/mL and

collagen (Col) was added at 0.1, 0.5, 1, 2.5 and 5 μg/mL for binding. (C) A 96-well plate was coated with different matrix PGs including Ver, V3, decorin (Dec), lumican (Lum) and aggrecan (Agg) at 0.25 μg/mL and Col was added at 0.1, 0.5, 1, 2.5 and 5 μg/mL for binding. (D) A 96-well plate was coated with Ver, V3 and versican core protein (Ver-ChABC, generated by ChABC digestion) at 0.25 μg/mL and Col was added at 0.1, 0.5, 1, 2.5 and 5 μg/mL for binding. In binding curves, error bars represent SD. (E-G) The Scatchard analysis of (D) by plotting ΔA/C versus C with R^2 (mean of three individual experiments) indicating linear fitting quality. (H) K_d was calculated from the slope of the linear fitting of the Scatchard plot. (I) A_{max} was the X-intercept of the linear fitting of the Scatchard plot. Three independent experiments were carried out for each condition with one technical repeat in each experiment. Data represent mean ± SD, *P<0.05, **P<0.01, ***P<0.001 and ****P<0.0001.

2.3.4 Versican core protein interacts with collagen via its G3 domain

To narrow down the collagen binding sites on V3, I studied the interaction between collagen and the versican G1 and G3 domains (which are the two parts of V3) using a solid phase binding assay in which a plate was coated with collagen and G1 or G3 added with comparison of their binding capacity. I observed that there was an interaction between collagen and the G3 domain but not between collagen and the G1 domain (Figure 2.4A). To confirm this finding, I also used a solid phase binding assay in which a plate was coated with collagen and bound with biotinylated G1 domain and I found that there was significantly less biotinylated G1 bound to collagen (Figure 2.4B).

Because versican binds HA via its G1 domain (S. Shi et al. 2004), a competition binding assay was designed to confirm that versican binds collagen and HA at different locations (G3 versus G1). Versican was used to coat 96-well plates and then exposed to collagen mixed with

increasing amounts of HA. The collagen-versican binding was not affected by additional HA (Figure 2.4C). In a reverse design in which versican was used to coat the plates and HA mixed with increasing collagen was added, HA-versican binding was also unchanged by additional collagen (Figure 2.4D). The competition binding assay thus supported the conclusion that versican binds to collagen via G3 and does so independently of the G1 domain binding HA.

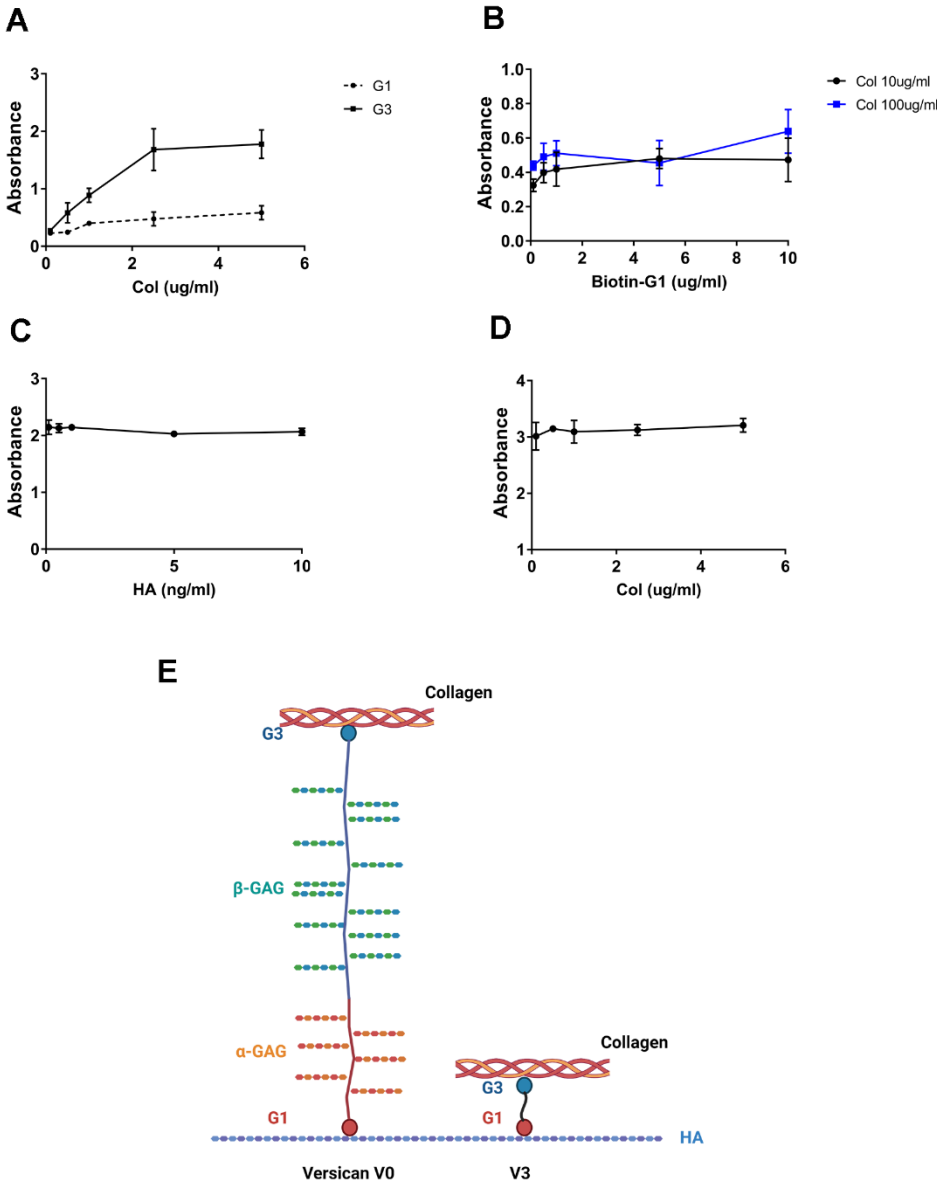

Figure 2.4 Versican binds collagen via its G3 domain in contrast to its G1 domain binding HA. (A) A plate was coated with recombinant G1 and G3 domains at 0.25 µg/mL and Col was added at 0.1, 0.5, 1, 2.5 and 5 µg/mL for binding. (B) A 96-well plate was coated with Col at 10 and 100 µg/mL and biotinylated G1 was added at 0.1, 0.5, 1, 5 and 10 µg/mL. (C) A plate was coated with V3 and bound with collagen mixed with increasing amounts of HA. (D) A plate was coated with V3 and bound with HA mixed with increasing amounts of collagen. (E) A diagram shows the

proposed collagen/versican and HA/versican interaction (created with BioRender.com). Three independent experiments were carried out for each condition with one technical repeat in each experiment. Data represent mean ± SD.

2.3.5 The collagen/versican interaction is sensitive to pH and ionic strength

To further characterize the interaction between collagen and versican, the impact of pH and ionic strength was examined. With increasing pH, the interaction between collagen and versican was attenuated (Figure 2.5A), suggesting an important role for negatively-charged GAG side chains as well as other charged amino acids on the core protein. The same trend was also observed for the interaction between collagen and V3 (Figure 2.5B), which was also consistent with the charged residues of the versican core protein having a regulatory role, altering the versican/collagen interaction capacity regardless of versican's GAG side chains. Both collagen/versican and collagen/V3 interactions were found to be downregulated with increasing ionic strength (Figure 2.5C), which further supported that charged residues modulated their binding. The amount of collagen binding was gradually decreased when NaCl was increased from 0 to 0.15 M and was not affected when NaCl was higher than 0.2 M. As the physiological ionic strength is 10-20 mM, my data supported the conclusion that the collagen/V3 interaction was sensitive to ionic strength changes in the physiological range while the collagen/versican interaction remained constant.

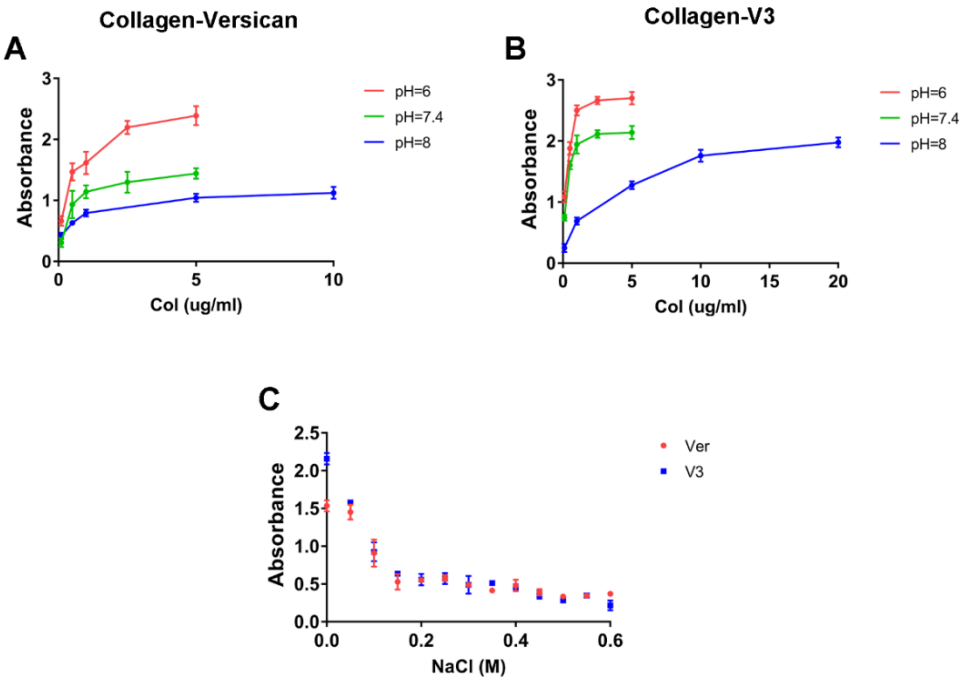

Figure 2.5 pH and ionic strength modulate collagen/versican and collagen/V3 interactions. (A, B) Solid phase binding assay using binding buffer at different pH values (pH 6, pH 7.4 as physiological condition and pH 8) indicated that increased pH downregulated collagen/versican and collagen/V3 binding. (C) Solid phase binding assay using binding buffer with increasing ionic strength (modified by adding NaCl at 0.05-0.6 M). Three independent experiments were carried out for each condition with one technical repeat in each experiment. Data represent mean ± SD.

2.3.6 Potential versican binding sites on collagen are identified using the Collagen Toolkit

The Collagen Toolkit II is a library of synthetic type II collagen peptides which covers the whole triple helical region (aa. 201 – aa. 1214). Each Toolkit peptide has 27 amino acids (9 G-X-Y repeats) with overlap of 3 G-X-Y repeats between sequential peptides (Table 2.1). Because the

sequence of collagen II is similar to collagen I, it can be used for identifying the protein binding sites on collagen I.

Table 2.1 The amino acid sequence of 56 Collagen Toolkit II (O represents hydroxyproline).

Peptide	Sequence	MW
TK-II-1	GPC-$(GPP)_5$-GPMGPMGPRGPOGPAGAOGPQGFQGNO-$(GPP)_5$-GPC-NH_2	5558
TK-II-2	GPC-$(GPP)_5$-GPQGFQGNOGEOGEOGVSGPMGPRGPO-$(GPP)_5$-GPC-NH_2	5648
TK-II-3	GPC-$(GPP)_5$-GPMGPRGPOGPOGKOGDDGEAGKOGKA-$(GPP)_5$-GPC-NH_2	5572
TK-II-4	GPC-$(GPP)_5$-GEAGKOGKAGERGPOGPQGARGFOGTO-$(GPP)_5$-GPC-NH_2	5621
TK-II-5	GPC-$(GPP)_5$-GARGFOGTOGLOGVKGHRGYOGLDGAK-$(GPP)_5$-GPC-NH_2	5710
TK-II-6	GPC-$(GPP)_5$-GYOGLDGAKGEAGAOGVKGESGSOGEN-$(GPP)_5$-GPC-NH_2	5533
TK-II-7	GPC-$(GPP)_5$-GESGSOGENGSOGPMGPRGLOGERGRT-$(GPP)_5$-GPC-NH_2	5668
TK-II-8	GPC-$(GPP)_5$-GLOGERGRTGPAGAAGARGNDGQOGPA-$(GPP)_5$-GPC-NH_2	5503
TK-II-9	GPC-$(GPP)_5$-GNDGQOGPAGPOGPVGPAGGOGFOGAO-$(GPP)_5$-GPC-NH_2	5385
TK-II-10	GPC-$(GPP)_5$-GGOGFOGAOGAKGEAGPTGARGPEGAQ-$(GPP)_5$-GPC-NH_2	5423
TK-II-11	GPC-$(GPP)_5$-GARGPEGAQGPRGEOGTOGSOGPAGAS-$(GPP)_5$-GPC-NH_2	5447
TK-II-12	GPC-$(GPP)_5$-GSOGPAGASGNOGTDGIOGAKGSAGAO-$(GPP)_5$-GPC-NH_2	5295
TK-II-13	GPC-$(GPP)_5$-GAKGSAGAOGIAGAOGFOGPRGPOGPQ-$(GPP)_5$-GPC-NH_2	5417
TK-II-14	GPC-$(GPP)_5$-GPRGPOGPQGATGPLGPKGQTGEOGIA-$(GPP)_5$-GPC-NH_2	5510
TK-II-15	GPC-$(GPP)_5$-GQTGEOGIAGFKGEQGPKGEOGPAGPQ-$(GPP)_5$-GPC-NH_2	5607
TK-II-16	GPC-$(GPP)_5$-GEOGPAGPQGAOGPAGEEGKRGARGEO-$(GPP)_5$-GPC-NH_2	5558

TK-II-17	GPC-$(GPP)_5$-GKRGARGEOGGVGPIGPOGERGAOGNR-$(GPP)_5$-GPC-NH_2	5628
TK-II-18	GPC-$(GPP)_5$-GERGAOGNRGFOGQDGLAGPKGAOGER-$(GPP)_5$-GPC-NH_2	5680
TK-II-19	GPC-$(GPP)_5$-GPKGAOGERGPSGLAGPKGANGDOGRO-$(GPP)_5$-GPC-NH_2	5529
TK-II-20	GPC-$(GPP)_5$-GANGDOGROGEOGLOGARGLTGROGDA-$(GPP)_5$-GPC-NH_2	5606
TK-II-21	GPC-$(GPP)_5$-GLTGROGDAGPQGKVGPSGAOGEDGRO-$(GPP)_5$-GPC-NH_2	5562
TK-II-22	GPC-$(GPP)_5$-GAOGEDGROGPOGPQGARGQOGVMGFO-$(GPP)_5$-GPC-NH_2	5650
TK-II-23	GPC-$(GPP)_5$-GQOGVMGFOGPKGANGEOGKAGEKGLO-$(GPP)_5$-GPC-NH_2	5625
TK-II-24	GPC-$(GPP)_5$-GKAGEKGLOGAOGLRGLOGKDGETGAA-$(GPP)_5$-GPC-NH_2	5536
TK-II-25	GPC-$(GPP)_5$-GKDGETGAAGPOGPAGPAGERGEQGAO-$(GPP)_5$-GPC-NH_2	5447
TK-II-26	GPC-$(GPP)_5$-GERGEQGAOGPSGFQGLOGPOGPOGEG-$(GPP)_5$-GPC-NH_2	5577
TK-II-27	GPC-$(GPP)_5$-GPOGPOGEGGKOGDQGVOGEAGAOGLV-$(GPP)_5$-GPC-NH_2	5458
TK-II-28	GPC-$(GPP)_5$-GEAGAOGLVGPRGERGFOGERGSOGAQ-$(GPP)_5$-GPC-NH_2	5638
TK-II-29	GPC-$(GPP)_5$-GERGSOGAQGLQGPRGLOGTOGTDGPK-$(GPP)_5$-GPC-NH_2	5917
TK-II-30	GPC-$(GPP)_5$-GTOGTDGPKGASGPAGPOGAQGPOGLQ-$(GPP)_5$-GPC-NH_2	5401
TK-II-31	GPC-$(GPP)_5$-GAQGPOGLQGMOGERGAAGIAGPKGDR-$(GPP)_5$-GPC-NH_2	5561
TK-II-32	GPC-$(GPP)_5$-GIAGPKGDRGDVGEKGPEGAOGKDGGR-$(GPP)_5$-GPC-NH_2	5525
TK-II-33	GPC-$(GPP)_5$-GAOGKDGGRGLTGPIGPOGPAGANGEK-$(GPP)_5$-GPC-NH_2	5444
TK-II-34	GPC-$(GPP)_5$-GPAGANGEKGEVGPOGPAGSAGARGAO-$(GPP)_5$-GPC-NH_2	5344
TK-II-35	GPC-$(GPP)_5$-GSAGARGAOGERGETGPOGPAGFAGPO-$(GPP)_5$-GPC-NH_2	5450
TK-II-36	GPC-$(GPP)_5$-GPAGFAGPOGADGQOGAKGEQGEAGQK-$(GPP)_5$-GPC-NH_2	5495
TK-II-37	GPC-$(GPP)_5$-GEQGEAGQKGDAGAOGPQGPSGAOGPQ-$(GPP)_5$-GPC-NH_2	5475
TK-II-38	GPC-$(GPP)_5$-GPSGAOGPQGPTGVTGPKGARGAQGPO-$(GPP)_5$-GPC-NH_2	5412
TK-II-39	GPC-$(GPP)_5$-GARGAQGPOGATGFOGAAGRVGPOGSN-$(GPP)_5$-GPC-NH_2	5436
TK-II-40	GPC-$(GPP)_5$-GRVGPOGSNGNOGPOGPOGPSGKDGPK-$(GPP)_5$-GPC-NH_2	5525
TK-II-41	GPC-$(GPP)_5$-GPSGKDGPKGARGDSGPOGRAGEOGLQ-$(GPP)_5$-GPC-NH_2	5561

TK-II-42	GPC-$(GPP)_5$-GRAGEOGLQGPAGPOGEKGEOGDDGPS-$(GPP)_5$-GPC-NH_2	5561
TK-II-43	GPC-$(GPP)_5$-GEOGDDGPSGAEGPOGPQGLAGQRGIV-$(GPP)_5$-GPC-NH_2	5531
TK-II-44	GPC-$(GPP)_5$-GLAGQRGIVGLOGQRGERGFOGLOGPS-$(GPP)_5$-GPC-NH_2	5705
TK-II-45	GPC-$(GPP)_5$-GFOGLOGPSGEOGKQGAOGASGDRGPO-$(GPP)_5$-GPC-NH_2	5551
TK-II-46	GPC-$(GPP)_5$-GASGDRGPOGPVGPOGLTGPAGEOGRE-$(GPP)_5$-GPC-NH_2	5514
TK-II-47	GPC-$(GPP)_5$-GPAGEOGREGSOGADGPOGRDGAAGVK-$(GPP)_5$-GPC-NH_2	5491
TK-II-48	GPC-$(GPP)_5$-GRDGAAGVKGDRGETGAVGAOGAOGPO-$(GPP)_5$-GPC-NH_2	5449
TK-II-49	GPC-$(GPP)_5$-GAOGAOGPOGSOGPAGPTGKQGDRGEA-$(GPP)_5$-GPC-NH_2	5431
TK-II-50	GPC-$(GPP)_5$-GKQGDRGEAGAQGPMGPSGPAGARGIQ-$(GPP)_5$-GPC-NH_2	5534
TK-II-51	GPC-$(GPP)_5$-GPAGARGIQGPQGPRGDKGEAGEOGER-$(GPP)_5$-GPC-NH_2	5644
TK-II-52	GPC-$(GPP)_5$-GEAGEOGERGLKGHRGFTGLQGLOGPO-$(GPP)_5$-GPC-NH_2	5746
TK-II-53	GPC-$(GPP)_5$-GLQGLOGPOGPSGDQGASGPAGPSGPR-$(GPP)_5$-GPC-NH_2	5427
TK-II-54	GPC-$(GPP)_5$-GPAGPSGPRGPOGPVGPSGKDGANGIO-$(GPP)_5$-GPC-NH_2	5409
TK-II-55	GPC-$(GPP)_5$-GKDGANGIOGPIGPOGPRGRSGETGPA-$(GPP)_5$-GPC-NH_2	5528
TK-II-56	GPC-$(GPP)_5$-GPRGRSGETGPAGPOGNOGPOGPOGPO-$(GPP)_5$-GPC-NH_2	5521

To identify the versican binding sites on collagen, I compared the versican binding capacity of these Toolkit peptides to the versican binding of full-length collagen. V3 showed a relatively high binding when interacting with Toolkit peptides 4, 8, 11, 15 and 18 (Figure 2.6A). Toolkit peptides 4, 8, 11 and 18 also showed up as positive binding candidates for G3 (Figure 2.6B). In addition, Toolkit 5 and 44 were identified as potential binding sites for the G3 domain (Figure 2.6B).

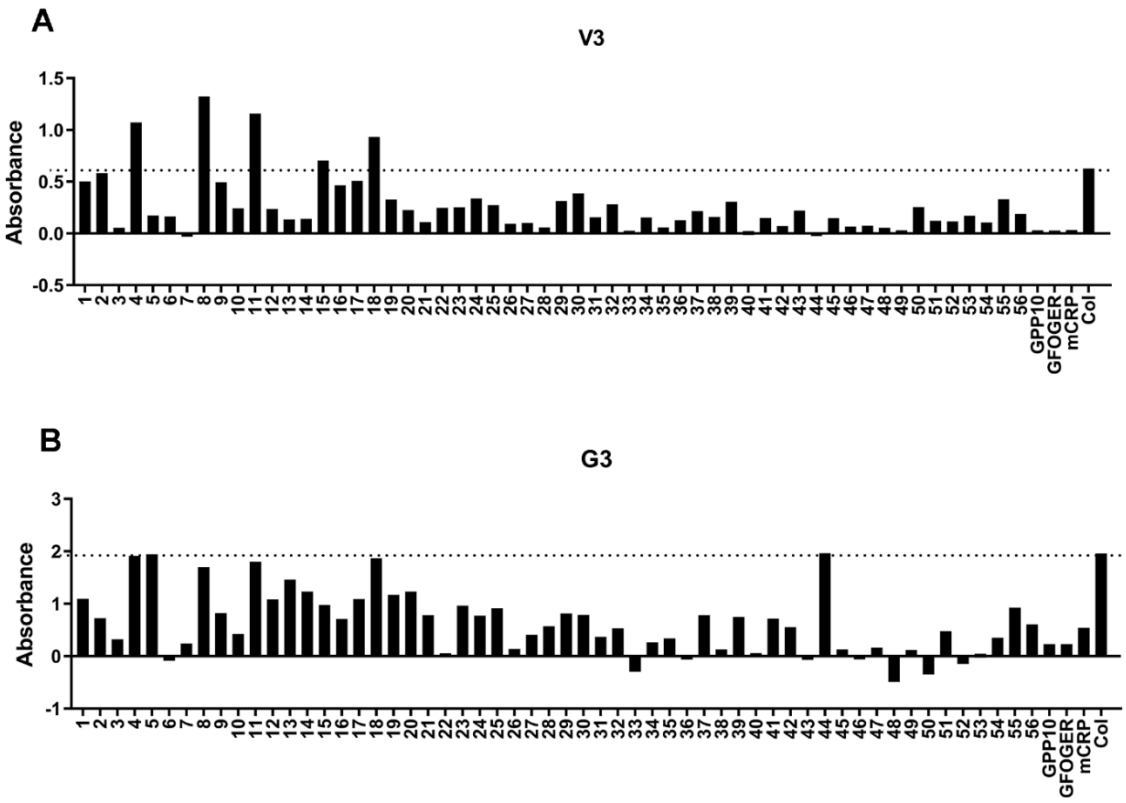

Figure 2.6 Potential V3 isoform and its G3 domain binding sites on collagen were identified using the Collagen Toolkit. Toolkit peptide-coated 96-well plates were tested with the addition of recombinant V3 or G3 (both have His tags), and bound V3 or G3 was detected using an HRP conjugated anti-His antibody. Empty wells in the plate provided by Camcol were coated with full-length collagen as a positive control. Two independent experiments were done with V3 with one representative graph shown. One experiment was done with G3.

2.4 DISCUSSION

Matrix PGs, especially SLRPs, have been well studied and reported to be important collagen binding ECM proteins and key regulators for collagen fibrillogenesis during development. I report here that versican, a universally distributed hyalectan PGs, can interact with collagen both in vitro

and in vivo, and may modulate collagen fiber formation maturation and organization during development. IEM successfully confirms the colocalization of versican and collagen fibers in the extrahepatic bile duct, with decreased versican deposition during development. A solid phase assay identified G3 domain as the collagen binding site on versican, and the Collagen Toolkit assay identified Toolkit peptides 4, 8, 11, 15 and 18 as potential V3 binding peptides, with the study on G3 adding Toolkit peptides 5 and 44 to the candidate list.

SLRPs, the small matrix PG subfamily, have been heavily studied as regulators of the size, morphology and organization of collagen networks during development and appear to be especially important for tissues such as cornea (S. Chen et al. 2014) and tendon (G. Zhang et al. 2006) that require well-organized fibrous networks for their physiological functions. For example, lumican and biglycan deficiency cause an impaired lamellar organization of collagen fibers and damage the transparency of cornea (S. Chen et al. 2014); the loss of lumican and fibromodulin leads to abnormal fiber structure and irregular interfibrillar spaces in tendon (Ezura et al. 2000). Unlike SLRPs, large hyalectan PGs including versican have not been well investigated as mediators of collagen maturation during development. Our lab has published that versican expression decreases during extrahepatic bile duct development, as determined by immunostaining neonatal and adult bile duct samples (Khandekar et al. 2020) and I further validated this observation by using IEM, which shows the colocalization of versican with collagen fibers and a decrease in versican deposition in the region of collagen fibers during development. IEM has also been used to study the interaction between collagen and other matrix PGs: in fetal dermis, a large amount of decorin has been observed that colocalizes with collagen fibers and forms a spiral like decoration along individual fibers (Fleischmajer et al. 1991); in cartilage, a small number of aggrecan KS domains colocalize with collagen (type II) fibers while others mainly stay in the interfibrillar space (forming large HA-aggrecan aggregates) (Hedlund et al. 1999). To further validate this versican/collagen colocalization, IEM was carried out on a collagen-versican

co-gel which illustrates that there is a direct interaction between collagen and versican in vitro. However, the mechanism of the collagen/versican interaction and its regulation of collagen fibrillogenesis and organization remains unclear.

To understand the collagen binding sites on versican, solid phase binding assays were used. It is important to clarify that isolated versican from bovine liver is contaminated with aggrecan and decorin. Although isolated versican, isolated versican core protein (generated by ChABC digestion), and recombinant V3 isoforms all demonstrate a collagen binding capacity, recombinant V3, as a pure core protein, has a particularly high binding affinity and capacity. Given the fact that isolated versican was contaminated with aggrecan and decorin, the direct binding between collagen and pure recombinant V3 confirm the actual binding between collagen and versican core protein. As V3 only contains N-terminal G1 and C-terminal G3 domain (lacking GAG domain), my further investigation in comparing the collagen binding capacity of G1 versus G3 further demonstrates that it is versican core protein G3 domain that directly bind collagen. As further validated by competition experiments, the collagen-binding site and the HA-binding site on versican are distinct: collagen binds to the C-terminal G3 domain of versican while HA binds to the N-terminal G1 domain, without evidence of interactions between the binding sites. Although aggrecan is thought to be structurally similar to versican, it has distinct interactions with collagen compared to versican given that the collagen binding site on aggrecan is in the KS domain (the core protein of this domain), a domain that versican lacks (Hedlund et al. 1999). Compared to isolated versican (K_d=1.29 nM) and its core protein (K_d=2.23 nM), recombinant V3 shows a higher binding affinity (K_d=0.69 nM) suggesting that the GAG residues, which are highly negatively charged, might play a negative role in interactions between collagen and versican. The K_d for collagen/fibromodulin and collagen/decorin interactions are 9.9 nM (Hedbom and Heinegard 1993) and 14 nM (Vynios et al. 2001), while the K_d is 1.1 μM for collagen/aggrecan binding (Hedlund et al. 1999). This indicates that there is a strong interaction between collagen and V3 compared to

the weak electrostatic interaction between collagen and aggrecan. Importantly, both collagen/versican and collagen/V3 interaction are pH and ionic strength sensitive indicating that charged residues play an important role in these interactions. Given that G3 domain is the collagen binding sites, I have analyzed the charged tracts on its amino acid sequence (Figure 2.7) and found that positive tracts including 3182-KYFAHRR-3188, 3306-KTFGKMKPR-3324, 3360-RTYSMKYFK-3368 and 3386-RWSRR-3390 and negative tracts including 3122-DQCELDFDE-3130 and 3163-EQDTETCD-3170 are potential binding residues which require further investigation using a solid phase binding assay with recombinant binding residues to identify the actual collagen binding motifs of versican.

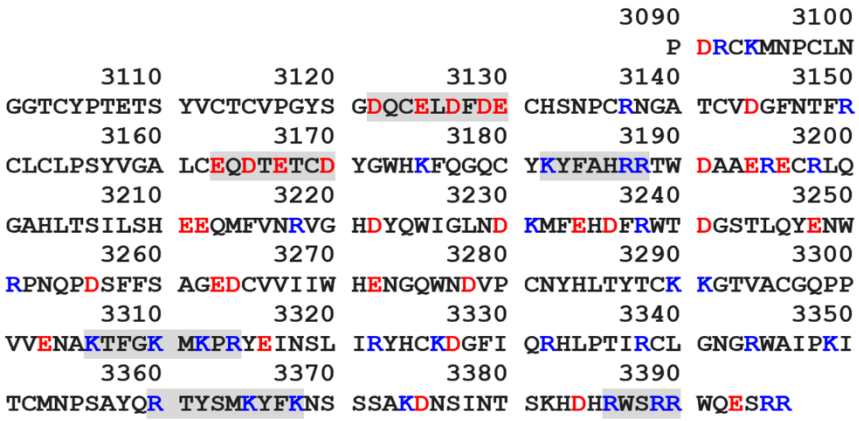

Figure 2.7 The highly charged tracts on the amino acid sequence of G3 core protein. Blue – positive charged; red – negative charged; grey highlights – highly charged tracts. (This analysis was done by R. W. Farndale.)

Based on the data from the solid phase assay and collagen/HA/V3 competition experiments, I have confirmed that the V3 isoform binds collagen via its G3 domain, but I have not studied the core protein of the α and β-GAG domains. There are some limitations to these studies: (1) purification of versican from native tissue is difficult and we have been unable to isolate pure protein; (2) there is not any normal tissue that has a large accumulation of versican; (3) versican has over 3000 amino acids which makes it hard to synthesize fragments covering the entire core protein for screening binding sites. In future experiments, using recombinant versican α and β-GAG domains in a solid phase assay will shed light on potential binding sites in these two large domains of versican core protein.

To identify the versican binding sites on collagen, the Collagen Toolkit solid phase assay has been used to detect potential binding peptides. After comparing the binding capacity of 56 synthetic collagen memetic peptides (Toolkits) to that of native collagen, Toolkit peptides 4, 8, 11, 15 and 18 show high binding to V3 and Toolkit peptides 4, 5, 8, 11, 18 and 44 show high binding to G3. This is a strong evidence that V3 and G3 share the same binding sequence as they all bind to Toolkit 4, 8, 11 and 18, which are not published as common binding peptides (except Toolkit 8, known as an integrin binding site) (Farndale 2019). Importantly, G3 adds Toolkit 5 and 44 to the candidate list. 5 and 44 both have important biological functions, having been reported as crosslinking and collagenase sites, respectively, which suggests a potential regulatory role of versican in collagen crosslinking and degradation. Why G3 binds to these peptides and V3 does not is unclear. There might be conformational changes in V3 compared to G3 alone (potentially with the G1 and G3 domains in V3 binding to each other, or dimerizing) which effectively sequester the binding sites of Toolkit 5 and 44. In this case, different versican isoforms may have different conformations and 3D crystal structures, which have not been studied. The structural variances of versican isoforms may lead to distinct binding capabilities and binding partners and might explain the diverse and opposing biological functions of these isoforms (Ricciardelli et al.

2009). After assessing the alignment of these Toolkit candidates, the R-G-Hydrophobic-O motif is highly aligned among all these candidates (Figure 2.8). R can be substituted by K in Toolkit 15, and the aliphatic stems of E, R and P provide hydrophobic interactions. Another possible motif is the GPA triplets that has also been found in some Toolkits which the small sidechain of alanine might avoid steric hindrance but not contribute to binding directly. In addition, GPP might also function similarly as GPA given that the ring of proline does not protrude too far from the axis of the helix. In the future, the binding between versican and R-G-Hydrophobic-O motif will be validated by using corresponding collagen mimetic peptides in a solid phase binding assay and studying versican binding with Toolkit III (synthetic collagen peptides of type III collagen) will explore additional versican/collagen binding sites. In addition, understanding the 3D conformational structure of V3 and G3 as well as the binding motif (R-G-Hydrophobic-O in the helix) will shed light on building the 3D binding model of collagen/versican interaction.

Figure 2.8 The binding motifs analyzed by the alignment of versican-binding Toolkits. The alignment analysis was done by R. W. Farndale.

In addition, collagen fibers form a 3D dynamic fibrous network via strong covalent interactions including LOX mediate crosslinks (Robins 2007) and weak interactions including electrostatic interactions between charged residues (Wallace 1990). Thus, the presence of versican in collagen matrices can regulate the organization of collagen fibers through binding between collagen and the G3 domain. This is particularly important given the evidence that G3 interacts with collagen crosslink sites. A future investigation into the 3D structural collagen/versican binding model will help understand the mechanisms of versican/collagen interactions in modulating collagen fibrous networks, specifically the promotion of fiber fusion into bundles and increased fiber alignment (shown in Chapters 3 and 4). The pH sensitivity of the versican/collagen interaction has a potentially crucial physiological relevance in vivo, considering the acidic tumor microenvironment as an example (Justus, Dong, and Yang 2013). The pH of the tumor microenvironment can be as low as 5.6 (Griffiths 1991) and acidic pH (pH=6) is preferred for versican/collagen interactions (Figure 2.5A, B). Thus, increased deposition of versican in cancer (Ricciardelli et al. 2009) could modulate the collagen fibrous network via upregulating versican/collagen interactions that facilitate the accumulation of a collagen rich matrix with highly aligned fibers (Figure 4.2, 4.4), which could enhance metastasis (Han et al. 2016).

In sum, versican colocalizes with collagen fibers both in vitro and in vivo, supporting the presence of a direct interaction between collagen and versican. There is decreased versican expression during bile duct development, suggesting a regulatory role in collagen fibrillogenesis and fibrous network maturation. Versican directly interacts with collagen via its C-terminal G3 domain, in contrast to its N-terminal G1 domain which binds HA. Highly charged residues on the binding sites, four positively charged tracts and two negatively charged tracts as potential binding motifs on G3, are important for collagen/versican interaction given its pH and ionic strength sensitivity. The Toolkit results further confirm the direct interaction between collagen and versican, indicate

the importance of R-G-Hydrophobic-O motifs in collagen/versican binding and identify a potential role for G3 in collagen crosslinking and degradation.

CHAPTER 3 VERSICAN REGULATES COLLAGEN FIBRILLOGENESIS AND ORGANIZATION DIFFERENTLY COMPARED TO OTHER MATRIX PROTEOGLYCANS

This chapter is adapted from the publication: D. Chen, L.R. Smith, G. Khandekar, P. Patel, C.K. Yu, K. Zhang, C.S. Chen, L. Han, R.G. Wells, Distinct effects of different matrix proteoglycans on collagen fibrillogenesis and cell-mediated collagen reorganization, Sci. Rep. 10 (2020) 1–13. doi:10.1038/s41598-020-76107-0.

L.R. Smith and P. Patel helped with versican isolation from bovine liver.

3.1 INTRODUCTION

Type I collagen is the most abundant structural protein in the ECM. It is synthesized and folded into a triple helix in the endoplasmic reticulum, post-translationally modified and transferred via the Golgi apparatus and then secreted into the ECM (Canty and Kadler 2005). After the cleavage of N- and C-propeptides, collagen monomers can form internal and external crosslinks and self-assemble into collagen fibrils which show a typical 67 nm D-periodicity as part of a well-organized banding pattern (Yamauchi and Sricholpech 2012). Fibrils can further form large fibers (although the distinction between fibril and fiber remains unclear) and they can undergo lateral fusion into larger bundles, form a complex fibrous network and build up higher tissue-level organization. Collagen fibrillogenesis is precisely controlled and dynamically regulated during tissue development and abnormal fibrillogenesis has been observed during collagen-related disorders. Collagen also has a crucial role in maintaining appropriate structural and mechanical complexity of the ECM in specific tissues (Banos, Thomas, and Kuo 2008). Importantly, the structure and organization of collagen fibrous networks is highly regulated by interacting with other ECM components including PGs and GAGs (Kalamajski and Oldberg 2010). PGs are highly glycosylated proteins attached to negatively-charged GAG side chains; the negative charges on

GAGs enable them to attract water, increase swelling and resist compression (Yanagishita 1993). PGs as well as GAGs have been widely studied as regulators for collagen fibrillogenesis and therapeutic targets for ECM-related diseases including inflammation, fibrosis and cancer (Theocharis 2008).

Matrix (interstitial) PGs are divided into two subgroups: SLRPs and hyalectans (large CSPGs). SLRPs have 50-60 kDa core proteins with only 1-4 GAG side chains (DS, CS or KS) and the family includes decorin, lumican, and fibromodulin. As important collagen binding partners, SLRPs have been well studied as key regulators of fibrillogenesis both in vitro and in vivo. An in vitro spectrophotometric (turbidity) assay has been widely applied to study various factors, such as pH, ionic strength and polyanions, that regulate fibril formation and fibrous network organization (Yan et al. 2012)(Wood 1960). As demonstrated using the turbidity assay, decorin and lumican have negative effects on fibrillogenesis such that they decrease both the rate and plateau of fibril formation (Rada, Cornuet, and Hassell 1993). During development, SLRPs are required for maintaining normal fiber formation and organization, especially for tissues like cornea and tendon, which need highly organized collagen networks for their regular functions. Lumican- and biglycan-deficient mice have disrupted lamellar fiber structures in the cornea that affect corneal transparency (S. Chen et al. 2014), and decorin-, fibromodulin- and lumican-deficient mice show abnormal fiber morphology, altered fiber size distributions and atypically non-uniform interfibrillar space in tendon (Ezura et al. 2000)(G. Zhang et al. 2006). However, the roles of large CSPGs, the other matrix PG subfamily, in regulating collagen fibrillogenesis and fibrous network organization are still unclear. The large hyalectan PG family includes versican (which contains a 360 kDa core protein with up to 23 CS side chains for the largest V0 isoform), aggrecan (which contains a 250 kDa core protein with over 100 GAG side chains, including both CS and KS) and others that are defined based on their ability to bind HA (Dours-Zimmermann and Zimmermann 1994)(Kiani et al. 2002). Compared with SLRPs, these large PGs have a significantly longer core

protein with a larger mass of negatively charged GAGs. The molecular weight of full-length large CSPGs can reach up to 1-2.5 MDa and when bound to long HA chains they can form larger space-filling bottlebrush-like aggregates. Their GAG side chains have been shown previously to have distinct impacts on collagen fibrillogenesis (Stuart and Panitch 2008), and small compositional changes in GAGs, such as addition of different types of hexuronic acids and altered sulfation levels, can also affect collagen fibrillogenesis. For example, dermatan sulfate (DS) epimerase 1-null mice have decreased iduronic acid in their GAGs, including on versican, and demonstrated abnormal collagen fibril formation and irregular collagen structure in skin (Maccarana et al. 2009). Unlike aggrecan, which is predominantly expressed in cartilage, versican is more universally distributed throughout the human body and shows increased deposition and turnover during numerous fibroproliferative process (Theocharis 2008)(Bode-Lesniewska et al. 1996). Although aggrecan and versican interact with collagen differently, the effects of large PGs on regulating fibrillogenesis are not well understood. There is a particular need to clarify the role of versican in regulating collagen fibrillogenesis and the organization of the collagen fibrous network given its widespread distribution and altered expression in collagen-related disorders.

In this chapter, distinct effects of different matrix PGs, even within a particular subfamily, on regulating in vitro collagen gelation (in part representing fibrillogenesis) are investigated using an in vitro turbidity assay. The impacts of isolated versican, its core protein, GAG side chains and the small V3 isoform on collagen behaviors in the turbidity assay are studied. The effects of different matrix PGs on the organization of collagen fibrous networks are visualized and analyzed by scanning electron microscopy (SEM). Both assays highlight the unique role of versican, even compared to the large PG aggrecan, in mediating fibrillogenesis and collagen network organization.

3.2 METHODS

3.2.1 Reagents

Bovine type I atelo-collagen (lacking N- and C-terminal telopeptide regions) was from Advanced Biomatrix (San Diego, CA, USA) and rat tail type I telo-collagen (with intact telopeptide regions) was from Corning (Corning, NY, USA). Versican was isolated from bovine liver. Aggrecan isolated from bovine cartilage was a gift of Lin Han (Drexel University) (Lee et al. 2013) and was also purchased from Sigma (A1960) (St. Louis, MO, USA). Decorin (D8428), CS sodium salt isolated from bovine cartilage and ChABC from *Proteus vulgaris* were from Sigma. Recombinant human lumican protein (lacking GAG chains) was from R&D Systems (Minneapolis, MN, USA).

3.2.2 In vitro spectrophotometric (turbidity) assay

Type I bovine atelo-collagen was diluted to a final concentration of 1.5 mg/mL. All solutions were kept on ice before gelation. Briefly, 187.5 µL collagen solution (3.2 mg/mL) was gently mixed with 40 µL 10× PBS, 4 µL 1N NaOH, and 168.5 µL diH_2O. All collagen solutions were kept on ice before testing. In some cases, type I rat tail telo-collagen was used and prepared similarly. For testing different wavelengths of spectrophotometry, the absorbances of both atelo- and telo-collagen solution were read under 313, 400, 500, 600, 700 and 800 nm. For some experiments, versican, aggrecan and decorin were added to the collagen solution to a final concentration of 0.1 mg/mL; lumican was added to 0.01 and 0.05 mg/mL (which were used at physiological relevant collagen:PG ratio according the 1.6:1 Col:GAG ratio in native liver (unpublished data quantified by L. Chin)). CS were tested by adding to final concentrations of 0.01, 0.04, 0.07 and 0.1 mg/mL. The versican core protein was obtained by treating the intact protein with 250 mU ChABC (per mg substrate) in 50 mM sodium acetate (pH=8.0) overnight at 37°C, followed by dialysis with diH_2O. The pH of the collagen solution was carefully adjusted to 7.4 and the solution was always incubated on ice for 1 h before pipetting into a 96-well plate. The absorbance of the solution was

read at 37°C by a plate reader (Infinite 200 Pro, Tecan Life Sciences) at 400 nm until gelation was complete (when the absorbance curve reached the plateau) (Vogel and Trotter 1987).

3.2.3 Scanning electron microscopy

Rat tail type I collagen was diluted to a final concentration of 1.5 mg/ml and supplemented with different PGs as descried above for the turbidity assay. It was polymerized at 37°C on 8 mm coverslips in a 6-well plate for 25 min (the plate was covered with wet Kimwipes and sealed with paraffin). The collagen gels were fixed with 2.5% glutaraldehyde in cacodylate buffer overnight at 4°C. The samples were further processed by the Cell and Developmental Biology Microscopy Core (University of Pennsylvania, Philadelphia, PA, USA). Briefly, samples were dehydrated with a graded series of ethanol washes (50, 75, 90, 95, 100%) and incubated with 50% hexamethyldisilazane (HDMS) for 30 min. Samples were then incubated with 100% HDMS for 3 times and air dried before mounting on stubs. Samples were imaged on a FEI Quanta 250 FEG scanning electron microscope (Thermo Scientific). Bovine collagen (atelo-collagen) was prepared and studied in the same manner. 5 figures were taken per each gel at 5 random locations at 10,000×. 5 randomly cropped figures (384×256 pixels) from each SEM figure were analyzed using DiameterJ, an image J plugin, which was used to quantify fiber diameter and length, porosity, pore size and connections.

3.2.4 Statistical analysis

All results were analyzed by GraphPad Prism 7 (San Diego, CA, USA) using an unpaired t test or one-way ANOVA. P values were determined by Tukey's multiple comparison test, in which *P<0.05 was considered to be statistically significant.

3.3 RESULTS

3.3.1 The spectrophotometric (turbidity) assay is a valid in vitro method for studying collagen gelation (fibrillogenesis)

The in vitro turbidity assay, which tracks the turbidity changes during collagen gelation using a spectrophotometer, has been used for decades to study the potential regulators of collagen gelation (partially representing fibrillogenesis) in vitro (Wood and Keech 1960). It generates a sigmoidal curve with a lag phase (representing nucleation), followed by a growth phase (representing lateral growth) and finally a final plateau representing complete gelation. During the growth phase, the formation of large aggregates (fibrils) contributes to the quick increase in turbidity due to an increased molecular weight and altered light scattering. While this assay does not directly measure fibrillogenesis, the increments in turbidity partially represent collagen fibril formation and alterations in collagen organization. This assay has been widely used to test various fibrillogenesis regulators and most researchers have used two different wavelengths, 313 and 400 nm, in this spectrophotometric assay (Wood and Keech 1960)(Harris, Soliakov, and Lewis 2013). In this case, I tested the effects of different wavelengths (including 313 and 400 nm) on the turbidity assay using both telo- and atelo-collagen. All of the different wavelength measurements resulted in typical sigmoidal kinetic curves representing gelation (Figure 3.1). The kinetic curves from 313 nm and 400 nm both showed significant changes in absorbance during gelation compared to other wavelengths. I chose to use the 400 nm wavelength to study the roles of different matrix PGs in regulating collagen gelation in vitro because 400 nm was used in previously published work for comparing the effects of small tendon PGs and large cartilage PGs on fibrillogenesis (Vogel and Trotter 1987).

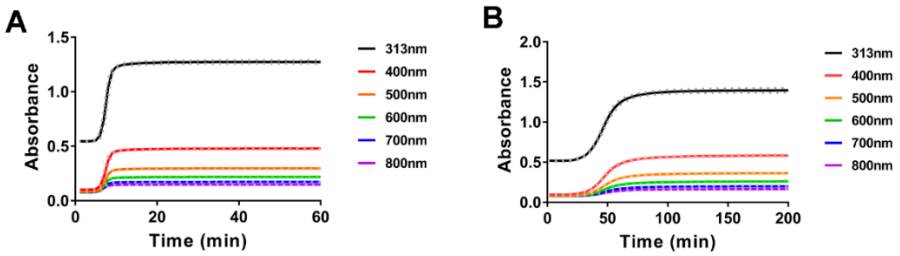

Figure 3.1 Results from in vitro turbidity assays carried out at different wavelengths. (A) 1.5 mg/mL telo-collagen, (B) 1.5 mg/mL atelo-collagen. The lines represent mean curves, and the dotted lines represent SD for the technical replicates. This experiment was performed once with three technical replicates.

3.3.2 Versican regulates collagen fibrillogenesis differently compared to other matrix PGs

I tested both rat tail telo-collagen and bovine atelo-collagen gelation and studied the effect of versican on gelation in both cases. I found that telo- and atelo-collagen showed different kinetic curves; it took a longer time for atelocollagen to reach full gelation (Figure 3.2A). Telo-collagen is acid-extracted and includes intact telopeptides while atelo-collagen is pepsin-extracted and lacks telopeptides. Telopeptides function as docking sites for collagen crosslinking, which guides the alignment of collagen monomers and promotes lateral growth. Thus the diffusion time of the monomer addition during fibril formation is impacted for atelocollagen compared to telocollagen (Shayegan et al. 2016). In both cases, the addition of isolated full-length versican, which consists mainly of βGAG-attached large V0 and V1 isoforms (shown in Figure 2.2 that there is positive staining of βGAG in isolated versican sample), accelerated collagen gelation and increased the final fibril formation plateau regardless of the two different collagens (Figure 3.2A, purple and blue curves). Because of the rapidity of telo-collagen gelation and the goal of studying different

modulators of gelation, I used atelo-collagen for all following turbidity experiments; this made it easier to compare the distinct roles of different matrix PGs in modulating collagen fibrillogenesis. To compare the effect of large CSPGs, versican and aggrecan, on collagen fibrillogenesis, I mixed either of the two large PGs with atelo-collagen before initiating the turbidity assay. When collagen was mixed with versican, the increase in absorbance was more rapid and the gelation plateau was higher compared with collagen alone (Figure 3.2B, purple and black curves); as a control, versican alone tested under identical conditions showed no change in absorbance (Figure 3.2C), suggesting that the dramatic change in the gelation curve with versican added to collagen was due to the interaction between the two proteins. Interestingly, the addition of aggrecan, which is structurally similar to versican, slowed the rate of fibrillogenesis without changing the gelation plateau (Figure 3.2B, blue curve). Because my isolated bovine versican was contaminated with decorin, which has been reported to be an inhibitor of collagen fibrillogenesis in vitro (Reese, Underwood, and Weiss 2013), I also tested the effect of decorin (intact structure with GAGs, from bovine articular cartilage) and lumican (recombinant core protein only, without GAGs) on collagen gelation, as controls. I found that the addition of either decorin or lumican led to a decreased rate of collagen fibrillogenesis. Decorin had particularly marked effects on both the rate and plateau (Figure 3.2D, green curve) while lumican downregulated collagen gelation in a dose-dependent manner (Figure 3.2D). Thus, the presence of decorin in my isolated native versican is unlikely to account for the effects observed in the turbidity assay given that decorin alone had the opposite effect as the isolated versican and the recombinant V3 isoform of versican core protein (Figure 3.3C) has similar effects as the form I isolated.

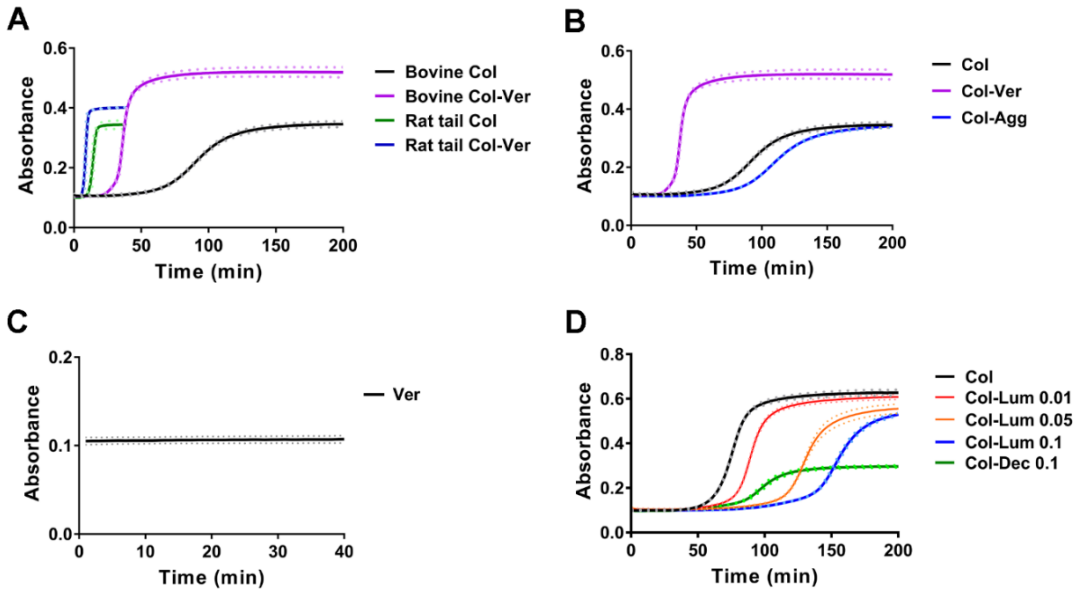

Figure 3.2 Different matrix proteoglycans have distinct effects on collagen gelation in the in vitro turbidity assay. (A) Versican (Ver; 0.1mg/mL) was added to rat tail telo-collagen (Col; 1.5 mg/mL) and bovine atelocollagen (1.5 mg/mL). (B) Versican (Ver; purple curve) or aggrecan (Agg; blue curve), both at 0.1 mg/mL, were added to atelocollagen (Col; 1.5mg/mL, black curve). Versican accelerated gelation dramatically while aggrecan slightly right-shifted the turbidity curve. (C) Versican alone (0.1 mg/mL) failed to gel and showed no change in turbidity over time under the assay conditions. (D) The SLRPs lumican (Lum; 0.01, 0.05 and 0.1 mg/mL) and decorin (Dec, 0.1 mg/mL) were added to atelocollagen (Col; 1.5 mg/mL). Decorin had a larger impact on decreasing fibrillogenesis than lumican. For all turbidity assays under all testing conditions, the pH and gelation temperature were the same. For all panels except C, three independent experiments were carried out for each condition, each with three technical replicates. Because there can be day-to-day differences in the absolute absorbance values for the assay, a representative figure from one experiment with mean curves is shown for each condition; however, all assays in a panel were carried out in parallel, and relative values among the different

conditions were consistent in each individual experiment. C was performed once with three technical replicates. The lines represent mean curves, and the dotted lines represent SD.

3.3.3 Versican core protein, with a minor contribution from the CS side chains, regulates collagen gelation

Because of the specific bottlebrush-like structure (a core protein attached with GAG side chains) of versican, I tested whether the versican core protein or the GAG side chains were the primary contributors to the effect of versican on collagen fibrillogenesis. Firstly, I studied the effect of CS, part of the GAG side chains of both versican and aggrecan, on collagen gelation in vitro. The addition of CS left-shifted the absorbance curve in a dose-dependent manner but less markedly than observed for intact versican at a comparable concentration (Figure 3.3A), suggesting that the interaction between collagen and versican was mainly via the core protein, not the GAG side chains. This is consistent with the finding reported in Chapter 2, from a solid phase assay, that versican binds collagen via its G3 domain. Secondly, I studied the role of the versican core protein in the turbidity assay. To obtain versican core protein, isolated intact versican was digested with ChABC to detach CS side chains, was dialyzed against diH_2O to remove digested CS, and then added to atelo-collagen for the turbidity assay. I observed that the impact of the versican core protein on the rate and plateau was slightly less than for the intact versican (Figure 3.3B, purple and pink curves). For experiments regarding enzyme-treated material, I confirmed that the heat-inactivated enzyme had minimal effects on fibrillogenesis (Figure 3.3B, blue curve). Additionally, I studied the effect of the recombinant V3 isoform, which only contains the G1 and G3 domains of versican without GAG modification, on collagen fibrillogenesis for both collagen types. I observed the same pattern as with intact full length versican, which showed an increase of both the rate and plateau for both telo- and atelo-collagen (Figure 3.3C, blue and purple curves). Thus, the versican core protein, with at best a minor contribution from its CS side chains, modulated collagen fibrillogenesis in vitro.

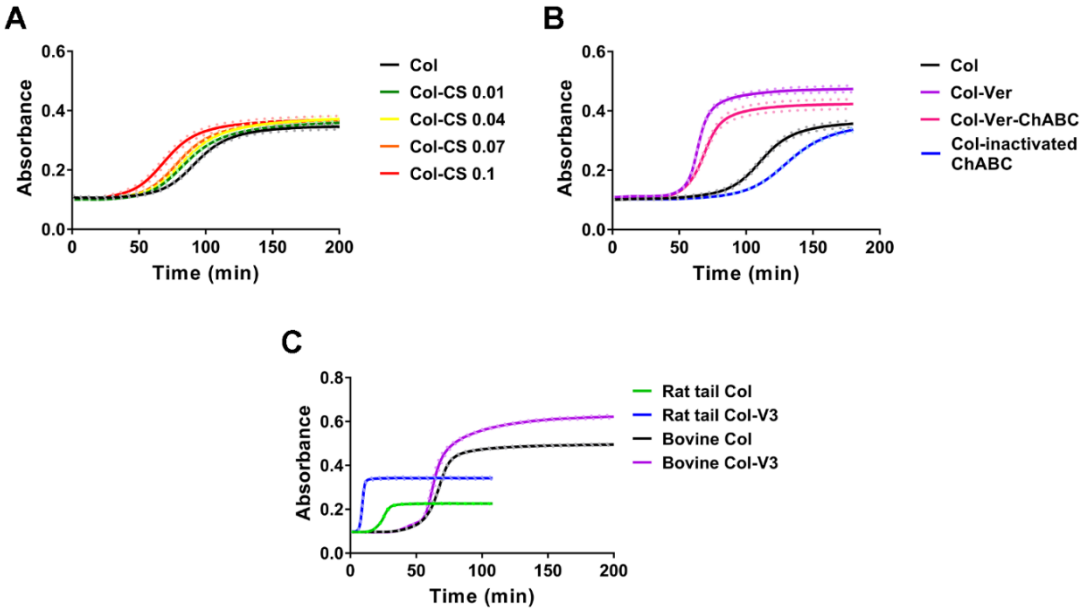

Figure 3.3 The versican core protein plays a major role in regulating collagen gelation. (A) Chondroitin sulfate (CS; 0.01, 0.04, 0.07 and 0.1 mg/mL; green, yellow, orange and red curves) was added to collagen (Col; 1.5 mg/mL; black curve). (B) After digestion of the versican CS side chains with ChABC, the remaining versican core protein was added at 0.1 mg/mL (pink curve) to atelo-collagen (1.5 mg/mL) and caused a similar although slightly blunted right shift to the curves. Heat-inactivated ChABC had minimal effect on collagen gelation (blue curve). (C) Recombinant V3 isoform (V3, 0.1 mg/mL) was added to rat rail telo-collagen (1.5 mg/mL) and bovine atelo-collagen (1.5 mg/mL). Three independent experiments were carried out for each condition, each with three technical replicates. Because there can be day-to-day differences in the absolute absorbance values for the assay, a representative figure from one experiment with mean curves is shown for each condition; however, all assays in a panel were carried out in parallel, and relative values among the different conditions were consistent in each individual experiment. The lines represent mean curves, and the dotted lines represent SD.

3.3.4 Versican alters the organization of collagen fibrous networks differently than other matrix PGs

To investigate the role of PGs in regulating the organization of collagen fibers, I used SEM to visualize individual fibers in collagen networks modified with different matrix PGs. Firstly, I compared the structure of both telo- and atelo-collagen networks (Figure 3.4A, B) and found that atelo-collagen formed a looser network with thicker fibers, decreased total fiber length and increased pore size (Figure 3.4C-G). The telo-collagen network had significantly fewer connections (crosslinks) than the telo-collagen network, consistent with the fact that atelo-collagen lacks the telo-peptides that are the most common sites of covalent crosslinking. Because the gelation time of atelo-collagen was three times longer than of telo-collagen (Figure 3.2A) and concerns that dehydration might occur during the gelation of atelo-collagen, telo-collagen was used in the SEM assay to evaluate the effect of PGs on the collagen fibrous network.

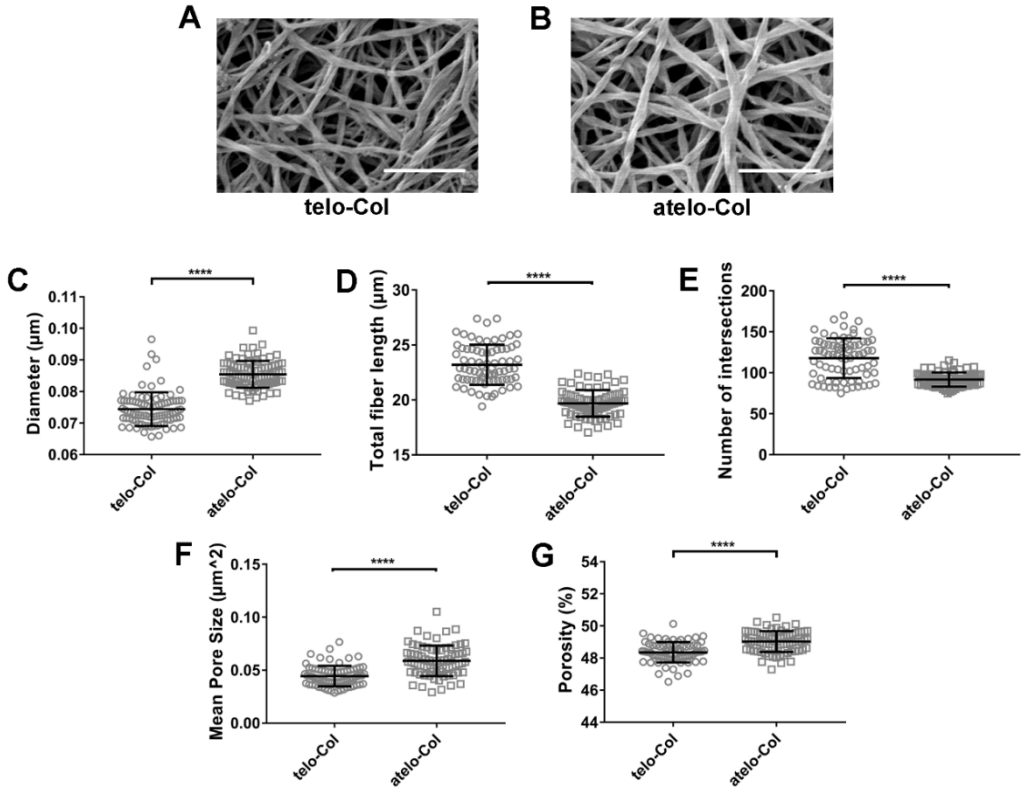

Figure 3.4 Matrices made from telo- and atelo-collagen show different structural features, as visualized by SEM. (A, B) Representative SEM imaging of collagen matrices: (A) 1.5 mg/mL telo-collagen; (B) 1.5 mg/mL atelo-collagen. (C-G) Fiber diameter (µm), total fiber length (µm), number of intersections, mean pore size (μm^2) and porosity (%) were quantified using the ImageJ plugin, DiameterJ. Three independent experiments were carried out for each condition and one gel was generated for each condition in each experiment. 5 SEM images were taken for each gel at random locations. When analyzing images using DiameterJ, 5 figures were cropped from each SEM image and a measurement was taken on each cropped figure. Each data point represents a single measurement. Scale bar = 1 µm. Data represent mean ± SD. ****P<0.0001.

The SEM imaging of collagen matrices manipulated with different matrix PGs showed distinct fiber and structural features of the collagen networks (Figure 3.5A-D). The addition of versican to

collagen matrices resulted in a looser network with fewer fiber connections, significantly enlarged fiber diameter, decreased total fiber length and decreased pore size (Figure 3.5E-I). Importantly, an increased number of fibers fused into large bundles was also observed when versican was present in the collagen network (Figure 3.5A, J). Because of the formation of large collagen bundles, the number of intersections (network connections/crosslinks) in the collagen-versican network was significantly lower (Figure 3.5G). The addition of aggrecan, another large CS proteoglycan that is structurally similar to versican, had no significant impact on fiber diameter, total fiber length or mean pore size but showed a slight decrease in connections (Figure 3.5E-I). For SLRPs, the addition of decorin to collagen resulted in a denser network, decreased fiber diameter and pore size, and increased total fiber length (Figure 3.5E-I). However, the addition of another SLRP, lumican, had a different impact on the structure of the collagen network. It had no impact on fiber diameter and porosity, but resulted in significantly increased mean pore size and decreased total fiber length and intersections (Figure 3.5E-I). Importantly, collagen gel samples, which naturally contained certain amount of water (like a hydrogel), were dehydrated during the sample fixation and preparation for SEM, causing the network to lose its native hydrated structure. The volume occupied by PGs and the water attracted by negatively charged GAGs were also affected during the sample preparation process. The relative collagen fiber morphology, diameter, and connections as well as the pore area of the fibrous network, however, were likely to persist and were comparable among different collagen/PG networks.

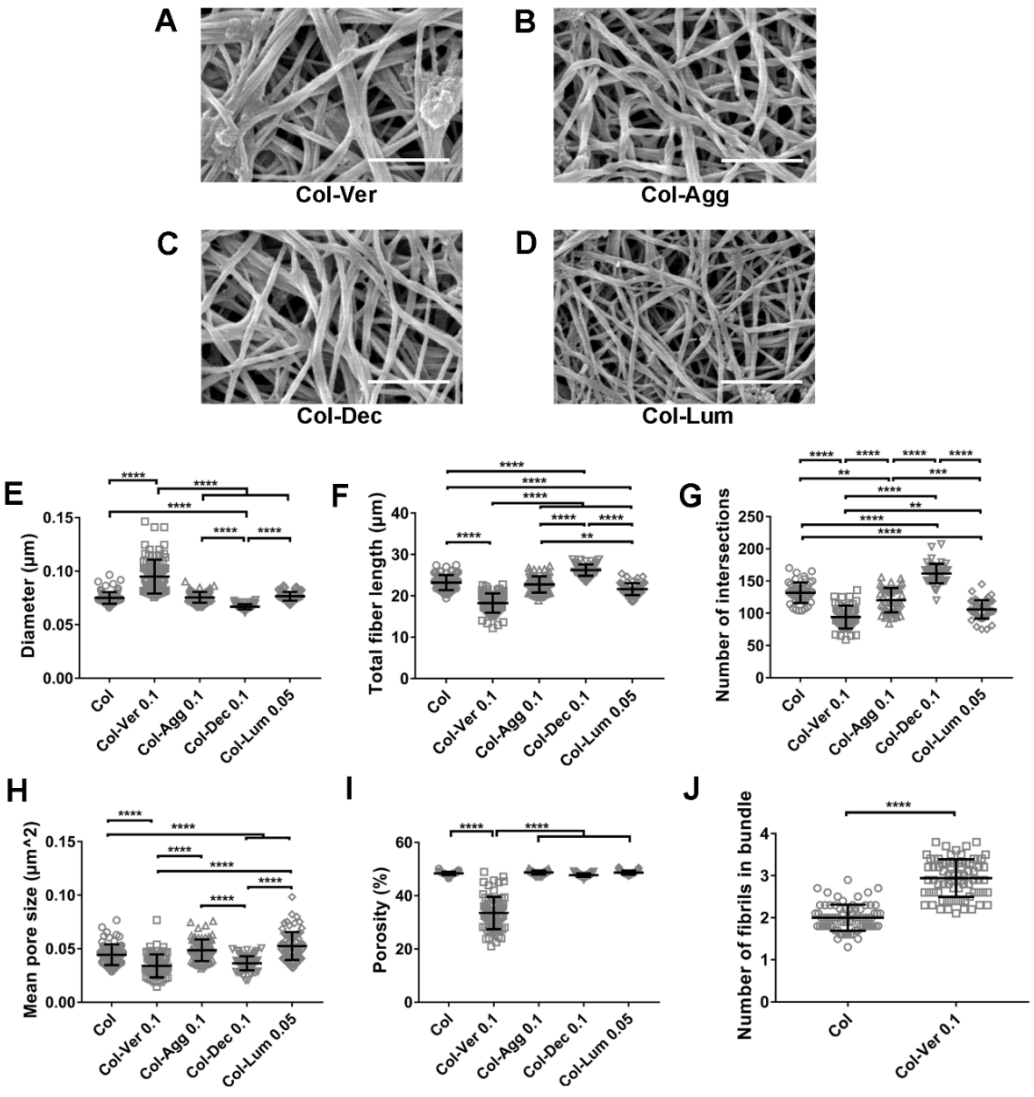

Figure 3.5 Matrix PGs have different effects on the structure of collagen networks. (A-D) Representative SEM images of telo-collagen matrices manipulated with different PGs. Telo-collagen (Col; 1.5 mg/mL) with 0.1 mg/mL versican (Ver) (A); 0.1 mg/mL aggrecan (Agg) (B); 0.05 mg/mL lumican (Lum) (C) and 0.1 mg/mlL decorin (Dec) (D). (E-I) Fiber diameter (µm), total fiber length (µm), number of intersections, mean pore size (µm^2) and porosity (%) were quantified using DiameterJ. (J) Numbers of fibrils in bundles were counted manually for each cropped figure. Three independent experiments were carried out and one gel was generated for each condition in

each experiment. 5 SEM images were taken for each gel at random locations. When analyzed using DiameterJ, 5 sections were cropped from each SEM image and a measurement was taken on each cropped figure. Each data point represents a single measurement. Scale bar = 1 μm. Data represent mean ± SD. **P<0.01, ***P<0.001 and ****P<0.0001.

3.4 DISCUSSION

Matrix PGs are important regulators of collagen fibrillogenesis and regulate the organization of collagen fibrous networks. I report here that different matrix PGs, regardless of their structural similarity, demonstrate distinct roles in modulating collagen gelation (fibrillogenesis) and alter fibrous network organization differently in vitro. Versican, a widely distributed hyalectan PG, has particularly specific effects on collagen behaviors in contrast to other matrix PGs, including the structurally similar hyalectan aggrecan.

The in vitro spectrophotometric (turbidity) assay has been used since the 1960s for studying the kinetics of collagen gelation (Wood and Keech 1960). The sigmoidal curves generated by recording the dynamic turbidity changes during the entire gelation process represent, in part, information about the kinetics of collagen fibrillogenesis. It can show the early nucleation (the lag phase) and lateral growth (the rapid growth phase) clearly. The weakness of this assay is that the absorbance readout only represents the molecular weight of aggregates (fibrils) and the different light scattering factors of these aggregates (fibrils) (Silver and Birk 1983), which does not provide details about the number and size of individual fibrils. This assay also only reports the properties of collagen gelation in vitro and cannot mimic the complex environment in vivo, including cell-mediated collagen expression and deposition. Thus, caution needs to be taken with any application of the conclusions from this assay to in vivo situations. This assay has also been used to investigate the role of matrix PGs, as important collagen binding proteins, in fibrillogenesis.

Previously published in vitro turbidity data has shown that decorin, lumican and biglycan (intact full length proteins as well as their core proteins) inhibit collagen gelation by decreasing the gelation rate and the fibril formation plateau (Rada, Cornuet, and Hassell 1993)(G. Zhang et al. 2009). Similarly, we observed here the same negative effect of decorin and lumican on collagen gelation using the turbidity assay, with the alterations in the kinetic curves for collagen/decorin gelation are more pronounced (much flatter with a lower plateau) than for collagen/lumican. One explanation for this difference between decorin and lumican is that the decorin core protein has 12 leucine rich repeats (LRRs) while lumican has 10 LRRs (Appunni et al. 2019). In this case, the similar horseshoe shaped structures of SLRPs turn out to have different geometries, especially the concave distance between N- and C-terminus. Importantly, the collagen binding sites on SLRPs are located on LRRs suggesting that different numbers of LRRs may have significant effects on modulating collagen lateral growth and organization during fibrillogenesis (Kalamajski and Oldberg 2009). There is also evidence indicating that decorin and lumican interact with collagen at different sites (Svensson, Närlid, and Oldberg 2000)(Hedbom and Heinegard 1993), which might lead to differential regulation of collagen fibril formation. Another reasonable explanation relates to the source of the SLRPs I used. The decorin, which has one GAG (CS or DS) side chain, was a native intact PG isolated from bovine cartilage, while lumican was the recombinant core protein, which lacks GAG side chains (there are 4 KS side chains on native lumican) (Appunni et al. 2019). As different GAGs have distinct effects on fibrillogenesis, the types, numbers and locations of GAG side chains may dramatically alter the role of SLRPs in regulating collagen fibrillogenesis.

In contrast to SLRPs, large hyalectan PGs including versican and aggrecan have not been well studied as regulators of collagen fibrillogenesis. Unlike aggrecan, which is more widely studied as an abundant structural and functional ECM protein in cartilage, the role of versican in regulating collagen behaviors has been neglected despite its universal distribution in various human tissues

and altered expression in collagen-related diseases. As assessed using the in vitro turbidity assay, versican has a particularly notable ability to upregulate the rate and plateau of collagen gelation, while aggrecan has a modest negative effect. My finding with aggrecan is consistent with previously reported in vitro turbidity results that aggrecan does not have a significant influence on gelation (Vynios et al. 2001). One explanation for the different effects of versican and aggrecan on regulating collagen gelation is that the binding sites – the versican G3 domain versus the aggrecan KS domain – interact with collagen differently. Another explanation is the distinct numbers and types of GAG side chains for versican and aggrecan. A typical intact aggrecan has over 100 GAG (both CS and KS) side chains and the physical repulsion caused by these highly negatively-charged GAGs may affect the lateral fibril growth by limiting fibril fusion and crosslinks between adjacent collagens. Versican, depending on its isoforms, has up to 23 GAG side chains (only CS), suggesting that the physical repulsion caused by its GAGs is significantly lower. Additionally, CS has been shown to have complicated and controversial effects on fibrillogenesis: some published literature (Öbrink 1973) has found that CS accelerates fibrillogenesis while others (Mathews and Decker 1968) have reported the opposite observation. Importantly, my data illustrate that CS slightly upregulates the rate of gelation in a dose-dependent manner, suggesting that minor changes in CS concentration can play its role which has also been shown previously by using a rheometer to study fibrillogenesis in vitro (Y. Yang et al. 2011). Other factors including the molecular weight and sulfation level of GAGs can also affect their regulation of collagen fibrillogenesis.

Given that different matrix PGs show distinct alterations during in vitro collagen gelation, I used SEM imaging of collagen matrices to compare the contribution of matrix PGs in altering collagen fibrous network organization. SEM provides detailed visualization into the fibrous network and helps to generate quantitative data, but a limitation of the technique is that the matrix is in a dehydrated state that may not represent the actual fiber morphology and pore size. The relative

structural features, however, are likely to persist. My SEM data indicate that versican and aggrecan, both large hyalectan PGs, regulate collagen networks differently. The results, showing that versican leads to the formation of a looser network with larger fiber bundles and smaller pores compared to a modest effect only for aggrecan on network connections, emphasize the unique role of versican amongst the PGs tested. Previously published work has shown that the presence of large cartilage PGs (mainly aggrecan) or small tendon PGs (mainly decorin) decreases fiber size using the in vitro turbidity assay (Vogel and Trotter 1987). Evidence addressing the influence of SLRPs on the structure of the collagen fibrous network is contradictory. Reese et al. have found that the inclusion of decorin into collagen gels (at 1:40 weight ratio) led to a denser network with thinner fibers (Reese, Underwood, and Weiss 2013). However, Raspanti et al. have reported that the addition of decorin to collagen (at 1:5 weight ratio) induced the fusion of collagen fibrils, resulting in fibrils with increased diameter (Raspanti et al. 2007). However, my data indicate that the presence of decorin in collagen matrices (1:15 weight ratio) results with a looser network with thinner fibers. Combining these data, there might be a dose-dependent regulation by decorin of the collagen network. For lumican, Rada et al. have shown that its inclusion into the collagen network in vitro decreases fibril diameter, as visualized by transmission electron microscopy (Rada, Cornuet, and Hassell 1993), and Chakravarti et al. have found that the size of fibrils in vivo in the corneal stroma is increased in lumican-deficient mice (Chakravarti et al. 2006). My data indicate that lumican leads to the formation of a loose network with no influence on fiber size. There are no published SEM data for comparison.

In sum, I observe distinct roles of matrix PGs, even within the same subfamilies, on regulation of collagen gelation (fibrillogenesis) and in modulating the organization of collagen fibrous networks. This suggests that the precisely-controlled deposition and the relative amounts of different PGs expressed in normal and diseased tissues, including in development and collagen-related disorders such as fibrosis and cancer metastasis, may have important impacts on collagen

behavior. Temporally and spatially dynamic collagen organization in native ECM is poorly understood but investigating the expression of different PGs quantitatively and comparing their distinct roles in fibrillogenesis might improve understanding of collagen fibrous network maturation and reorganization during development and collagen-related pathology. Given the evidence that versican has unique regulations in fibrillogenesis and collagen network organization compared to other matrix PGs, it is particularly important to investigate versican, which is a universally distributed large PG that is upregulated in disease, as a potential therapeutic target for collagen-related fibrotic disorders. I speculate that the progression of fibrogenesis could be potentially controlled and reversed by modulating versican expression, deposition and degradation so as to mediate collagen fibrillogenesis and organization.

CHAPTER 4 VERSICAN REGULATES CELL-MEDIATED COLLAGEN ORGANIZATION, ALIGNMENT AND CONTRACTION

This chapter is adapted from the publication: D. Chen, L.R. Smith, G. Khandekar, P. Patel, C.K. Yu, K. Zhang, C.S. Chen, L. Han, R.G. Wells, Distinct effects of different matrix proteoglycans on collagen fibrillogenesis and cell-mediated collagen reorganization, Sci. Rep. 10 (2020) 1–13. doi:10.1038/s41598-020-76107-0.

Parts of the collagen plug assay data involving versican are adapted from my master thesis, Effect of versican on collagen fibrous networks and long-range force transmission by contractile cells (2016).

G. Khandekar contributed to the engineered microtissue assay (focusing on lumican).

J. Llewellyn contributed to the isolation of portal fibroblasts.

4.1 INTRODUCTION

In native ECM, the collagen fibrous network is highly organized and dynamically mediated by not only ECM proteins, but also various types of cells (especially contractile cells) embedded in the network. There is a reciprocal interaction between contractile cells and collagen networks in the ECM. On the one hand, cells can sense structural and mechanical stimuli from the ECM and convert them into biochemical signals via mechano-transduction through various cell membrane receptors; these can further modulate cell behaviors such as adhesion, proliferation, migration and differentiation (Y. Chen et al. 2017). On the other hand, the organization of collagen fibrous networks can be regulated by forces generated by contractile cells that can stretch and align collagen fibers via focal adhesions (Abhilash et al. 2014). This cell-ECM reciprocal crosstalk is crucial for regulating cell function and tissue morphogenesis and is also important in maintaining normal development and homeostasis. To better understanding the role of versican in regulating

various collagen behaviors in native ECM, the impact of versican on cell behaviors needs to be investigated, including the impact of versican on cell-mediated regulations of collagen fibrillogenesis (deposition), organization and contraction.

Versican, a universally distributed large hyalectan, has an atypical effect on in vitro collagen fibrillogenesis (shown to upregulate fibrillogenesis, as studied by an in vitro turbidity assay) and on the organization of collagen network (as visualized by SEM). However, the role of versican in cell-mediated collagen deposition and organization is still unclear. In native tissues, fibroblasts are the most common cell type participating in the production of ECM components like collagen and PGs. Thus, a fibroblast-derived matrix (FDM) assay can be used as an in vitro model to study the effect of versican on fibroblast-mediated collagen deposition and organization. Abnormal organization of collagen fibrous networks (such as caused by collagen fiber realignment and compaction), accumulation of ECM proteins, and activation of fibroblasts into myofibroblasts have been observed for multiple ECM (collagen)-related disorders. Taken hepatic fibrosis as an example, the deposition of collagen (type I) increases up to 10-fold (Kershenobich Stalnikowitz and Weissbrod 2003) and the accumulation of versican is also upregulated about 4 fold (Bukong et al. 2016). Importantly, one typical tissue pattern observed during advanced hepatic fibrosis is bridging fibrosis, where highly compacted and aligned collagen regions develop between groups of activated fibroblasts, likely mediated via long range force transmission (Wang et al. 2015). The presence of cross-linked collagen networks and collagen fiber re-organization are thought to be required for this long distance mechanotransduction (Ma et al. 2013). Matrix PGs, as important collagen binding proteins, could play a key role in this cell-mediated collagen realignment. The collagen plug assay, in which fibroblast spheroids are seeded on collagen gels, is a reasonable in vitro model of bridging fibrosis that has been used to study collagen re-organization via long range force transmission. This is particularly important for understanding the role of versican, as a unique regulator (among those tested) in fibrillogenesis, in regulating fiber rearrangement and

condensation during fibrogenesis. Higher level tissue contraction, which is regulated by collagen organization and cellular contractility, is a crucial function of native tissue during morphogenesis and wound healing (wound closure) (Desmoulière, Chaponnier, and Gabbiani 2005). Given that matrix PGs are important collagen regulators, they can modulate tissue contraction via rearranging collagen fibers. Microfabricated tissue gauges (also known as engineered microtissues), a recently developed technique to investigate biochemical, mechanical and other cues that mediate microtissue formation, can be used to compare the effects of different matrix PGs on microtissue contraction.

In this chapter, I report an investigation into the effects of versican (and other matrix PGs) on multiple cell-mediated collagen network behaviors. FDMs are used to mimic in vivo collagen deposition and to study the role of versican and its V3 isoform in cell-mediated collagen synthesis, deposition and arrangement. Due to the different interactions between PGs and collagen (Chapter 2, 3), I also compare the distinct effects of various PGs on mediating collagen realignment via long-range force transmission and on higher level tissue contraction.

4.2 METHODS

4.2.1 Reagents, antibodies, and cells

Rat tail type I collagen (with intact telopeptide regions) was from Corning (Corning, NY, USA). Versican was isolated from bovine liver. Aggrecan isolated from bovine cartilage was a gift of Lin Han (Drexel University) (Lee et al. 2013) and also purchased from Sigma (A1960). Decorin (D8428) was from Sigma (St. Louis, MO, USA) and human recombinant lumican and the versican V3 isoform protein were from R&D Systems (Minneapolis, MN, USA). Gelatin from porcine skin and ethanolamine were purchased from Sigma. Glutaraldehyde soludion (50%) was purchased from Fisher Scientific (Hampton, NH, USA). Dulbecco's phosphate buffered saline with calcium

chloride and magnesium chloride (DPBS+ (10×)) and Dulbecco's phosphate buffered saline without calcium chloride and magnesium chloride (DBPS- (1×)) were purchased from Life Technologies (Carlsbad, CA, USA). Vitronectin (recombinant human protein) was purchased from Fisher Scientific. Sylgard 184 polydimethylsiloxane (PDMS) and its curing agent were from Dow Corning (Midland, MI, USA). Trichloro silane, isopropanol, pluronic F127 and Medium 199 were purchased from Sigma; sodium bicarbonate from Corning; and CellPURE™ HEPES from Fisher Scientific. 40% acrylamide and 2% bisacrylamide stock solutions were purchased from Bio-Rad (Bio-Rad Laboratories, Hercules, CA, USA). Tetramethylethylene diamine (TEMED), ammonium persulfate (APS) and 0.2 μm fluorescent beads in solution were from Fisher Scientific. Coverslip activation reagents were aminopropyltrimethoxysilane (Sigma) and glutaraldehyde (Sigma). PAA gel surface activation reagents were ethyl(dimethylaminopropyl) carbodiimide (EDC) and N-hydroxysuccinimide (NHS) solution (Fisher Scientific). Collagenase from Clostridium histolyticum was purchased from Sigma. VECTASHIELD PLUS antifade mounting medium with 4′,6-diamidino-2-phenylindole (DAPI) was from Vector Laboratories (Burlingame, CA, USA).

Anti α-smooth muscle actin antibody (A2547) was from Sigma. Anti-fibronectin antibody (ab2413) was from Abcam. Cy™3 AffiniPure Donkey Anti-Mouse IgG (H+L) (715-165-151) and Cy™3 AffiniPure Donkey Anti-Rabbit IgG (H+L) (711-165-152) were from Jackson ImmunoResearch (West Grove, PA, USA).

NIH 3T3 fibroblasts (CRL-1658) were obtained from the ATCC (Manassas, VA, USA) and portal fibroblasts were isolated from rat liver as described (Wen et al. 2012). Both types of fibroblasts were cultured in DMEM (Dulbecco's Modification of Eagle's Medium with 4.5 g/L glucose and L-glutamine without sodium pyruvate (Corning)) with 10% fetal bovine serum (Gemini Bio-Products, West Sacramento, CA, USA) supplemented with 1% penicillin/streptomycin (Corning) and 0.5%

fungizone (Life Technologies) at 37°C in a humidified atmosphere with 5% CO2/balance air. For FDMs, DMEM was supplemented with 10% calf serum (Fisher Scientific) instead of fetal bovine serum.

4.2.2 Fibroblast-derived matrices

FDMs were generated according to a published protocol (Franco-Barraza et al. 2016). MatTek glass-bottomed dishes were rinsed with DPBS+ and incubated with 0.2% (w/v) gelatin solution (diluted in DPBS+ at 37°C and sterilized through a 0.2 μm filter) for 1 h at 37°C. After rinsing with DPBS+, dishes were incubated with 1% (v/v) glutaraldehyde (diluted in DPBS+ and sterilized through a 0.2 μm filter) at RT for 30 min. After rinsing with DPBS+ 5 min for 3 times, dishes were then incubated with 1 M ethanolamine (diluted in diH_2O and sterilized through a 0.2 μm filter) at RT for 30 min. After rinsing 3 times with DPBS+, DMEM culture media with 10% calf serum, 1% penicillin/streptomycin and 0.5% fungizone was added for checking the pH. After aspirating media, 0.1 mg/mL versican, V3 or vitronectin (as a control) was used to coat glass-bottomed culture dishes by incubating overnight at 37°C. After aspirating the coating solution, semi-confluent 3T3 fibroblasts were trypsinized and seeded at 2.5×10^5 cells/mL. After overnight culture, media were replaced with media containing 100 μg/mL ascorbic acid; this was freshly changed every 48 h. At the third media refresh, additional versican, V3 or vitronectin was added. After 7 days of culture, FDMs were rinsed with DPBS-, fixed with 10% formalin and stored at 4°C. Second harmonic generation (SHG) imaging was used to visualize collagen fibril organization; the orientation of collagen fibrils was analyzed by ImageJ and its plugin OrientationJ. Each image was adjusted to its average intensity using Z-stack and two channels (SHG signal and autofluorescence from fibroblasts) were split using the Stack to Images option. The dominant angle of collagen fibrils was calculated by using the Orientation Dominant Direction option of OrientationJ and was used for angle normalization. The distribution of fibril orientation was quantified using the OrientationJ Distribution option: the σ of pixels in the Gaussian window was set to 3; Gaussian Gradient was

chosen for the provided options; the Min. Coherency and Energy was set to 0%; and the following options were selected: Orientation in the Hue section, Coherency in the Saturation section and Original-image in the Brightness section. After running the analysis, the list of orientations (in degrees) and the distribution of orientations were normalized to the dominant angle, and the normalized data was plotted using GraphPad and analyzed using two-way ANOVA.

4.2.3 Immunostaining

FDMs were stained with anti-fibronectin (1:100) and anti α-smooth muscle actin (α-SMA, 1:100) antibody at 4°C overnight and then stained with Cy3 anti-rabbit secondary antibody (1:600) after rinsing. FDM samples were mounted with coverslips, imaged with confocal microscopy, and quantified using ImageJ.

4.2.4 Sirius red staining

Sirius red was used to stain collagen in fixed FDM samples. Briefly, FDMs were rinsed with PBS for 5 min and incubated with Sirius red for 1 h at RT. After staining, FDMs were rinsed twice with acidified water (5 mL acetic acid in 1 L water) and were dehydrated 3 times with 100% ethanol. After dehydration, FDMs were cleared with xylene and mounted with coverslips. The area fraction, which is the area with Sirius red staining over total area, was analyzed for each image using ImageJ.

4.2.5 Collagen plug assay

Rat tail type I collagen was diluted to a final concentration of 1.5 mg/mL using 10× PBS, distilled water and 1 N NaOH (for adjusting pH to 7.4) as described before. Isolated versican, aggrecan or decorin were added to the collagen solution to a concentration of 0.1 mg/mL; lumican was added

to 0.01 and 0.05 mg/mL. The pH of the collagen solution was adjusted to 7.4 and incubated on ice for 1 h before it was pipetted into a microwell dish with a glass-bottomed cutout (14 mm Microwell, MatTek, Ashland, MA). The dish was sealed with parafilm and kept in an incubator (5% CO_2/balance air) overnight at 37°C. Cells were trypsinized and suspended in DMEM at 25,000 cells/mL (for NIH 3T3 cells) and 200,000 cells/mL (for portal fibroblasts). Fibroblast spheroids were formed by the hanging droplet method (Kelm et al. 2003). Briefly, 20 µL droplets of suspension cell solution were placed on the underside of a petri dish lid. To avoid drying, 10 mL DMEM were added to the dish. After inversion of the lid, the cell droplets were cultured for 5 days (for NIH 3T3 cells) or 3 days (for portal fibroblasts). Cells proliferated and accumulated at the free liquid-air interface and formed spheroids. At the time of seeding, 1 mL media was added on top of each collagen gel. Spheroids were captured by a 20 µL pipette and carefully placed on the gel in pairs approximately 500 µm apart with about 4 pairs per gel. This distance ensured long-range force transmission happened between contractile cells and was suitable for SHG imaging in the same microscope frame. The gel was incubated for 4 h for spheroid attachment and 2 mL DMEM media were added. After culturing for another 20 h, gels were rinsed with PBS and fixed with 10% formalin for 10 min, and the samples were sealed with parafilm and stored in PBS at 4°C. To test the plasticity of collagen realignment in both plain collagen and collagen/versican plugs, plugs with live 3T3 cells were first imaged with SHG and then treated with sodium azide for 5 min to induce cell death, and plugs with dead cells were imaged again using SHG. To quantify plasticity, the intensity and anisotropy visualized after cell death was normalized to the original intensity and anisotropy in the presence of live cells.

4.2.6 Second harmonic generation imaging

SHG imaging requires a multiphoton microscope and is based on the hyperpolarizabilities of non-centro-symmetric molecular assemblies (Williams, Zipfel, and Webb 2005). Collagen networks produce second-harmonic generation images with a fibril-like pattern (Suzuki et al. 2012). A Leica

SP5 spectral imaging confocal/dual-photon microscope (Leica Microsystems, Inc., Mannheim, Germany) was used to collect SHG signals from spheroid-seeded collagen gels. The coherent Chameleon Ultra II Ti:Sapphire laser (Coherent Inc., Santa Clara, CA) was tuned to 800 nm in wavelength, and images were captured on a non-descanned detector configured to wavelengths smaller than 495 nm. The parameters were set up as following: Trans = 34%, Gain = 85%, Offset = 47% and Smart Gain at 900 V. The lens (20×, 1.0 NA water immersion lens) was submerged in PBS during imaging. SHG images of collagen gels were collected at a Z-stack height of 20 μm (with 28 steps, 0.74 μm of each step) with a resolution of 1024×1024 at 200 Hz. The SHG image of the background of each gel was captured from an area without nearby spheroids. Image J was used to analyze the collagen alignment between two spheroids. The SHG images were adjusted by applying average intensity in the Z-stack. The region of interest was determined by using the polygon tool and the mean pixel intensity was measured. An ImageJ plug-in, FibrilTool (Boudaoud et al. 2014), was used to analyze the anisotropy of alignment in the bridged region between two spheroids and, as background, the anisotropy of matrices distant from spheroids. The distance between two spheroids was measured with a line tool.

4.2.7 Engineered microtissue assay

Engineered microtissue gauges were fabricated using a published protocol (Ramade et al. 2014). The mold was a gift from Dr. Chris Chen (Boston University). The molds (stamps) were rinsed with isopropanol and sonicated for 10 min. After air drying, the molds were coated with plasma using a plasma etcher. Then the molds were placed in a vacuum chamber and salinized overnight. PDMS was mixed and stirred with its curing agent at a ratio of 10:1 for 5 min and was degassed until no bubbles were present. Some PDMS was placed in 35 mm petri dishes to cover the bottom and cured at 65°C for 30 min. Other PDMS was pipetted on top of the stamps and degassed again. After degassing, the stamps were inverted and placed in the center of PDMS covered dishes. The remaining dish areas were filled with PDMS and cured at 65°C overnight.

Stamps were then removed and the resulting μTUG platforms were rinsed with ethanol and isopropanol. 1.5 mg/mL collagen solution was prepared as described in Table 4.1. Isolated versican, aggrecan or decorin was added to reach a final concentration of 0.1 mg/mL while lumican was used at 0.01 and 0.05 mg/mL. The pH was adjusted to 7.4 and the collagen solution was incubated on ice. The platforms were sterilized with UV light for 15 min, rinsed with 70% ethanol following with 0.2% pluronic F127 and then centrifuged at 500×g until there were no bubbles in the wells. After rinsing the platforms twice with PBS, 1 mL collagen/PG solution was added to each dish and degassed for 3 min. The platforms were then centrifuged at 700×g for 2 min and stored at 4°C to avoid gelation. NIH 3T3 fibroblasts were harvested from culture plates and 150,000 cells were mixed gently with 0.5 mL collagen solution, and then added to each platform. The platforms were centrifuged at 206×g for 2 min and were turned 90 degrees for centrifugation again. Extra solution was carefully aspirated, and the platforms were placed inverted into a centrifuge and spun at 37×g for 15-20 s. 1 mL PBS was added to the lid and the platforms were incubated at 37°C for 20 min until gelation. 1.5 mL culture media was added to each platform and the platforms were cultured at 37°C for roughly 24 h, until microtissues had formed. Images were taken using a light microscope (Leica DM IRM) before and after the removal of microtissues by pipetting and rinsing wells with PBS. Cantilever displacements were measured and used to determine the contraction of engineered microtissues.

Table 4.1 Components in collagen solutions for engineered microtissue assay

diH_2O	1067 μL
M199 (10×)	200 μL
HEPES (250 mM)	80 μL
$NaHCO_3$ (5% w/v)	14 μL
NaOH (1 M)	24 μL

Collagen (4.88 mg/mL)	615 µL

4.2.8 Traction force microscopy

Traction force microscopy (TFM) was used to study the effect of matrix PGs on cell contractility. The protocol was modified from previous publications (Yeung et al. 2005)(Chopra et al. 2011). Quartz slides were salinized in a vacuum chamber overnight and cleaned with kimwipes before using. Circular coverslips were activated by plasma for 30 s and incubated in 0.5% (v/v) APTES in diH_2O for 30 min on a shaker. After rinsing several times, they were incubated with 0.5% (v/v) glutaraldehyde in diH_2O for 1 h on a shaker and then air dried. 7.9 kPa polyacrylamide gels (Table 4.2) were made by mixing 40% acrylamide and 2% bisacrylamide with TEMED and 1% APS. This gel solution was mixed with 0.2 µm fluorescent beads in solution (diluted at 1:1000) and placed on quartz slides, and then covered with a 25 mm glass coverslip pre-activated with 0.5% aminopropyltrimethoxysilane and 0.5% glutaraldehyde. After polymerization for 30 min in a moisture environment, quartz slides (facing up) were warmed in the UVO chamber for 2 min. The gels were submerged in water, then gently taken off from the quartz slides. The gel surface was activated with EDC/NHS solution (17.5 mg/mL NHS and 10 mg/mL EDC in milliQ water) for 15 min and then coated with collagen (10 µg/mL, mixed with different matrix PGs (0.1mg/mL for versican and aggrecan, and 0.05mg/mL for lumican) and either cellular or plasma fibronectin (0.1mg/mL)). Fibroblasts were seeded at 20,000 cells per gel and incubated overnight. Live cell imaging was applied using EVOS AUTO2 (Thermo Invitrogen) and single cell images were taken before and after removing cells with 10% sodium dodecyl sulfate. The average traction force was calculated by measuring the displacement of fluorescent beads (ImageJ plugin available at https://sites.google.com/site/qingzongtseng/tfm) (Chopra et al. 2018).

Table 4.2 The protocol for making 7.9 kPa polyacrylamide gel

Stiffness (Pa)	40% acrylamide (μL)	2% bisacrylamide (μL)	10×PBS (μL)	diH2O (μL)	TEMED (μL)	1% APS (μL)	Total volume (μL)
7900	187.5	35	100	576.5	1	100	1000

4.2.9 Fibroblast proliferation in contractile collagen gels

To test the effect of matrix PGs on fibroblast proliferation, the same number of NIH 3T3 fibroblasts cultured in engineered microtissues were cultured in contractile collagen gels modified with different PGs and the cell proliferation under various PG conditions was investigated. Collagen solutions manipulated with PGs were prepared as previously described in the engineered microtissue assay. 3T3 fibroblasts were mixed with the gel solution, added to 48 well plate and incubated at 37°C for 20 min for gelation. Plain collagen gels and collagen/PG co-gels were gently detached from each well and cultured for 24 h. The contractile gels were then digested with 10 mg/mL collagenase for 15 min at 37°C and the cell numbers were counted and compared among all conditions.

4.2.10 Statistical analysis

All results were analyzed by GraphPad Prism 7 (San Diego, CA, USA) using unpaired t test, one-way or two-way ANOVA. P values were determined by Tukey's multiple comparison test, in which *$P<0.05$ was considered to be statistically significant.

4.3 RESULTS

4.3.1 Versican promotes the deposition of collagen-rich matrix from fibroblasts

I showed in previous chapters that versican binds collagen and regulates fibrillogenesis and fiber organization in vitro, but it is also important to further investigate the role of versican in cell-mediated collagen fibrillogenesis and deposition. I used the FDM assay, an in vitro model that results in collagen deposition and organization mimicking the composition and structure of native ECM, to study the effects of versican and the small V3 isoform on fibroblast-mediated ECM deposition. For coating, 0.1 mg/mL versican or V3 was added to glass-bottomed culture dishes and incubated overnight at 37°C. Vitronectin was used as a coating control because it had minimal impact on fibroblasts in comparison to bovine serum albumin. To avoid fibroblast activation, 3T3 cells were cultured with 10% calf serum and used at passage numbers less than 15. After seeding on the coated dishes, 3T3 fibroblasts were cultured for 7 days to generate FDMs. Sirius red staining for collagen showed that all FDMs were collagen-rich matrices with nicely formed fibrous networks (Figure 4.1A-C). There were subtle increases in collagen area fraction for cells on dishes coated with versican and V3, although there is no significant difference (Figure 4.1D). While Sirius red highlighted the area fraction with collagen, the images could not show individual fibrils and the fibrous network organization clearly.

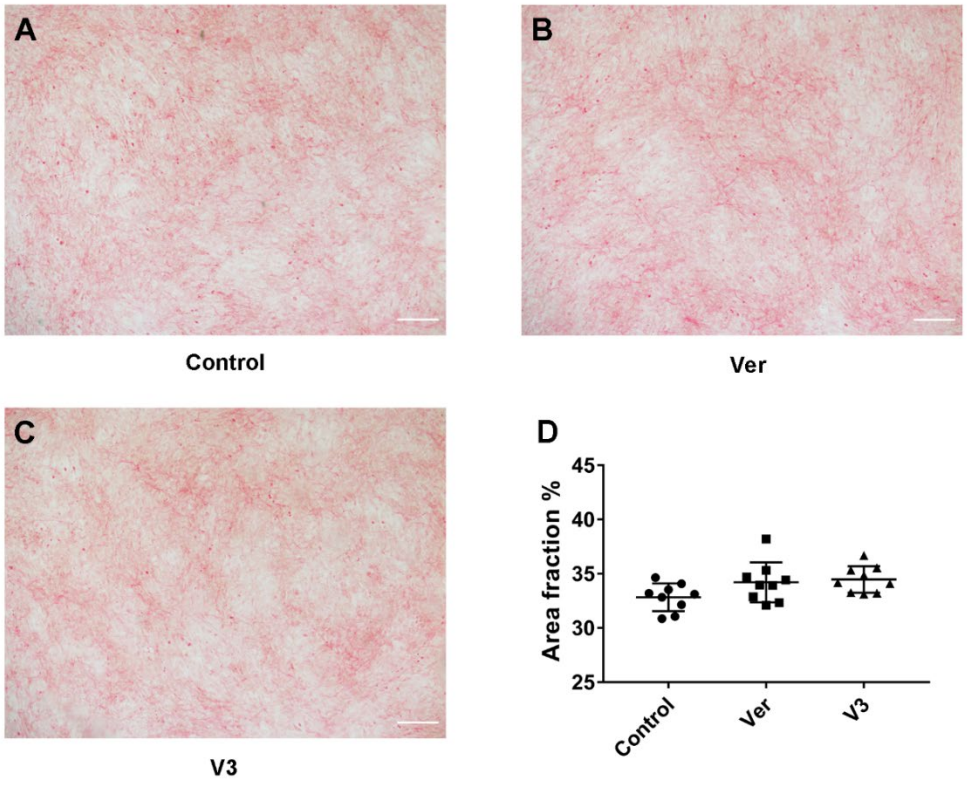

Figure 4.1 Sirius red staining illustrates collagen-rich matrices in FDMs. Only one representative FDM of each condition was stained with Sirius red because other samples were used for immunostaining purpose. (A-C) Representative Sirius red staining of FDMs: (A) vitronectin coating as a control, (B) versican coating, (C) V3 coating. (D) Area fraction with positive Sirius red staining was quantified using Image J. One FDM for each coating condition was stained and nine light microscopy images were taken. Scale bar = 100 μm. Data represent mean ± SD.

To better visualize the collagen fibrous network, SHG imaging was used. SHG detects collagen fibrils without staining as a result of its non-centro-symmetric organization (Suzuki et al. 2012). Using the multiphoton microscope, the intense excitation at 900 nm encounters the non-centro-

symmetric structural protein and induces a secondary harmonic generation signal at half the original wavelength. In this assay, SHG images showed a good resolution of collagen fibrils and the SHG signal intensity partially represented collagen content (the correlation between SHG intensity and collagen density is not linear, but can be used to identify differences between matrices). As shown in Figure 4.2A-C, fibroblasts cultured on differently-coated coverslips produced well-formed collagen fibrous networks with locally aligned fibers. Coating with versican or the V3 isoform significantly increased the SHG signal intensity (Figure 4.2D) suggesting the formation of collagen-rich matrices. Fibronectin, a cell-associated protein that interacts with collagen, was also expressed in FDMs, mainly surrounding fibroblasts (Figure 4.2E-G). The presence of versican and V3 isoform slightly increased fibronectin deposition (Figure 4.2H).

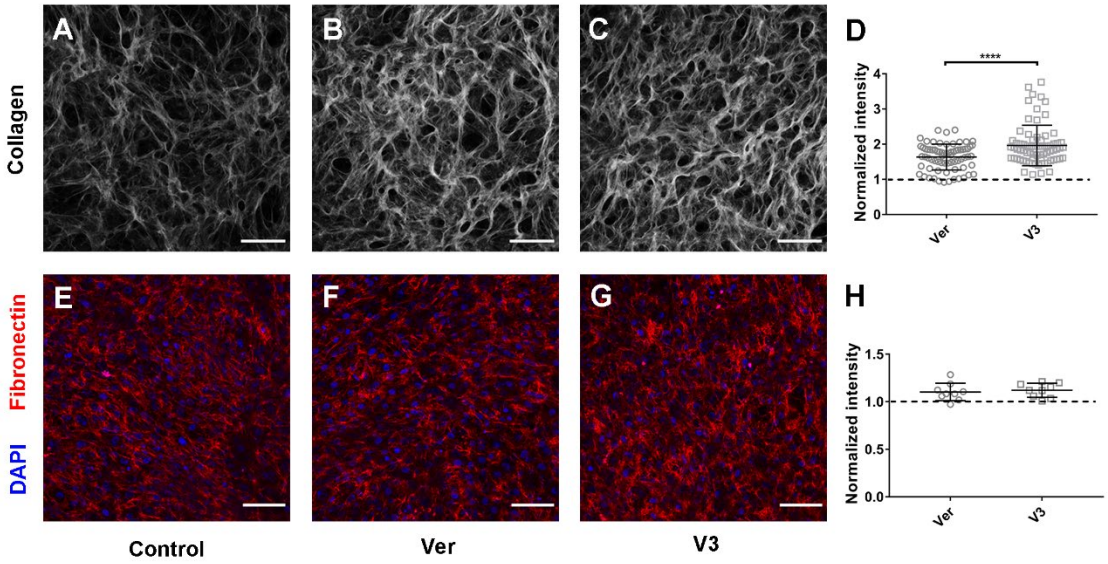

Figure 4.2 Versican and V3 isoform upregulate the formation of collagen rich matrices produced by fibroblasts. (A-C) Representative SHG imaging of FDMs: (A) vitronectin coating as a control, (B) versican coating, (C) V3 coating. (D) Quantification of the intensity of SHG signal. The data from each individual experiment were normalized to its control group (dashed line). (E-G)

Representative confocal imaging of fibronectin staining (red - fibronectin, blue - DAPI): (E) vitronectin coating as a control, (F) versican coating, (G) V3 coating. (H) Quantification of the intensity of fibronectin staining. The data from each individual experiment were normalized to its control group (dashed line). Four independent experiments were carried out with two technical repeats for each coating condition in each experiment. Scale bar = 100 μm. Data represent mean ± SD, *P<0.05 and ****P<0.0001.

To improve the accuracy of the FDM assay, I included additional steps to standardize the fibroblasts in a quiescent state. One step was to use calf serum instead of fetal bovine serum when culturing fibroblasts. Another step was to use fibroblasts that were not passaged more than 15 times. To assess the activation state, I stained FDMs with anti-α-smooth muscle actin (α-SMA) antibody, which is highly expressed in activated fibroblasts (myofibroblasts). As shown in Figure 4.3A-F, α-SMA staining was minimally positive in these fibroblasts and the stretched filament-like structures were rarely observed. The intensity of α-SMA staining was similar for all conditions (Figure 4.3G). Additionally, to control for the possibility that the increased SHG signal for the versican or V3 isoform coating condition (Figure 4.2A-D) might be due to altered cell proliferation, I also counted the cell number and found that the presence of versican or V3 isoform had no impact on fibroblast proliferation (Figure 4.3H).

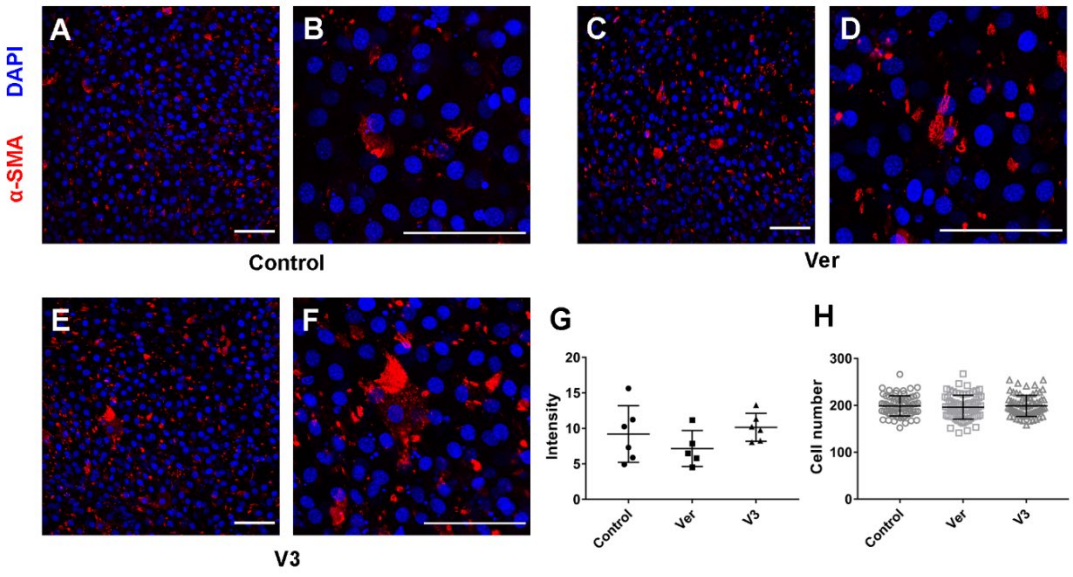

Figure 4.3 The presence of versican or V3 isoform in addition to collagen had no impact on fibroblast quiescence or proliferation. (A-F) Representative confocal imaging of α-SMA staining: (A, B) vitronectin coating as a control, (C, D) versican coating, (E, F) V3 coating. (G) Quantification of the intensity of α-SMA staining. (H) Quantification of cell number for each condition, from four independent experiments. One FDM for each condition was stained for α-SMA in each experiment. Scale bar = 100 μm. Data represent mean ± SD.

4.3.2 Versican improves fiber alignment in collagenous matrices deposited by fibroblasts

To analyze the fiber orientation in FDMs, OrientationJ, an ImageJ plugin, was used to analyze SHG images. Collagen fibers oriented at different angles were labeled with gradient colors (Figure 4.4A-C). To plot and compare the distribution of fiber orientation (angles), the number of fibers oriented at a certain angle was normalized to the dominant angle of each SHG image; after normalization, the dominant angle was set at 0° for all analyzed image. As shown in Figure 4.4D,

collagen fibers were highly aligned in the versican or V3 addition conditions compared to the control group (statistical significance was analyzed using two-way ANOVA and is shown in Table 4.3).

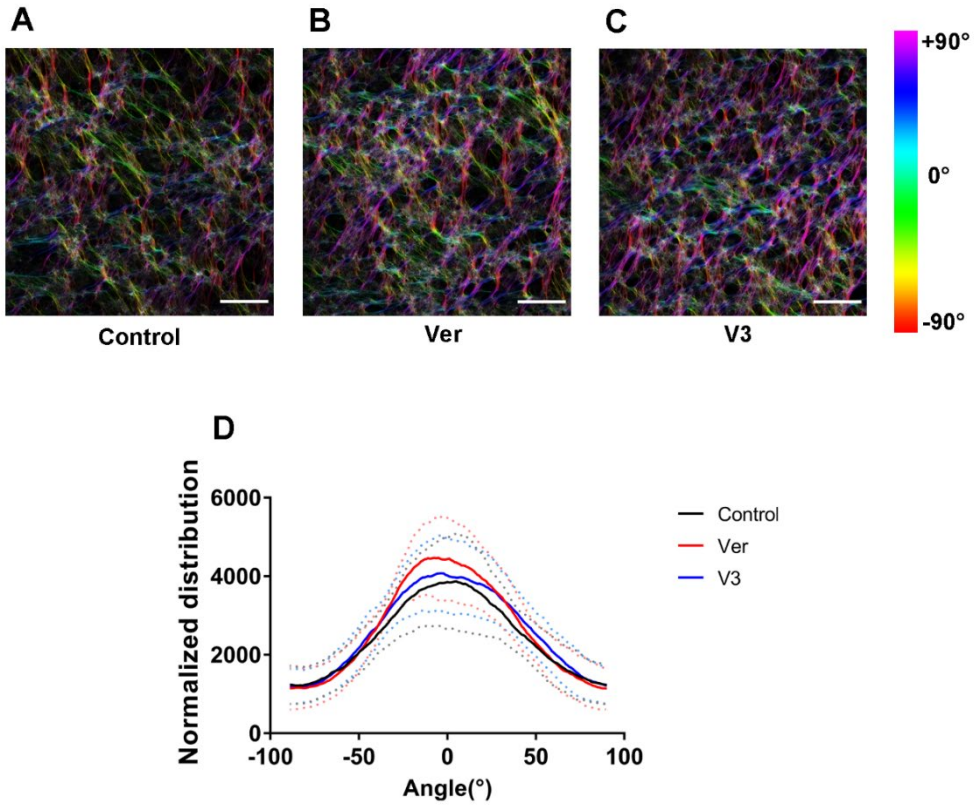

Figure 4.4 Versican and V3 promote the deposition of highly aligned collagen fibers in FDMs. (A-C) Representative SHG images (the same as in Figure 4.2A-C) analyzed by OrientationJ: (A) vitronectin coating as a control, (B) versican coating, (C) V3 coating. (D) The distribution of fiber orientation was quantified by OrientationJ and normalized to the dominant angle of each SHG image, which was then set to 0°. Four independent experiments were carried out with two technical repeats for each coating condition in each experiment. Scale bar = 100 μm. Data represent mean ± SD, *P<0.05, **P<0.01, ***P<0.001 and ****P<0.0001.

Table 4.3 Statistical significance of differences in fibril orientation between conditions. Data from Figure 4.4D were analyzed using two-way ANOVA.

Data #1	Data #2	Angle range	Significance
Control	Ver	-40° to -30°	**
Control	Ver	-30° to -20°	****
Control	Ver	-20° to -10°	****
Control	Ver	-10° to 0°	****
Control	Ver	0° to 10°	****
Control	Ver	10° to 20°	***
Control	Ver	20° to 30°	***
Control	Ver	30° to 40°	**
Control	V3	-40° to -30°	*
Control	V3	-30° to -20°	*
Control	V3	-20° to -10°	*
Control	V3	20° to 30°	**
Control	V3	30° to 40°	**
Control	V3	40° to 50°	**
Control	V3	50° to 60°	*
Ver	V3	-30° to -20°	*
Ver	V3	-20° to -10°	***
Ver	V3	-10° to 0°	***
Ver	V3	0° to 10°	**

4.3.3 Versican, unlike other matrix PGs tested, increases collagen compaction mediated by fibroblast spheroids

To evaluate the effect of matrix PGs as modulators of cell-mediated collagen re-organization and long-range cell-cell communication, the collagen plug assay (a pseudo-3D model) was used. In this assay, pairs of fibroblast spheroids were seeded atop collagen gels and collagen condensation and alignment between pairs were imaged and analyzed using SHG imaging. For quantitative analysis, I calculated the SHG intensity and anisotropy using ImageJ and its plugin FibrilTool. Anisotropy (normally a number from 0 to 0.2) reflects the alignment of fibrils: a higher anisotropy number indicates an increase in parallel aligned fibrils, while 0 means randomly distributed fibrils.

To compare the large hyalectan PGs, I mixed isolated versican or aggrecan with collagen and allowed gelation to occur, then placed 3T3 fibroblast-generated spheroids atop gels and imaged the collagen fibers after 24 h of culture, a sufficient time to enable cell-mediated collagen rearrangements to occur. The collagen fibrils visualized by SHG in the controls were highly compacted and aligned in the regions between pairs of spheroids (Figure 4.5A-C). The addition of versican increased cell-mediated collagen condensation while aggrecan had no significant effect on collagen compaction (Figure 4.5A-D). This was constant with the data shown in the in vitro turbidity assay suggesting that versican and aggrecan had distinct effects on collagen fibrillogenesis. Interestingly, cell-mediated compaction of collagen in the collagen-versican mixture was highly sensitive to pH at values ranging from 7.20 to 7.40 (Figure 4.5G). Cell-mediated compaction in a plain collagen plug, however, was not sensitive to pH in a similar range (Figure 4.5F). There was no significant difference in anisotropy between any of the conditions, indicating that fibers in all conditions were equally parallel in the aligned area (Figure 4.5E).

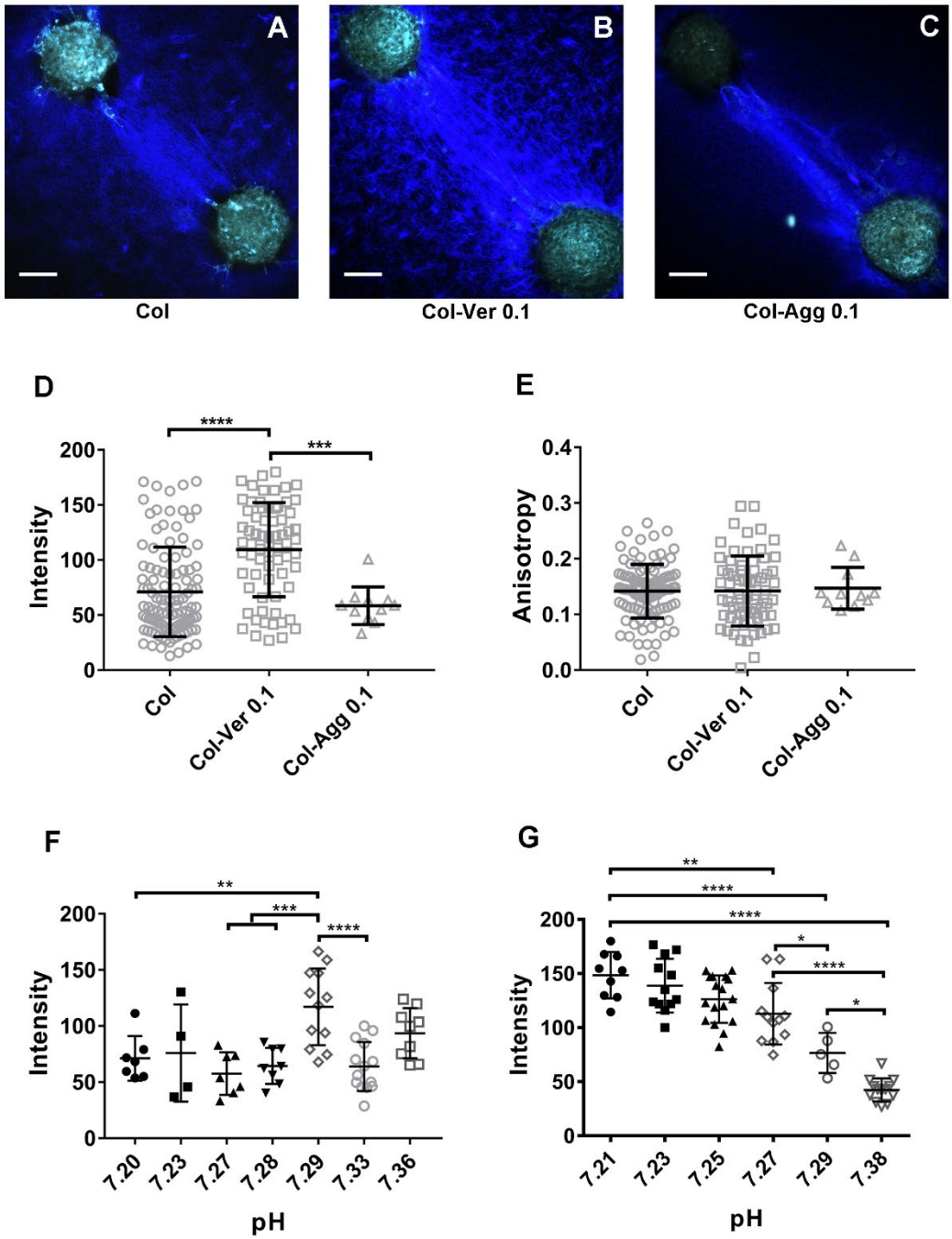

Figure 4.5 Large PGs have differential effects on cell-mediated collagen reorganization. (A-C) Representative SHG images of aligned collagen fibrils between pairs of NIH 3T3 spheroids. Blue represents the SHG signal from collagen; green is cell autofluorescence. (A) Plain collagen (Col;

1.5 mg/mL), (B) collagen-versican (Ver; 0.1 mg/mL) and (C) collagen-aggrecan (Agg; 0.1 mg/mL) plugs. (D & E) Quantification of intensity and anisotropy in the aligned collagen area for A-C. (F, G) Collagen compaction in plain collagen plugs (F) was not pH sensitive, but the impact of versican on collagen compaction was highly pH-dependent (G). Each data point in D-G represents collagen compaction between one pair of spheroids. At least 3 independent experiments were carried out for each condition, with at least 3 pairs of plugs examined for each experiment. For the pH testing in F and G, 4-12 pairs of spheroids were analyzed for each pH condition. Spheroids were seeded approximately 500 μm apart. Scale bars = 100 μm. Data represent mean ± SD. *P<0.05, **P<0.01, ***P<0.001 and ****P<0.0001.

I also used portal fibroblast-containing spheroids to assess the impact of SLRPs including decorin and lumican on cell-mediated collagen remodeling. These two SLRPs were shown to be negative regulators of collagen fibrillogenesis in the in vitro turbidity assay. Here I observed a consistent pattern. There was a significant decrease in collagen condensation with the addition of either SLRP (Figure 4.6A-E), although lumican did not show the dose-dependent effect that I observed from the in vitro turbidity assay (potentially because intensity was already low using these cells). Interestingly, the presence of decorin decreased the anisotropy significantly, although anisotropy was similar under all other conditions (Figure 4.6F).

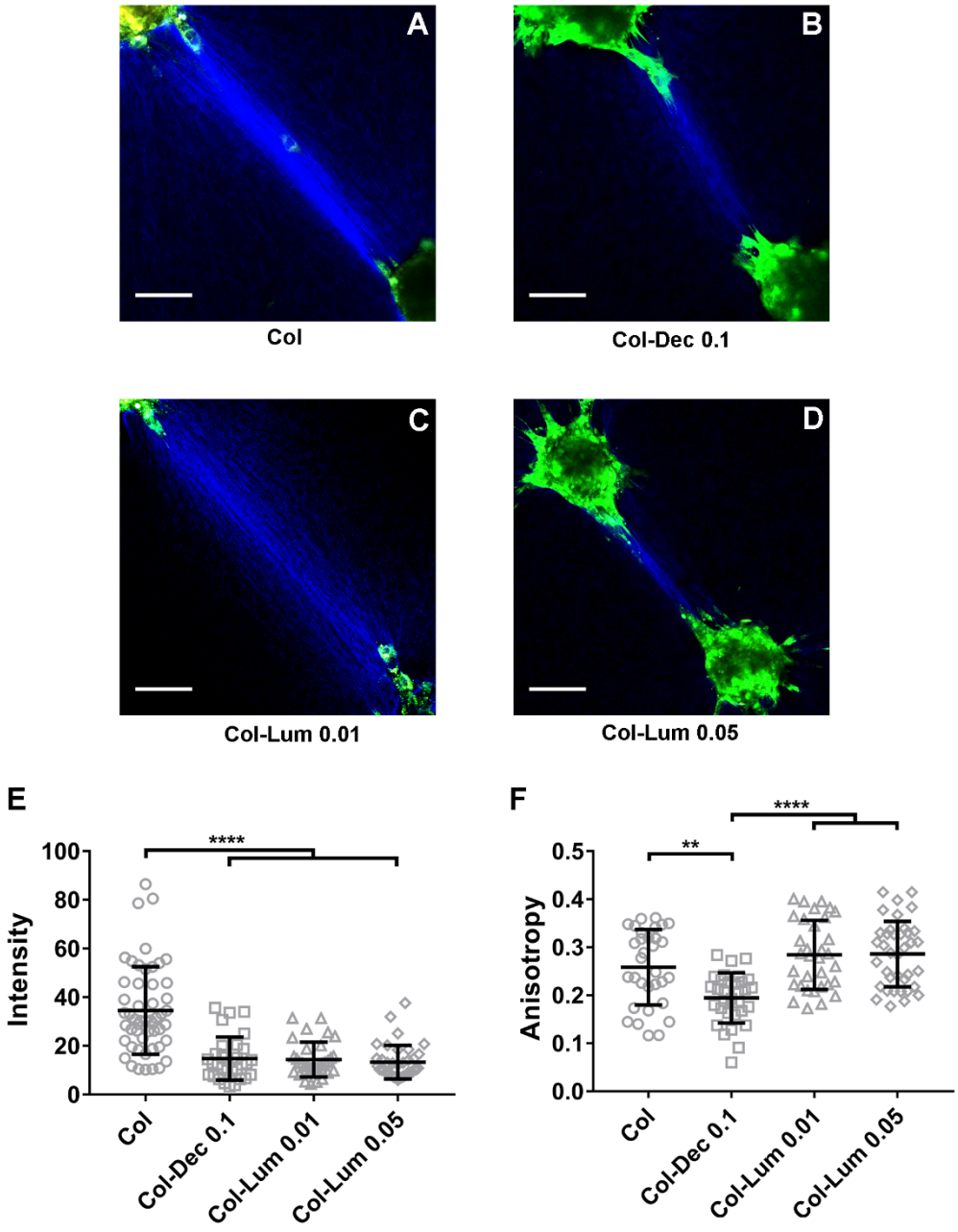

Figure 4.6 SLRPs regulate cell-mediated collagen reorganization differently. (A-D) Representative SHG images of collagen fibrils between portal fibroblast spheroids on (A) plain collagen (1.5 mg/mL), (B) collagen-decorin (Dec; 0.1 mg/mL) and (C, D) collagen-lumican (Lum, 0.01 or 0.05 mg/mL) plugs. (E, F) Quantification of intensity and anisotropy in the aligned

collagen area for A-D. Each data point in E and F represents collagen compaction between one pair of spheroids. At least 3 independent experiments were carried out for each condition, with at least 3 pairs of plugs in each experiment. Spheroids are seeded approximately 500 μm apart. Scale bar = 100 μm. Data represent mean ± SD, **P<0.01 and ****P<0.0001.

4.3.4 Versican has no alteration on the plasticity of cell-mediated collagen reorganization

To address the role of versican in the plasticity of cell-mediated collagen alignment (effectively, irreversible collagen reorganization), I used the collagen plug assay and imaged aligned areas using SHG before and after cell death. I compared the SHG signal intensity of plain collagen and collagen/versican co-gels. The normalized intensity and anisotropy (such that data after cell death were normalized to data before death) were approximately 1, which indicated that the intensity and anisotropy did not change after removing the contractile forces generated by fibroblasts (Figure 4.7A, B). It supported the conclusion that cell-mediated collagen alignment was a plastic (permanent) deformation. The addition of versican did not alter the plasticity of collagen reorganization.

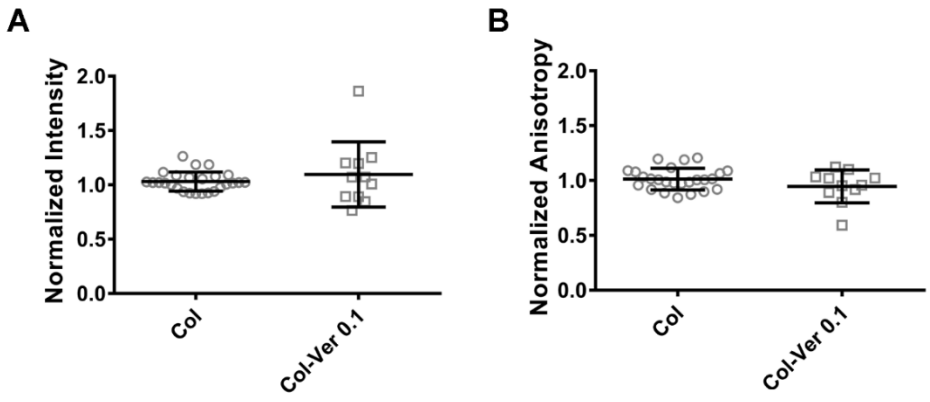

Figure 4.7 Cell-mediated collagen re-organization is plastic in both plain collagen and collagen-versican plugs. The intensity (A) and anisotropy (B) were quantified by ImageJ and FibrilTool. Data generated after cell death were normalized to data generated when cells were alive. Three independent experiments were carried out for each condition with 26 technical repeats for Col and 11 technical repeats for Col-Ver 0.1 in total. Data represent mean ± SD.

4.3.5 Matrix PGs have no impact on fibroblast contractility

As part of long-range force transmission, cells can generate forces that rearrange collage fibers. This is mediated by cell contractility. To rule out changes in cell contractility on different collagen/PG matrices as an explanation for the observed differences in collagen compaction, traction force microscopy (TFM) was used to measure 2D contractility directly. Polyacrylamide gels embedded with fluorescent beads were coated with collagen/matrix PG mixtures and 3T3 fibroblasts were cultured overnight; these contracted the gel, leading to bead displacement. The calculated average traction from bead displacement reflected the contractility. I also coated PAA gels with two types of fibronectins, cellular and plasma fibronectin, as positive controls. As shown

in Figure 4.8, both types of fibronectin increased fibroblast contractility (and cellular fibronectin showed a significant increase on contractility compared to plasma fibronectin). I also found that matrix PGs, regardless of the different subfamilies, had no effect on fibroblast contractility in 2D (Figure 4.8). This suggested that the role of PGs in regulating cell-mediated collagen organization is mainly due to interactions with collagen and alteration on the structure of the fibrous network.

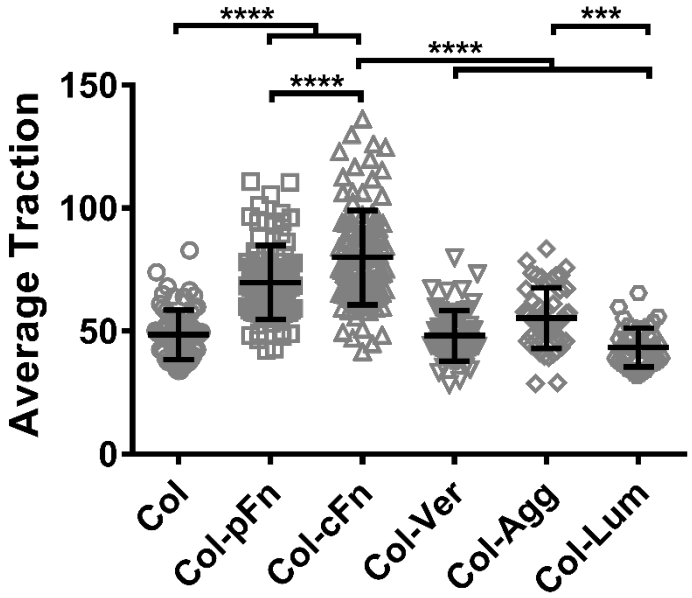

Figure 4.8 Matrix PGs have no impact on fibroblast contractility. 7.9 kPa polyacrylamide gels were coated with 0.1 mg/mL collagen (Col) mixed with plasma fibronectin (pFn), cellular fibronectin (cFn), versican (Ver), aggrecan (Agg) or lumican (Lum) at 0.1 mg/mL. The inclusion of PGs did not alter cellular contractility. In contrast, there was a significant increase with both variants of fibronectin, which were included for comparison. Three independent experiments were carried out for Col-Agg and four independent experiments were carried out for all other conditions. Each point represents a single cell and N=72 for Col, N=93 for Col-pFn, N=111 for Col-cFn, N=62 for Col-Ver, N=52 for Col-Agg and N=44 for Col-Lum. Data represent mean ± SD. **P<0.01 and ****P<0.0001.

4.3.6 Versican, unlike other matrix PGs, increases fibroblast contractility in engineered microtissues

At a higher level, tissue contraction can occur as a result of cell-mediated reorganization of the collagen fibrous network. The TFM assay only evaluated the cellular level contractility in 2D while here I used engineered microtissue gauges, which enable study of both ECM (collagenous matrices) contraction and cell contractility, to determine the role of versican and other matrix PGs in higher level 3D tissue contraction. Engineered microtissues were generated by gelling collagen/fibroblast mixtures in PDMS microwells with pairs of PDMS cantilevers; cell contractility and ECM re-organization resulted in the displacement of the cantilevers. Representative light microscopic images of microtissues (plain collagen with 3T3 fibroblasts) showed the displacement of the cantilevers in the presence and absence of microtissues (Figure 4.9A, B). SHG imaging showed that the collagen fibrils in engineered microtissues were well organized and highly aligned (Figure 4.9C). Quantification of the cantilever displacement from a large number of engineered microtissues with and without PG addition showed that the addition of versican significantly increased microtissue contraction while the addition of aggrecan had no effect (Figure 4.9D, E). For the SLRPs, the addition of decorin (0.1 mg/mL) decreased the contraction compared to plain collagen (Figure 4.9E), while the presence of lumican showed a dose-dependent effect: 0.05 mg/mL lumican addition led to a decrease in the contraction while the addition of lumican at a lower concentration (0.01 mg/mL) had no effect (Figure 4.9E). Because tissue contraction is correlated with the number of cells embedded and cell contractility, I quantified fibroblast proliferation in contractile collagen gels to rule out the effects of PGs on cell proliferation. I counted the cell number in contractile collagen gels manipulated with different PGs after 24 h of culture. The addition of different PGs did not alter fibroblast proliferation in contractile collagen gels (Figure 4.9F). In addition, it was shown previously that matrix PGs had no impact on fibroblast contractility in 2D as assessed by TFM (Figure 4.8). Thus, the distinct regulations of

matrix PGs on microtissue contraction appeared mainly due to their different interactions with collagen and diverse effects on collagen network organization.

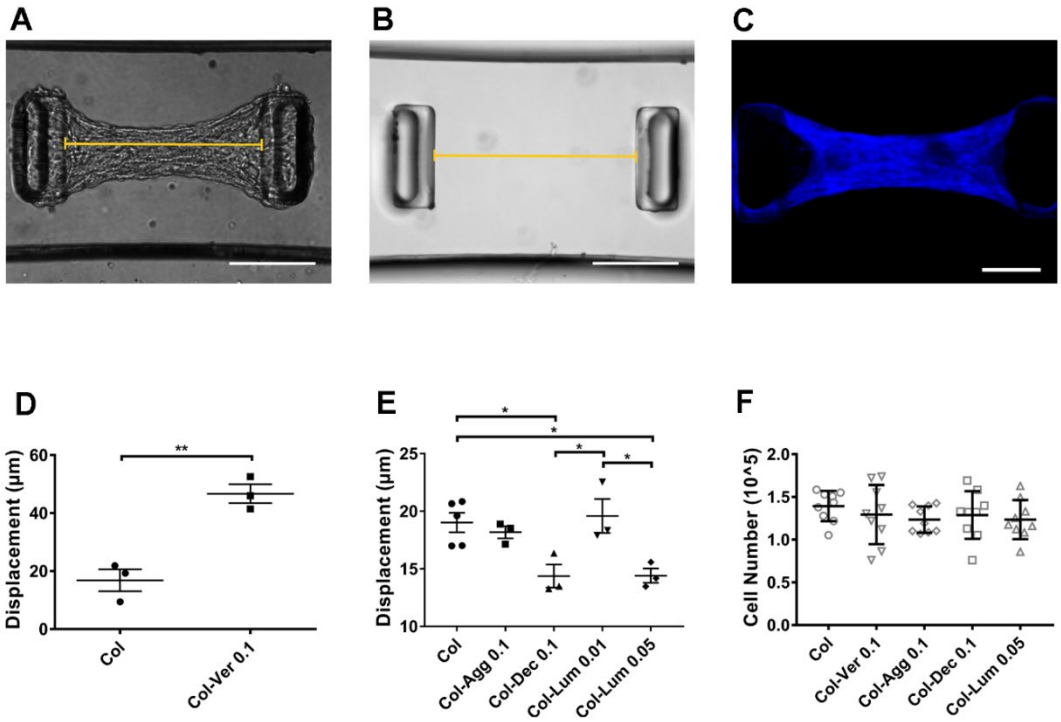

Figure 4.9 Matrix PGs have different effects on the contraction of engineered collagenous microtissues. (A, B) Representative light microscopic images of PDMS cantilever displacement in engineered microtissues. (C) SHG imaging of a representative engineered microtissue formed by NIH 3T3 fibroblasts cultured in plain collagen. (D) Quantification of increased displacement observed with inclusion of 0.1 mg/mL versican (Ver) in 1.5 mg/mL collagen (Col) microtissue. (E) Quantification of the displacement observed in collagen microtissues with or without aggrecan (Agg; 0.1 mg/mL), decorin (Dec; 0.1 mg/mL), or lumican (Lum; 0.01 mg/mL or 0.05 mg/mL). N>30 microtissues per each platform, at least three independent experiments (platforms) per condition. Points represent mean per platform. Scale bar = 200 μm. Data represent mean ± SD. *P<0.05

and **P<0.01. (F) The number of fibroblasts counted in contractile collagen gels manipulated with PGs after 24 h of culture. Three independent experiments were carried out for each condition and three technical repeats for each experiment. Data represent mean ± SD.

4.4 DISCUSSION

Versican and other matrix PGs, as collagen-binding proteins and key regulators of collagen fibrillogenesis and organization, have distinct impacts on modulating cell-related collagen behaviors. The combination of FDM, collagen plugs and engineered microtissue assays illustrates the importance of matrix PGs in mediating multiple cell-mediated collagen behaviors. It also highlights again the unusual role of versican amongst the PGs in modulating cell-mediated collagen behaviors, particularly in contrast to similar large PG aggrecan. SLRPs, another matrix PG subfamily as discussed in previous chapters, consistently show effects on cell-mediated collagen behaviors that are in contrast to versican.

I showed in Chapter 3 that versican upregulates collagen gelation (fibrillogenesis) and promotes the formation of a looser network with thicker fibers. It is thus key to assess the potential effect of versican on collagen deposition in native ECM where cells dynamically synthesize and organize collagen fibers. By analyzing the SHG images of FDMs, the presence of versican or V3 isoform has been found to upregulate the production of collagen-rich matrices and improve fiber alignment locally, which is consistent with the turbidity data showing that versican increases the rate and plateau of in vitro collagen fibrillogenesis. Additionally, these observations further support the previously described IEM data showing that versican could play a key role in mediating fibrillogenesis in vivo. Because of the formation of collagen-rich matrices with aligned fibers, versican accumulation and versican/collagen interactions can play important roles in fibrotic disorders (Taufalele et al. 2019). For example, versican expression and its cleavage via

ADAMTS are upregulated during liver fibrosis and downregulated during recovery (Bukong et al. 2016). Additionally, aligned collagen fibers can direct the invasion of carcinoma cells (Ray et al. 2018)(Han et al. 2016), which indicates that a potential mechanism of metastasis is upregulated by versican (due to the reorganization and alignment of collagen networks I observed). The validity of my findings regarding the role of versican in FDM deposition, however, would be improved by using versican-knockout fibroblasts in future experiments.

Cell-ECM reciprocal crosstalk, particularly cell-mediated collagen reorganization and long-range cell-cell mechanosensing, has been investigated here using the collagen plug assay. This assay is of particular interest because it may serve as a model of in vivo pathology such as bridging fibrosis, which is typical of advanced hepatic fibrosis (Herrera, Henke, and Bitterman 2018). Versican, but not the structurally similar large hyalectan PG aggrecan, increases collagen compaction in the fibroblast-generated bridging area. Interestingly, the pH-dependent effects observed for collagen/versican plugs suggest that the highly negatively-charged GAGs and charged residues on versican/collagen binding sites may play a significant role in reorganizing the collagen network. In this case, although versican and the V3 isoform (which lacks the GAG binding domain) interact with collagen similarly. They may regulate the organization of fibrous network differently due to the physical repulsion caused by negative charges. For SLRPs, decorin and lumican both decrease collagen condensation in the aligned area which aligns well with previously described results from the turbidity assay that SLRPs are negative regulators of fibrillogenesis. Importantly, the TFM data indicating that matrix PGs do not affect fibroblast contractility strongly support that the different observations from the collagen compaction and alignment mediated by fibroblast spheroids are mainly caused by distinct collagen/PG interactions and various structural alterations in the collagen/PG network. The horseshoe-like 3D structure of decorin can occupy the space around collagen monomers to limit parallel fibril assembly via interacting with collagen α1 chain on its concave surface (Orgel et al. 2009), which

is a potential explanation for our observation that the addition of decorin blunted the increase in anisotropy of collagen fibers in response to cell contractility in the plug assay. Decorin, as a structural spacer, would make it harder for contractile forces to stretch fibers closer and align them in a linear fashion. Lumican, however, which shares a similar horseshoe-like structure, has no impact on anisotropy. One potential explanation for these differences is that lumican and decorin bind collagen at different LRRs. Additionally, the geometry of their concave structures may be distinct due to the number of LRRs (decorin has 12 while lumican only has 10). They also have different types and numbers of GAG side chains that may affect their interactions with collagen: decorin has 1 CS or DS close to the N-terminus; native lumican has 4 KS on LRRs (Appunni et al. 2019), while the recombinant lumican core protein that was used here was not GAG modified. In addition, this work indicated that collagen compaction and realignment generated by contractile cells cause plastic deformation (permanent reorganization).

An engineered microtissue assay was used here to evaluate tissue contraction in 3D. This technique has been widely used for screening drugs (West et al. 2013), for studying magnetic force derived cell responses (Zhao et al. 2013) and for investigating mechanical and cellular force-induced reorganization of collagen and fibronectin networks (van Spreeuwel et al. 2014). This technique has advantages compared to traditional collagen gel contraction assays: (1) quantification of tissue contraction by measuring cantilever displacement is straightforward and accurate; (2) collagen fibers become highly aligned between cantilevers, which can mimic fibrogenesis (as observed during fibrosis and metastasis); (3) it provides a large quantity of data with a small amount of sample used. This latter was particularly important for my project as I only have limited amounts of isolated full-length versican and the recombinant V3 isoform. By using engineered microtissues, different matrix PGs showed distinct effects on tissue contraction. Decorin has been reported previously as an inhibitor of collagen gel contraction when mixed with collagen gel or added to culture media (Bittner et al. 1996)(Z. Zhang et al. 2009), which is

consistent with my findings in engineered microtissues. In contrast to decorin, lumican as reported in the published literature, at a very low concentration (approximately 0.4 ng/mL), increases fibroblast-mediated collagen gel contraction (Liu et al. 2013). In contrast, I have found that 10 ng/mL (consistent with the lumican concentration in native tissues (Svensson, Närlid, and Oldberg 2000)) has no effect on contraction, while the inclusion of lumican at 50 ng/mL decreases microtissue contraction. Understanding the potentially dose-dependent effect of lumican on multiple collagen behaviors will require further investigation. Importantly, versican shows an unusual impact on collagen behaviors such that the addition of versican into engineered microtissues increases contraction, which is consistent with data in a previous publication indicating that versican upregulates fibroblast-mediated collagen gel contraction (J. Carthy et al. 2008). However, aggrecan has no effect on microtissue contraction. As matrix PGs have no effects on either cell contractility in 2D or cell proliferation culturing within contractile collagen gels, I conclude that the distinct effects of PGs on altering tissue contraction are mainly due to their different roles in binding collagen and regulating the organization of the collagen fibrous network. Assessment of the impacts of PGs on cell contractility in 3D needs to be carried out as a future experiment.

In sum, different matrix PGs, even within the same subfamilies, show distinct roles in regulating multiple cell-mediated collagen behaviors. The observations from all three assays further support that versican is a unique collagen regulator among the PGs tested. This suggests that the precisely controlled expression of PGs during normal and collagen-related disease states may have a significant influence on collagen network organization and on cell-ECM crosstalk. In liver fibrosis for example, both versican and lumican are upregulated during fibrogenesis (Bukong et al. 2016)(Krishnan et al. 2012), but I report here that they have opposite effects on modulating cell-mediated collagen condensation. Other work has also indicated that lumican and aggrecan have distinct but time-dependent expression patterns during liver fibrosis (Krull and Gressner 1992).

Thus, investigating the time-dependent deposition of different PGs quantitatively would be a way to start testing my hypothesis that specific PGs are potential therapeutic targets; it may be possible to control long range force transmission, cell-mediated collagen reorganization and tissue contraction by altering the expression of specific PGs.

CHAPTER 5 VERSICAN REGULATES THE MECHANICS OF COLLAGEN IN THE ECM

Y. Du helped with the liver perfusion.

5.1 INTRODUCTION

The mechanics as well as the structure of collagen fibrous networks are highly regulated, and this is necessary for maintaining normal cell and tissue functions. The mechanical properties of collagen networks are regulated by various factors including fiber sizes, fiber orientation/organization, number and types of crosslinks, the presence of collagen-binding proteins and others. Although there is a correlation between the structure and the mechanics of collagen networks, the relationship is neither fully understood nor defined. It has been reported that in vitro collagen gelation under different temperatures changes fiber diameters and pore sizes, leading to altered shear moduli (G) and strain stiffening behaviors: gelation at 26°C, for example, causes an increased fiber diameter and an increased G' (Jansen et al. 2018). In addition to temperature, pH also alters the structure and mechanics of collagen networks. The structural observations that collagen networks gelled at pH=6.9-8.0 form larger fibers (Y. Li et al. 2009) correlate well with the mechanical findings that collagen gels formed at pH=8 show increased G' (Diamantides et al. 2017). Increasing fibrous network crosslinks via chemical and photo crosslinker additions during collagen gelation significantly increases the stiffness (Diamantides et al. 2017)(Tian, Liu, and Li 2016). Given the compositional complexity of the ECM, other ECM components, especially collagen binding partners, are likely to be important regulators of the mechanics of collagen networks. GAGs are negatively charged polysaccharide chains formed by disaccharide repeats which can interact with collagen and regulate collagen structure and mechanics. The addition of HA into a collagen network decreases fiber diameter and pore size resulting in an increased G' (Y. Yang and Kaufman 2009). The addition of CS increases pore

size and fiber diameter by promoting lateral fibril fusion, and the G' of collagen/CS networks are upregulated in a CS dose-dependent manner (Y. Yang et al. 2011). The importance of GAGs in collagen network mechanics suggests that PGs, as core proteins for GAG attachment, may also play a role in regulating the mechanics of in vitro collagen gels.

As the most fundamental structural protein, collagen is a key element in predicting and modeling the mechanics of collagenous tissues. As the mechanics of in vitro collagen gels are highly regulated by the fibrous network organization, tissue mechanics in vivo can also be modulated by collagen/ECM fiber organization. In a number of pathological states, alterations in tissue mechanics have been observed along with the accumulation of ECM proteins including collagen and matrix PGs. Alterations in collagen arrangement may enhance the progression of these disorders including fibrosis and cancer (Piersma, Hayward, and Weaver 2020). Meanwhile, a significant increase in stiffness has been found preceding increased collagen deposition (Georges et al. 2007) suggesting that potential early alterations such as collagen crosslinking and fiber reorganization/realignment may play a role in initiating tissue stiffening and thereby fibrogenesis. In this case, matrix PGs, as important modulators of collagen fibrous networks, are candidate regulators of tissue mechanics. Aggrecan, which is primarily expressed in articular cartilage, modulates cartilage mechanics via the osmotic pressure derived from its fixed negatively-charged GAGs and via the bulk mass of large HA-aggrecan aggregates (Lu et al. 2004). The nano-mechanics of aggrecan, which are mainly represented by solid-fluid interactions and electrostatic interactions between GAGs, have been used as primary cues for predicting the macro-mechanics of cartilaginous tissues (Tavakoli Nia et al. 2015). The loss of aggrecan expression in cartilage results in ECM stiffening, osteoarthritis, and damage to skeletal growth (Alberton et al. 2019). Upregulated versican deposition has been found in both liver and pulmonary fibrosis (Bukong et al. 2016)(Bensadoun et al. 1996), in which there is a 30-fold increase in stiffness in fibrotic tissues (Wells 2008)(Hinz 2012). Less is known, however, about

the role of versican in tissue mechanics, in contrast to the structurally-similar large hyalectan PG aggrecan. Interestingly, externally applied mechanical force can alter the expression of certain matrix PGs. For example, external mechanical ventilation of the rat lung causes significantly increased deposition of versican and biglycan, and it also upregulates tissue resistance and elasticity as measuring by complex impedance using volume oscillation (Al-Jamal and Ludwig 2001). Additionally, asymmetric compressive loading of the intervertebral disc increases the degradation of aggrecan, upregulates the expression of ADAMTS-4 and induces stiffening (Walter et al. 2011). Thus, there may be a reciprocal interaction between PG deposition and mechanics: PGs can regulate tissue mechanics via their distinct functional interactions with collagen and different effects on the organization of fibrous networks; mechanical changes can also alter the deposition of different PGs differentially.

In this chapter, I investigate the specific role of versican in regulating the mechanics of collagenous matrices and tissues. Shear rheology is used to assess the viscoelasticity and non-linear behaviors of collagen matrices and tissues. The effects of different matrix PGs on in vitro collagen gel mechanics are compared. To study the functional interaction between collagen and versican in vivo, liver tissues were perfused with ADAMTS-5 or ChABC and evaluated by shear rheometry to identify the role of versican in native tissue mechanics, particularly compression stiffening and plasticity.

5.2 METHODS

5.2.1 Reagents and Antibodies

Type I collagen from calf skin was purchased from MP Biomedicals (Irvine, CA, USA) for rheometry. Versican was isolated from bovine liver. Recombinant human versican isoform V3 and recombinant lumican protein (without GAGs) were from R&D Systems (Minneapolis, MN, USA).

Aggrecan (A1960), decorin (D8428), ChABC from Proteus vulgaris and recombinant human ADAMTS-5 (cc1034) were purchased from Sigma (St. Louis, MO, USA). Sodium hyaluronate (1.5 MDa) was from Lifecore (Chaska, MN, USA). HBSS (without calcium and magnesium, no phenol) were from Fisher Scientific (Waltham, MA, USA). Heparin (5000 USP unit/mL) was from Medline Industries (Westampton, NJ, USA). Tissue-Teck O.C.T. Compound was from Sakura Finetek (Torrance, CA, USA). VECTASHIELD PLUS antifade mounting medium with DAPI was from Vector Laboratories (Burlingame, CA, USA). Blyscan GAG assay was purchased from Biocolor (Carrickfergus, County Antrim, UK).

Anti-versican (β-GAG domain, Ab1033) was from Millipore Sigma (Burlington, MA, USA) and anti-versican ab19345 (against the neoepitope generated by ADAMTS-5 cleavage) was from Abcam (Cambridge, UK). Cy™3 AffiniPure Donkey Anti-Mouse IgG (H+L) (715-165-151) and Cy™3 AffiniPure Donkey Anti-Rabbit IgG (H+L) (711-165-152) were from Jackson ImmunoResearch (West Grove, PA, USA).

5.2.2 Collagen gel rheology

Type I collagen from MP Biomedicals was reconstituted at 5 mg/mL in 0.02 N acetic acid and stored at 4°C, then diluted to a final concentration of 2.5 mg/mL in 1x PBS at pH=7.4. Briefly, 1000 µL collagen solution (5 mg/mL) was gently mixed with 200 µL 10× PBS, 20 µL 1 N NaOH, and 780 µL diH_2O. All collagen solutions were kept on ice before rheology measurements. For some experiments, versican, the V3 isoform, aggrecan, or decorin was added to the collagen solution to a final concentration of 0.167 mg/mL (Col:PG weight ratio = 15:1, a physiological ratio). For other experiments, HA (1.5 MDa) was added to the collagen solution to a final concentration of 0.1 mg/mL, or HA and V3 were added to the collagen solution together to a final concentration of 0.1 mg/mL (for HA) and 0.167 mg/mL (for V3). A shear rheometer (Kinexus, Malvern) with

rSpace software was used to evaluate the rheological (mechanical) properties. The temperature was set to 37°C for polymerization and a 20 mm plate was used. 314 µL collagen solution was added between plates (gap=1 mm). Both shear storage and loss moduli (G' and G") were measured during gelation by applying an oscillatory shear strain of 2% at a frequency of 10 rad/sec (1.592 Hz). When the shear modulus reached equilibrium indicating full gelation, the freshly formed collagen gel was tested under a strain sweep, during which the shear strain was increased from 1% to 100% at a frequency of 1 rad/s (0.159 Hz). Some freshly formed gels were tested for plasticity using creep and recovery measurements: 5 Pa shear stress was applied for 300 s during the creep phase and the gel was recovered for 300 s during a recovery phase. For measuring G' under compression, the gap was set to 0.9 mm to reach 10% compression. G' measured under 10% compression was normalized to the uncompressed G' for comparing compression softening behavior. Both the G' and G" during gelation were plotted against time. The G' values after full gelation for each condition were compared using one-way ANOVA in ImageJ. The shear strain during creep and recovery was plotted against time. For strain sweep, G' values were plotted against the shear strain on a logarithmic scale and compared among all conditions using two-way ANOVA.

5.2.3 Animal Studies

All animal studies followed the Guide for the Care and Use of Laboratory Animals of the National Institutes of Health. The animal protocol (#804031) was approved by the Institutional Animal Care and Use Committee of the University of Pennsylvania. 300-350 g Sprague-Dawley rats (Charles River Laboratories, Malvern, PA) were housed in pairs strictly following the specifications of the protocol.

5.2.4 Liver perfusion

Rats were anesthetized with pentobarbital by intraperitoneal injection (1 mL per 500 g). The abdomen was opened, 5 mL 1000 USP unit/mL heparin was injected, and the portal vein was catheterized (BD Insyte™ 18GA 1.16IN 1.3×30 mm catheter) and flushed with warm HBSS (without Ca^{2+}, at 37°C). The inferior vena cava was then transected. To enzymatically digest versican into versikine, livers were perfused with 5 µg/200 mL ADAMTS-5 for 1h. To digest CS, livers were perfused with 5 U ChABC for 1h. For control groups, livers were perfused with HBSS for 1h. After starting the perfusion, the inferior vena cava was pressed with a cotton tipped applicator to cause tissue swelling and push buffer through the entire liver. After perfusion, livers were harvested, and the largest lobule was used for rheology testing. Other lobules were fixed in two different ways. Some samples were fixed with 4% paraformaldehyde overnight and stored in 70% ethanol for processing. The Molecular Pathology and Imaging Core (MPIC) processed these by paraffin embedding and sectioning. Other samples were frozen in OCT: liver tissues were embedded with OCT compound in cassettes placed in a liquid nitrogen chamber and stored at -80°C. Frozen tissues were also sectioned by MPIC.

5.2.5 Liver Rheology

Liver tissues were kept in HBSS on ice and rheology studies were performed within 2h of tissue harvest. A 20 mm punch was used to prepare liver samples and samples were kept hydrated throughout testing. A shear rheometer (Kinexus, Malvern) with rSpace software was used to quantify the rheological (mechanical) properties. The plate-tissue adhesive contact point was set as the normal force reaching 10 g (equals to 0.1 N for a 20 mm plate). The rheological testing sequence was done in the following order: (1) dynamic time sweep; (2) creep and recovery; (3) dynamic strain sweep. During the time sweep test, G', G" and normal force were measured under 2% strain with an oscillation frequency of 1 rad/s (0.159 Hz) for 120s. This measurement was then taken under increasing uniaxial compression at 10, 15, 20 and 25% (returning to 0% in the

end) by setting the gap. Young's modulus was calculated by normal forces and gap changes. G' and Young's modulus were plotted against time. To study plastic deformation, shear creep and recovery was assessed by applying 5 or 15 Pa shear stress for 300s with 300s of recovery. The shear strain data were plotted against time, and the creep deformation (strain after creep), plastic deformation (strain after recovery) and plasticity (plastic deformation/creep deformation) were compared among all conditions. The strain sweep test was set up by increasing strain amplitude from 1% to 50% (by logarithmic progression) with an oscillation frequency of 10 rad/s (1.59 Hz). G' was plotted against increasing shear strain.

5.2.6 Immunostaining

All paraffin-embedded sections were deparaffinized by washing with xylene (3 times, 2 min each), washing with 100% ethanol (2 times, 2 min each), and then washing with 95%, 95%, 80%, and 70% ethanol and diH_2O (1 min each). Slides were incubated with 10 mM citric acid buffer (pH = 6) using a pressure cooker and rinsed with gently running water. For frozen sections, slides were warmed to RT, incubated with 10% neutral buffered formalin for 4 min and rinsed with gently running water for 5 min. Both kinds of sections were blocked with protein blocking agent (Thermo Scientific Starting Block T20 Blocking Buffer, Fisher #PI-37539) for 1h and rinsed with PBS. Frozen slides were then incubated with anti-versican β-GAG antibody (ab1033) and paraffin slides were incubated with anti-versikine antibody (ab19345) (diluted 1:200 in PBT (0.2% Triton X-100, 0.1% BSA in PBS)) at 4°C overnight. After washing with PBS 3 times (5 min each), all slides were then incubated with secondary antibody (1:600 in PBT) in dark for 1 h and washed with PBS. Each slide was mounted with mounting media with DAPI and a coverslip, and then sealed with nail polish. Stained slides were stored in dark at 4°C up to 2 weeks before confocal microscopy.

5.2.7 Sulfated glycosaminoglycan quantification

The Blyscan sulfated GAG assay was used to quantify sulfated GAGs in enzyme-perfused liver tissue; the protocol was adapted from the general protocol from Biocolor. Briefly, approximately 20 µg frozen liver tissue was digested with 4 M guanidine hydrochloride buffer and homogenized using a Bullet Blender. The tissue buffer was shaken overnight at 4°C. After centrifugation, 100 µL of the supernatant was mixed with 1 mL Blyscan dye reagent. GAG standards were prepared to 10, 20, 30, 40 and 50 µg/mL and were mixed with 1 mL dye reagent. After shaking at RT for 30 min, tubes were spun at 12,000 rpm for 10 min. The supernatant was removed, and the pellet was dissolved with 0.5 mL dissociation reagent. After another centrifugation at 12,000 rpm for 5 min, 150 µL of the supernatant was added to a 96-well plate and the absorbance was read at 656 nm.

5.2.8 Statistical analysis

All results were analyzed by GraphPad Prism 7 (San Diego, CA, USA) using an unpaired t test, one-way or two-way ANOVA. P values were determined by Tukey's multiple comparison test, in which *P<0.05 was considered to be statistically significant.

5.3 RESULTS

5.3.1 Versican accelerates collagen gelation on a rheometer in contrast to other matrix PGs

In chapter 3, I reported that versican upregulated collagen fibrillogenesis as determined by the in vitro turbidity assay. Here, I used shear rheology to record the changes in G' and G" during collagen gelation at 37°C while on the rheometer. The kinetic curves measured by rheometry (Figure 5.1A-E) were not the typical sigmoidal shape observed in the turbidity assay. To compare the gelation quantitatively, I recorded the time when G reached equilibrium and found that the

addition of versican or the V3 isoform significantly accelerated collagen gelation (Figure 5.1F). Because the isolated full-length versican is contaminated with small amounts of aggrecan and decorin (Figure 2.2), I also tested them as controls. The addition of aggrecan and decorin had no impact on gelation time (Figure 5.1F).

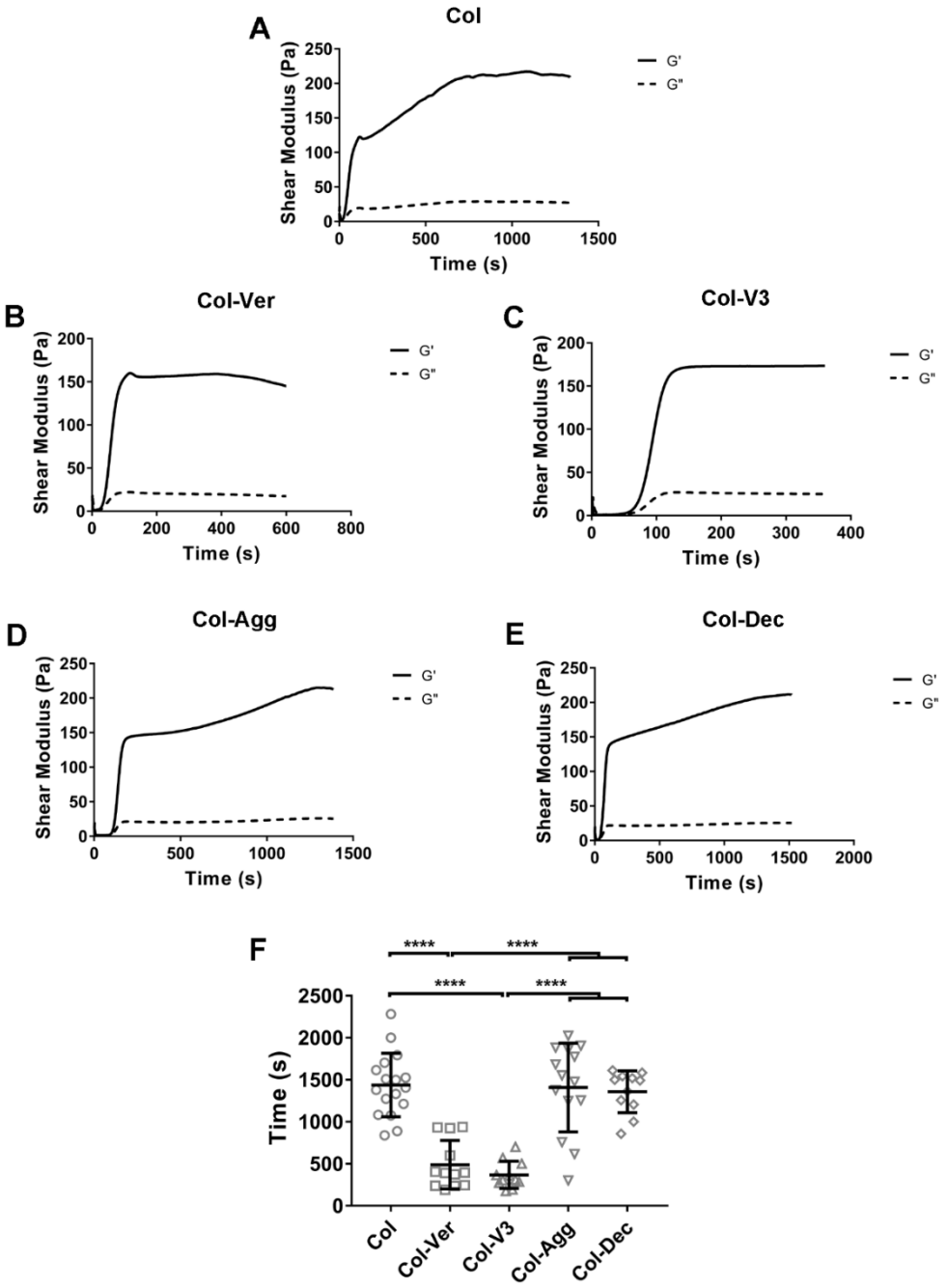

Figure 5.1 Versican and its V3 isoform accelerate collagen gelation on a shear rheometer. (A-E) Representative kinetic curves for collagen gelation measured by shear rheometry: (A) collagen (Col; 2.5 mg/mL) alone, (B) collagen-versican (Ver; 0.167 mg/mL), (C) collagen-V3 isoform (V3; 0.167 mg/mL), (D) collagen-aggrecan (Agg; 0.167 mg/mL) and (E) collagen-decorin (Dec; 0.167

mg/mL). (F) The gelation time was considered to be the time when G reached equilibrium. N=17 for Col, N=12 for Col-Ver, N=11 for Col-V3, N=15 for Col-Agg and N=11 for Col-Dec. Data represent mean ± SD. *P<0.05, **P<0.01, ***P<0.001 and ****P<0.0001.

5.3.2 The effect of versican on the viscoelasticity of collagen gels differs from other matrix PGs

The mechanics of collagenous matrices can be regulated by structural factors of collagen fibrous network such as fiber size and crosslinking density (Valero et al. 2018)(Lin and Gu 2015). I observed by SEM that collagen matrices co-gelled with different matrix PGs had distinct network organization (Figure 3.5). Here, I used a shear rheometer to study viscoelasticity and non-linear rheological behaviors of collagen matrices and compared the effects of different PGs. Both G' and G" were measured during gelation. When G reached equilibrium for each gel condition, G', G" and tan δ (which is G"/G', representing the viscosity to elasticity ratio of collagen gels) were compared for the different conditions. I found that the addition of versican or the V3 isoform significantly decreased G', while aggrecan, which belongs to hyalectan family and is structurally similar to versican, had no influence on collagen gel stiffness (G'). Decorin, a SLRP, also showed no impact on G' (Figure 5.2A). Additionally, the presence of versican decreased G" significantly; V3 also led to a decreased G" although it was not significantly different from collagen (Figure 5.2B). Aggrecan and decorin had no influence on viscosity (G") (Figure 5.2B). Interestingly, the inclusion of the V3 isoform significantly increased tan δ suggesting an increased energy dissipation potential for Col-V3 co-gels (Figure 5.2C).

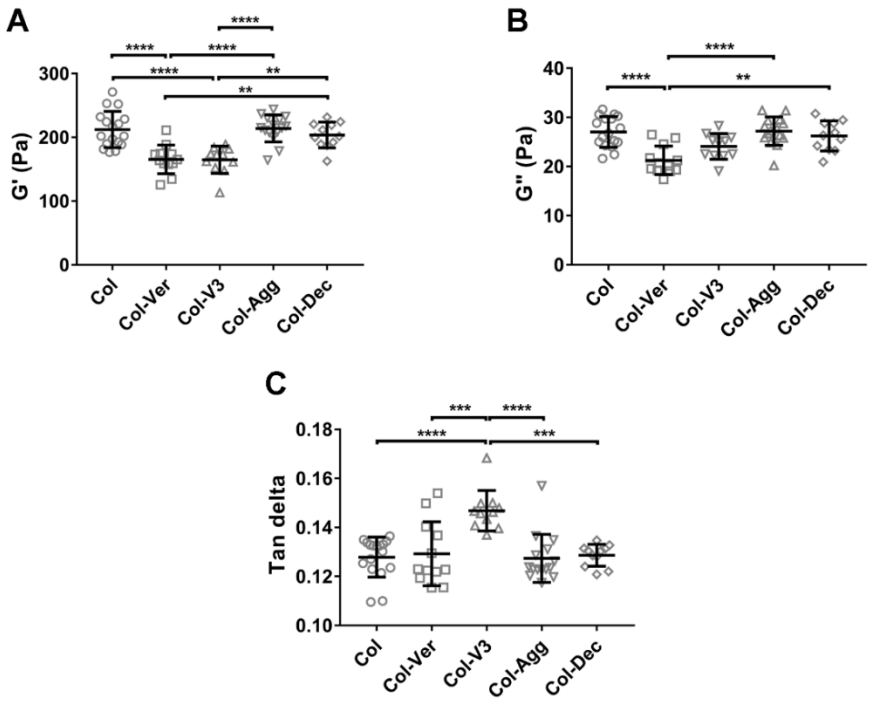

Figure 5.2 Versican and its V3 isoform have distinct effects on the viscoelasticity of collagen gels. (A) G', (B) G", and (C) tan δ (which is G"/G') of Col (2.5 mg/mL), Col-Ver (Ver; 0.167 mg/mL), Col-V3 (V3; 0.167 mg/mL), Col-Agg (Agg; 0.167 mg/mL) and Col-Dec (Dec; 0.167 mg/mL). N=17 for Col, N=12 for Col-Ver, N=11 for Col-V3, N=15 for Col-Agg and N=11 for Col-Dec. Data represent mean ± SD. **P<0.01, ***P<0.001 and ****P<0.0001.

5.3.3 Versican modulates non-linear rheological behaviors of collagen gels differently than other matrix PGs

It is known that networks formed by biopolymers (including collagen), which are semiflexible filaments, show complex non-linear behaviors such as compression softening and strain stiffening (Van Oosten et al. 2016). To study the compression behavior in collagen gels and co-gels, the

gap was set to 0.9 mm to reach 10% compression after full gelation. Normalizing G' at 10% compression to its G' at equilibrium and quantification of the softening rate (the slope of Figure 5.3A) were used to compare the compression softening behavior of the different gels. All types of collagen gels showed compression softening behaviors (Figure 5.3A, B). Only the presence of aggrecan significantly attenuated compression softening (Figure 5.3B blue). After calculating the slopes in Figure 5.3A (shown as absolute values in Figure 5.3C), I found that there was no difference on the rate of G' decay after compression between any conditions. By applying increasing shear strain to the gel, I observed that the inclusion of versican eliminated the strain stiffening behavior (Figure 5.3D red and Table 5.1) and the addition of the V3 isoform led to markedly blunted strain stiffening behavior (Figure 5.3D orange and Table 5.1). Collagen co-gelled with aggrecan or decorin strain stiffened, but slightly less than for the plain collagen gel (Figure 5.3D purple and blue). The strain at which the plain collagen gel failed was significantly higher than for collagen co-gelled with V3, aggrecan and decorin (the failure strain is 8% for Col-V3, 15.85% for Col-Agg and Col-Dec, but 19.95% for plain collagen). Given that I observed previously that the plastic re-organization of a collagen network could be generated by cell contractile force (Figure 4.7), here I used a creep and recovery test to study the plastic deformation of collagen networks by applying external shear stress. I observed that there was plasticity (plastic deformation) for all different types of collagen gels and found that there was no significant difference among these gels (Figure 5.3E).

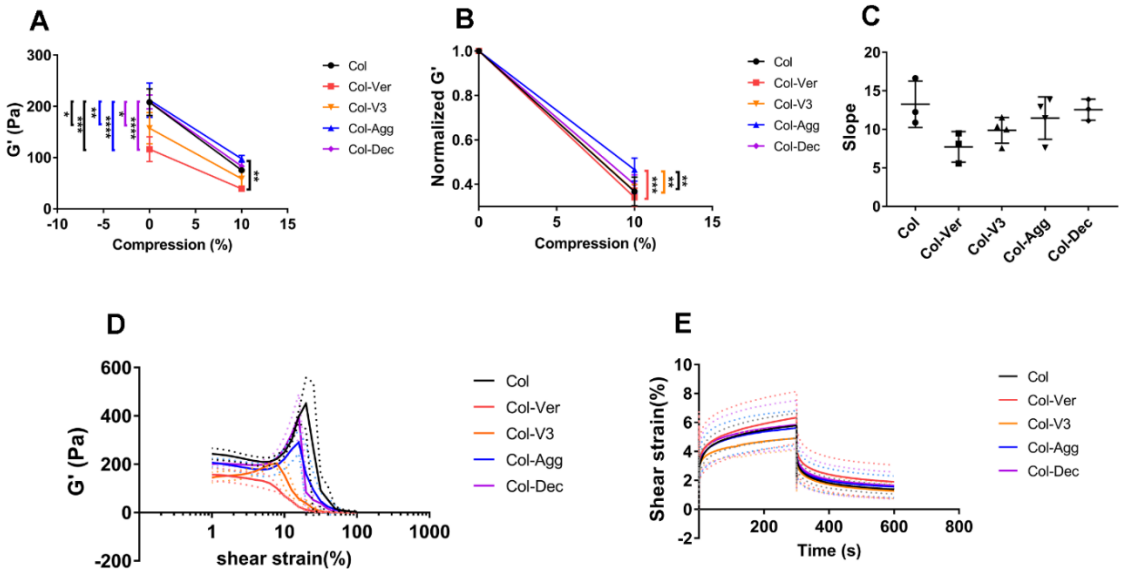

Figure 5.3 Matrix PGs show different regulation of non-linear mechanical behaviors of collagen gels. (A) G' was measured at equilibrium and under 10% compression. (B) G' at 10% compression was normalized to G' at equilibrium. (C) The slopes of curves in (A) were calculated and are shown as absolute values. (D) G' was measured under increasing shear strain from 1% to 100%. (E) Plasticity was measured by a creep and recovery test. Collagen gels were deformed at 5 Pa for 5 min and recovered for another 5 min. Col (2.5 mg/mL), Col-Ver (Ver; 0.167 mg/mL), Col-V3 (V3; 0.167 mg/mL), Col-Agg (Agg; 0.167 mg/mL) and Col-Dec (Dec; 0.167 mg/mL). Freshly gelled samples were used separately for compression, strain sweep or creep and recovery testing. For 10% compression testing, N=3 for Col, N=3 for Col-Ver, N=4 for Col-V3, N=4 for Col-Agg and N=3 for Col-Dec; for strain sweep, N=3 for Col, N=3 for Col-Ver, N=3 for Col-V3, N=4 for Col-Agg and N=3 for Col-Dec; for creep and recovery, N=5 for Col, N=4 for Col-Ver, N=3 for Col-V3, N=4 for Col-Agg and N=4 for Col-Dec. Data represent mean ± SD. *P<0.05, **P<0.01, ***P<0.001 and ****P<0.0001.

Table 5.1 Significant differences in G' of strain sweep testing (Figure 5.3D) when different PGs were added to collagen gels. Different collagen gel conditions were compared using two-way ANOVA. *P<0.05, **P<0.01, ***P<0.001 and ****P<0.0001.

Condition #1	Condition #2	Shear strain (%)	Significance
Col	Col-Ver	7.9433	**
Col	Col-Ver	10	****
Col	Col-Ver	12.5893	****
Col	Col-Ver	15.8489	****
Col	Col-Ver	19.9625	****
Col	Col-Ver	25.1189	****
Col	Col-V3	1	*
Col	Col-V3	10	*
Col	Col-V3	12.5893	****
Col	Col-V3	15.8489	****
Col	Col-V3	19.9625	****
Col	Col-V3	25.1189	****
Col	Col-Agg	15.8489	**
Col	Col-Agg	19.9625	****
Col	Col-Agg	25.1189	****
Col	Col-Dec	19.9625	****
Col	Col-Dec	25.1189	****
Col-Ver	Col-V3	7.9433	*
Col-Ver	Col-Agg	7.9433	*
Col-Ver	Col-Agg	10	****
Col-Ver	Col-Agg	12.5893	****
Col-Ver	Col-Agg	15.8489	****

Col-Ver	Col-Agg	19.9625	****
Col-Ver	Col-Agg	25.1189	*
Col-Ver	Col-Dec	7.9433	**
Col-Ver	Col-Dec	10	****
Col-Ver	Col-Dec	12.5893	****
Col-Ver	Col-Dec	15.8489	****
Col-V3	Col-Dec	10	**
Col-V3	Col-Dec	12.5893	****
Col-V3	Col-Dec	15.8489	****
Col-V3	Col-Agg	12.5893	****
Col-V3	Col-Agg	15.8489	****
Col-V3	Col-Agg	19.9625	**
Col-Agg	Col-Dec	15.8489	**

5.3.4 Versican and its chondroitin sulfate side chains regulate liver tissue mechanics

My in vitro data strongly support the conclusion that versican plays an important role in modulating the mechanics of collagenous tissues. To investigate the effects of versican and its CS side chains in tissue mechanics, I used a shear rheometer to measure the stiffness (G') and non-linear rheological behaviors of liver tissue (as an in vivo model) perfused with ADAMTS-5 (for versican cleavage at GAG domains) or ChABC (for CS removal). Neither enzymatic perfusion had any impact on the stiffness (G') in the un-compressed state but both attenuated the compression stiffening of G', resulting in a significant G' decrease under 25% compression after CS removal (Figure 5.4A). I also calculated the Young's modulus from the gap changes and normal forces, and the results indicated that perfusion with either enzyme significantly

downregulated the compression stiffening of Young's modulus, showing with a significant decreased Young's modulus at 22.5% compression (Figure 5.4B). In addition to compression stiffening, native collagenous tissues also undergo another non-linear behavior, strain softening. As shown in Figure 5.4C, normal liver strain softened, and this was not significantly affected by perfusion with either ADAMTS-5 or ChABC.

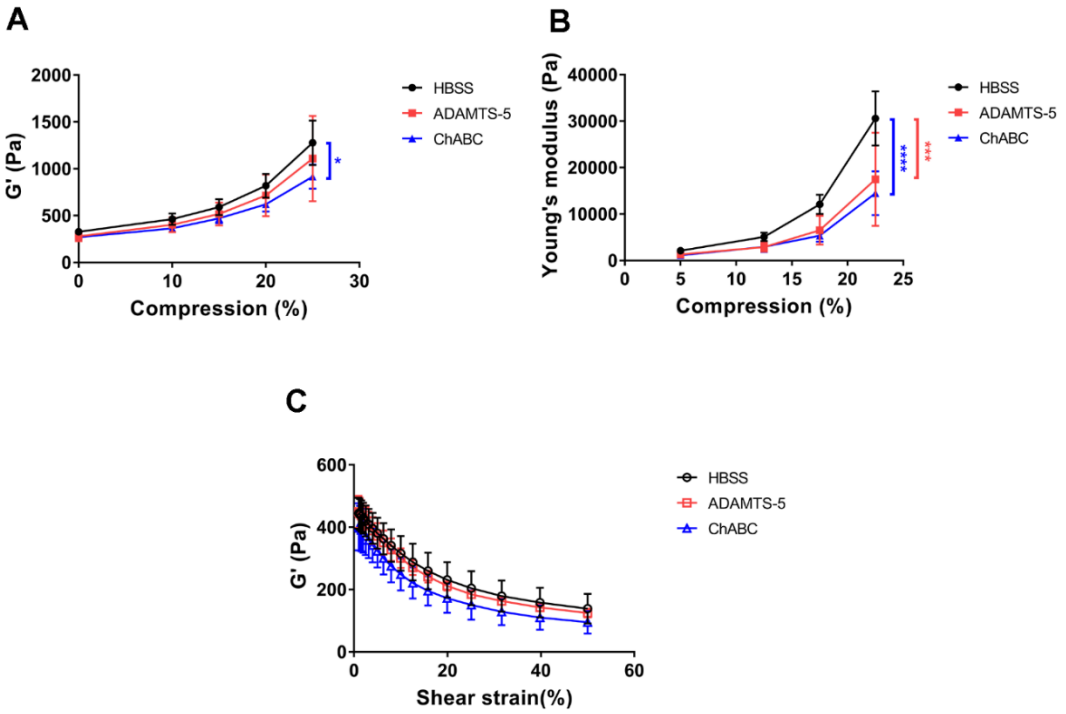

Figure 5.4 Versican and its CS side chains alter compression stiffening of liver tissues. (A) Compression stiffening behavior was studied by measuring G' under 10%, 15%, 20% an 25% compression via changing the gap of the rheometer. (B) Young's modulus at 5%, 12.5%, 17.5% and 22.5% compression. (C) G' measured by strain sweep with an increasing strain from 1% to 50%. N=3 for HBSS, N=4 for ADAMTS-5 and ChABC, the compression and strain sweep

experiments were done on the same liver sample. Data represent mean ± SD, *P<0.05, ***P<0.001 and ****P<0.0001.

To confirm the cleavage of versican by ADAMTS-5, I immunostained perfused tissue with anti-versican βGAG antibody (this versican antibody targets aa. 1360-1439, covering the cleavage site, and therefore only stains intact versican) and anti-DPEAAE (which recognizes the neoepitope exposed after cleavage). Liver tissue is highly cellular and ECM proteins, including collagen and PGs, are mainly located at the portal tract and vessel area. As shown in Figure 5.5A-C, intact versican was found in both HBSS and ChABC perfused samples but not in ADAMTS-5 perfused samples. Meanwhile, DPEAAE staining was observed in ADAMTS-5 perfused samples (Figure 5.5E); the control group showed no positive staining for this neoepitope (Figure 5.5D). To test the effectiveness of the enzymatic perfusions, sulfated GAGs from perfused liver tissues were quantified and showed a significant decrease after both ADAMTS-5 and ChABC perfusions (Figure 5.5F).

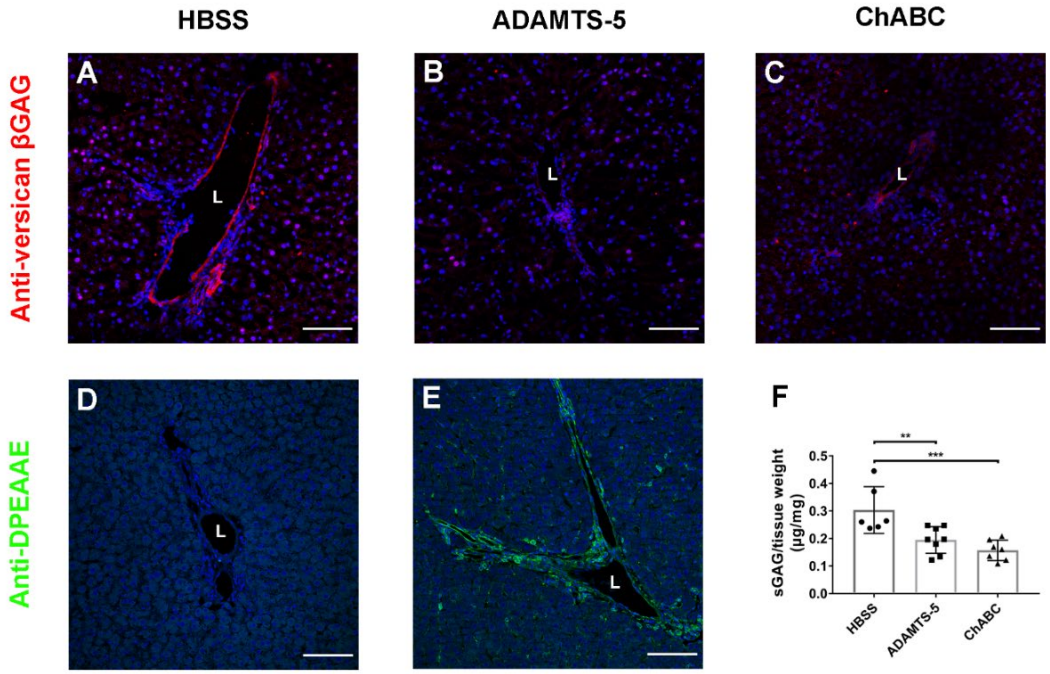

Figure 5.5 The enzymatic perfusions of liver tissues effectively alter versican and GAG content. (A-C) Representative confocal images of veriscan β-GAG-stained tissue in HBSS-, ADAMTS-5- and ChABC-perfused livers (the lumen of the portal tract or vessel was labeled with L). (D, E) Representative confocal images of neoepitope-DPEAAE-stained tissue in HBSS- and ADAMTS-5-perfused livers. (F) Quantification of sulfated GAGs in perfused liver tissues (N=6 for HBSS, N=8 for ADAMTS-5 and N=7 for ChABC). Data represent mean ± SD, **P<0.01 and ***P<0.001.

5.3.5 HA explains the distinct alterations of versican on the G' of collagenous matrices versus tissues

I observed that there was a decrease in G' for collagen gels manipulated with versican or its V3 isoform (Figure 5.2A), while in native tissue, the cleavage of versican did not lead to statistically-significant softening (Figure 5.6A). There is a large amount of HA in native ECM that can interact

with both collagen and versican to alter the structure and mechanics of collagen fibrous network, and I hypothesized that HA stiffens collagen network via upregulating swelling. I therefore investigated the G' of collagen-HA and collagen-HA-V3 co-gels in vitro. The inclusion of HA into plain collagen gels increased G' significantly while the addition of HA into collagen-V3 co-gels prevented the decrease in G' observed with the addition of V3 (Figure 5.2A), resulting in gels with the same G' as collagen alone (Figure 5.6B). Thus, the stiffening of the collagen network by HA could balance the softening caused by versican.

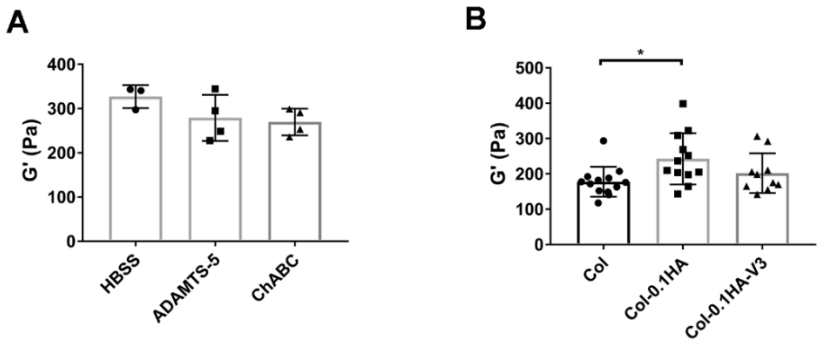

Figure 5.6 The presence of HA increases the stiffness of collagenous matrices. (A) G' measured under no compression for enzymatically-perfused liver tissues. (B) G' measured for Col (1.5 mg/mL) gels, Col-HA (1.5 MDa; 0.1 mg/mL) and Col-HA-V3 (HA 1.5 MDa, 0.1 mg/mL and V3, 0.167 mg/mL) co-gels. For G' measurements of liver tissue, N=3 for HBSS, N=4 each for ADAMTS-5 and ChABC; for G' measurements of collagen gels, N=13 for Col, N=12 for Col-0.1HA and N=10 for Col-0.1HA-V3. Data represent mean ± SD, *P<0.05.

5.3.6 Versican and its chondroitin sulfate GAGs participate in the plasticity of liver tissues

To investigate the plasticity of collagenous tissues, enzymatically-perfused livers were studied by creep and recovery using a shear rheometer. First, I induced small tissue deformations by applying 5 Pa shear stress and let it recovery. The creep deformation was the strain measured after creep, the plastic deformation was the remaining strain measured after recovery and the plasticity was defined as plastic deformation divided by creep deformation. The cleavage of versican or the removal of CS residues decreased the plasticity significantly (Figure 5.7A, D). Versican and CS had no impact on the shear deformation after the 5 Pa creep phase (Figure 5.7B) but both enzymatic perfusions resulted in a significant decrease in the plastic deformation after the recovery phase (Figure 5.7C). Under these creep conditions, the tissue deformation was only about 2%. Second, I used a 15 Pa shear stress to assess the role of versican and its GAGs in plasticity under larger tissue deformations. In this trial, plasticity was also observed in liver tissues regardless of the nature of the enzymatic perfusion (Figure 5.7E), with the tissue deformation reaching up to about 18% (Figure 5.7F) and returning to about 7% after recovery (Figure 5.7G). Under large deformations, neither ADAMTS-5 nor ChABC perfusions had any impact on the plasticity of liver tissue or on any other part of the creep and recovery process compared to control groups (Figure 5.7E-H).

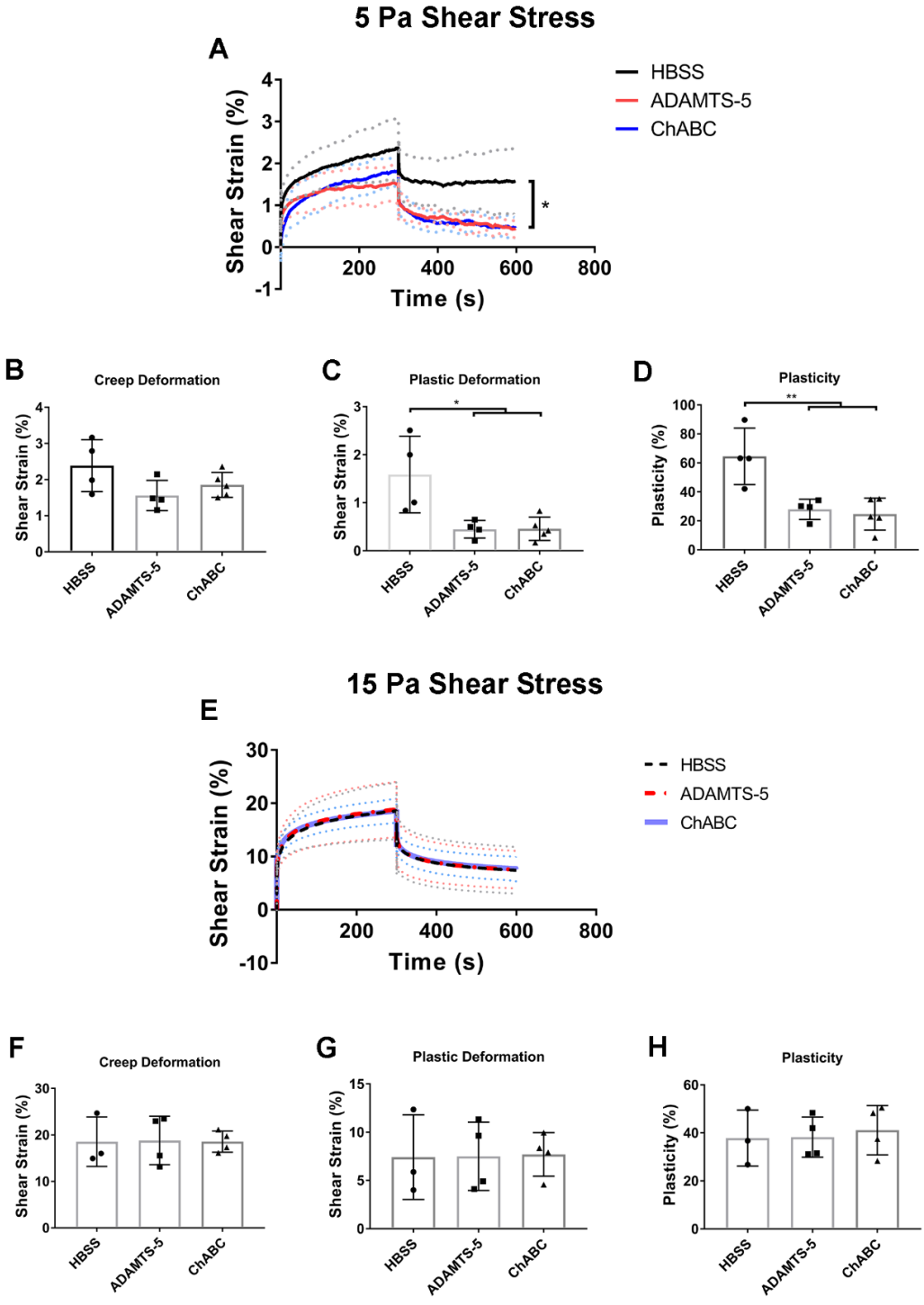
5 Pa Shear Stress
A
HBSS
ADAMTS-5
ChABC
Shear Strain (%)
Time (s)
*
B
Creep Deformation
C
Plastic Deformation
D
Plasticity
**
HBSS
ADAMTS-5
ChABC
15 Pa Shear Stress
E
F
G
H
Plasticity (%)

Figure 5.7 Versican and its CS side chains contribute to tissue plasticity at small deformations. (A-D) A 5 Pa shear stress was applied to ADAMTS-5- and ChABC-perfused livers during a creep and recovery test: (A) the shear strain curves generated by creep and recovery; (B) the creep deformation after a 5 min creep phase; (C) the plastic deformation after a 5 min recovery phase; (D) plasticity as calculated by dividing plastic deformation by creep deformation. (E-H) A 15 Pa shear stress was applied to ADAMTS-5- and ChABC-perfused livers during creep and recovery: (E) the shear strain curves generated by creep and recovery; (F) the creep deformation after a 5 min creep phase; (G) the plastic deformation after a 5 min recovery phase; (H) plasticity as calculated by dividing plastic deformation by creep deformation. For 5 Pa creep testing, N=4 for HBSS and ADAMTS-5, and N=5 for ChABC; For 15 Pa creep testing, N=3 for HBSS, N=4 each for ADAMTS-5 and ChABC; experiments with the two different shear stresses for creep were carried out on different samples. Data represent mean ± SD, *P<0.05 and **P<0.01.

5.4 DISCUSION

The mechanics of collagenous tissues are defined by the organization of collagen fibrous networks and are essential for maintaining normal cell and tissue functions. Abnormal mechanics have been observed for almost all collagen-related fibroproliferative diseases. Matrix PGs, which are key regulators of collagen fibrillogenesis and fibrous network organization, can play important roles in regulating the mechanics of collagen networks. Understanding the role of versican in collagen gel and tissue mechanics is particularly important because versican is universally distributed in various tissues; it has different effects on fibrillogenesis and fiber organization than other PGs; and its deposition is upregulated in various collagen-related diseases. I report in this chapter that the additions of versican and V3 to collagen matrices result in decreased stiffness and attenuate strain stiffening. Versican and its GAGs also contribute to tissue mechanics by maintaining tissue compression stiffening and participating in tissue plasticity at lower deformations.

In addition to the turbidity assay discussed previously in this thesis, rheometry can be used as a technique for studying collagen gelation in vitro. When a collagen solution is placed between the plates on the shear rheometer, both G' and G" can be tracked during collagen gelation (fibrillogenesis) at 37°C generating both the mechanics and kinetics of fibrillogenesis. This approach has been used with confocal reflectance microscopy to study the effect of HA on collagen fibrillogenesis as well as structural and mechanical alterations during gelation (Y. Yang and Kaufman 2009). I found consistently using both techniques that versican and V3 accelerate collagen gelation. Additionally, rheology data illustrate that aggrecan and decorin have no influence on collagen gelation while they both show inhibitive effects using the in vitro turbidity assay. Potential explanations for this difference are that: (1) rheometery and the turbidity assay measure different things: the rheometer measures the changes in G while the turbidity assay measures the changes in light scattering properties of collagen fibrils, neither of which is a direct measure of fibrillogenesis; (2) the rheometer applies 2% shear strain to the collagen gel while the effect of shear strain on gelation is unknown. The kinetic curves generated by rheometry only represent the gain in G during collagen gelation, while there is not a defined correlation between G and fibrillogenesis including fibril size, quantity and the structure of fibrous network. Thus, these kinetic curves are not sigmoidal and do not contain the lag and rapid growth phases which represent the nucleation and lateral growth in the kinetic curves generated by the turbidity assay (Silver and Birk 1983)(Zhu and Kaufman 2014).

I have previously reported and discussed the differential interactions between collagen and different PGs, which result in altered fibrillogenesis and fibrous network organization (Figure 3.2 and 3.5). In this chapter, I have also observed that different PGs have distinct effects on collagen gel mechanics, which further supports the conclusion there is a correlation between collagen structure and mechanics. Thus, understanding the relationship between matrix PGs and collagen

mechanics may be important to understanding the mechanisms of fibroproliferative disorders. Interestingly, in my shear rheometry studies, versican and the V3 isoform are unique among the PGs tested in their effect on viscoelasticity. SEM data suggest that the presence of versican in a collagen network can significantly increase fiber size and decrease network connections. It has been previously published that the G' of collagen gels is upregulated with increasing crosslinks (Valero et al. 2018)(Lin and Gu 2015); it is thus not surprising that the G' of collagen/versican gels is significantly lower in the context of a loosely connected network with thicker fibers and fewer connections. In addition, the inclusion of V3 into collagen matrices significantly decreased tan δ suggesting that V3 increases energy dissipation in the collagen network. Unlike versican, aggrecan and decorin have no impact on viscoelasticity in the assays reported in this chapter. It has been published that the inclusion of decorin into collagen gels increases stiffness as measured by a tensile test (Reese, Underwood, and Weiss 2013), and there are complicated dose- and location-dependent effects of decorin on the tensile stiffness of tendons (Dourte et al. 2012)(Robinson et al. 2005). The effects of aggrecan on tissue stiffness are controversial: in an in vitro engineered chondrocyte/collagen scaffold, local increases in stiffness are correlated with local increases of aggrecan, as shown by a combination of histological staining and confocal elastography (Middendorf et al. 2020); but an in vivo study yielded the opposite result that the loss of aggrecan triggers ECM stiffening in cartilage (Alberton et al. 2019). However, there are no published studies of rheological data of collagen/PGs co-gels that would allow me to compare and discuss my results directly.

Non-linear rheological behaviors, including strain stiffening, compression softening and plasticity, are typical mechanical features for semiflexible biopolymer network including collagen fibrous networks (Van Oosten et al. 2016).The mechanism of these non-linear mechanical behaviors and the relationship between physical and structural parameters and strain-dependent rheology is not fully understood and requires further investigation. After applying a strain sweep to collagen gels,

I observed strain softening (to a small degree) at low strains, strain stiffening at intermediate strains and failure/collapse (or gel slipping) at higher strains. One explanation for the mechanism underlying this observation is that strain softening at low strains is triggered by the slippage of physical crosslinks and strain stiffening at intermediate strains is caused by stretch-induced fiber alignment and stiffening (Kurniawan, Wong, and Rajagopalan 2012). Compression softening was also found in all of the collagen and collagen/PG gels. Among them, only the inclusion of aggrecan significantly attenuated compression softening, likely because it is modified by about 100 negatively charged GAG side chains, which is ten times the number for versican and hundred times that of decorin. These negative GAG side chains can attract water, increase swelling and cause resistance to compression as its native physiological function in cartilage tissues (Roughley and Mort 2014).

Plasticity, which is the permanent deformation and reorganization of the collagen network caused by cellular contractile forces or externally-applied mechanical forces, is another important mechanical behavior of collagen networks. Importantly, there is also a reciprocal crosstalk between the plasticity of collagen fibrous networks and cell behaviors: cell-generated forces cause irreversible alterations in collagen networks (Ban et al. 2018) and plasticity can modulate cell functions such as migration (Wisdom et al. 2018). After doing creep and recovery testing, I found that there was no significant difference in collagen gel plasticity among the different collagen co-gels, which is constant with my previous observation from the collagen plug assay (Figure 4.7) that there is no difference in cell-mediated plastic deformation in collagen/versican co-gels compared to plain collagen. Potential explanations are that: (1) interactions between collagen and PGs are not significantly altered during stress-induced collagen re-organization and (2) the effects of newly-formed or damaged collagen/PG interactions on the network organization are limited, in contrast to the re-arrangement of collagen fibers/bundles in a larger scale.

To further investigate the role of versican in native tissue mechanics, I used ADAMTS-5 perfusion in liver tissue to induce the cleavage of versican. CS is predominantly deposited in prenatal liver tissue and then largely converted into CSPGs in postnatal liver tissue, and it is particularly versican V1 isoform that is highly expressed in liver (Gressner and Vasel 1985)(Cattaruzza et al. 2002). Thus, versican, especially its V1 isoform, is the major cleavage target for ADAMTS-5 and ChABC. A well-studied cleavage site is in the βGAG domain (Glu441-Ala442 for the V1 isoform) (Sandy et al. 2001) and produces two versican fragments, G1-DPEAAE and a G3-containing fragment. My data support that there are G1-DPEAAE fragments remaining in liver tissue after perfusion (Figure 5.5E), and I hypothesize that this is G1-binds HA and, because of the size of HA, is retained. However, there are no antibodies available for staining the cleaved G3 fragment (βGAG-G3), making it difficult to determine whether or not it remains in the tissue after perfusion. A published study on aggrecan degradation by ADAMTS-5 strongly supports that HA, hyaladherins (G1 and link proteins) and the G3 fragment can be released from native tissue (Durigova et al. 2008)(Chockalingam et al. 2004). However, I have found significant differences in the behaviors of versican and aggrecan; the binding of collagen to the versican G3 domain (shown in Chapter 2) may protect the G3 fragment from removal. Given that I observed a significant loss of tissue GAGs after ADAMTS-5 perfusion, it is likely that a significant part of the versican GAG domain been cleaved and flushed out. There is also evidence that there are multiple ADAMTS-5 cleavage sites on versican core protein in addition to the canonical site, including Glu405-Gln406 on αGAG for V2 (Westling et al. 2004) and other cleavage sites on G1, βGAG and G3 of V1 (Martin et al. 2021), which makes it possible that small GAG domains are released from the core protein (and are potentially easily flushed from the tissue during perfusion). In another trial, I degraded and removed versican CS side chains via ChABC perfusion, which my control experiments showed also effectively removed GAGs (even better than ADAMTS-5). For tissue subject to either enzymatic perfusion, there were significant changes in tissue mechanics, namely the downregulation of compression stiffening behaviors as observed in both G' and Young's modulus values. Unlike collagen network which shows compression softening, the

opposing compression stiffening behavior observed in native tissue is due to the inclusion of inert particles such as cells (van Oosten et al. 2019). In ECM, collagen fibers are crosslinked and form the stress-bearing network and the volume-conserving cells are embedded. Increased fraction of closely packed cells can suppress the compression derived relaxation of nonlinear biopolymer network and contribute to tissue stiffening (van Oosten et al. 2019). The attenuation of compression stiffening observed here is mainly due to the natural physiological functions of highly negatively charged GAGs in ECM that they can attract water, cause swelling, increase osmotic pressure and resist compression. This finding aligns well with previously published work done by our lab indicating that liver perfusions with α-amylase, an enzyme that digests α-linked polysaccharides including GAGs, also eliminated compression stiffening (Perepelyuk et al. 2016).

Interestingly, the inclusion of versican into collagen gels decreases G' but the cleavage of versican has no effect on G' in the non-compressed state. One potential explanation is that the compositional, structural, and mechanical features of native tissues are remarkedly different from collagen matrices. For example, liver tissue is highly cellular, filled with cells which are normally regarded as incompressible particles. The deposition of ECM proteins, including collagen, HA and versican, is significantly increased during hepatic fibrosis (Bukong et al. 2016). The presence of HA, an important binding partner of both collagen and versican, in the ECM can also modulate the mechanics of collagenous matrices and tissues. For example, the G' for Col-HA-V3 co-gels is comparable to that of plain collagen gels while Col-HA co-gels are significantly stiffer (Figure 5.6). Thus, double perfusions targeting both versican and HA may cause a significant tissue softening. Another reason is that ADAMTS-mediated versican cleavage cannot remove the entire versican from ECM as the G1-DPEAAE fragment has been found remaining in perfused tissue and may still play a specific role in regulating tissue mechanics at least in part since it binds to HA.

Native ECM, which collagen provides the fundamental structure for, also shows a typical mechanical plasticity. After applying and removing external shear stress, tissue plasticity is reflected in the fact that the shear deformation cannot fully recover to its initial state. Although the mechanism underlying ECM plasticity is not fully understood, published works studying the plasticity of collagen networks via cell contractile force and shear stress support that the permanent reorganizations of collagen fibrils via crosslinking, fibrils sliding and fusion into large bundles are responsible for plasticity (Kim et al. 2017)(Nam et al. 2016). Versican, as a regulator of collagen fibrillogenesis and organization, alters tissue plasticity. Interestingly, I have observed that the cleavage of the versican core protein or the degradation of its CS side chains only downregulates plasticity under small shear deformations (1-2%) but not large deformations (15-25%). This hypothetically indicates that versican-modulated collagen reorganization is more effective at a lower magnitude of stress-induced deformation, whereas versican/collagen interactions contribute to irreversible fibril reorganization via maintaining new crosslinking and fibril bundles formation. For higher order plastic deformation, the dramatic alterations of the collagen network via large scale fiber sliding, realignment and merging may obscure the relatively minor structural alterations from the interactions between versican and collagen fibrils.

In sum, versican plays an important role in modulating the mechanics of collagen networks. In contrast to other matrix PGs, versican and V3 soften collagen matrices and attenuate strain stiffening behaviors in vitro. Given the distinct mechanical effects of different PGs, understanding the time-dependent expression of different PGs quantitatively will shed light on ECM stiffening and its potential reversal during fibrogenesis. Moving forward to native tissues, versican and its CS side chains contribute to compression stiffening likely mainly because of the natural features of negatively-charged GAGs which attract water and increase osmotic pressure. Although the role of versican and its cleaved fragments in tissue mechanics is not fully understood, this work still strongly supports the potential of versican as a therapeutical target in collagen-related

fibroproliferative disorders for which there are dramatic alterations, especially tissue stiffening, in mechanics.

CHAPTER 6 CONCLUSIONS AND FUTURE DIRECTIONS

6.1 CONCLUSIONS

The compositional, structural, and mechanical complexities of the ECM are important for maintaining normal cell and tissue functions during development and homeostasis. Collagen forms the most fundamental network in the ECM, providing cell and tissue structure and supporting and enabling biochemical and biomechanical cues. Collagen fibrous networks are highly regulated by numerous factors including cells (Hall et al. 2016), externally applied mechanical force (Vader et al. 2009) and other ECM components including PGs (D. Chen et al. 2020). Matrix PGs, especially the SLRP subfamily (Kalamajski and Oldberg 2010), have been well studied as collagen binding partners (Kalamajski and Oldberg 2007)(Hedbom and Heinegard 1993) and key regulators of both in vitro and in vivo collagen fibrillogenesis (Reese, Underwood, and Weiss 2013)(Robinson et al. 2005). The hyalectan family of large matrix PGs, however, in particular versican, have been underestimated as important modulators of collagen behaviors in spite of their important roles (and increased expression) in collagen-related diseases (Bukong et al. 2016)(Lohmander et al. 1999). Unlike versican, the hyalectan aggrecan has been studied as a collagen binding protein because of its abundant accumulation in cartilage (Hedlund et al. 1999). Given versican's wide distribution in human tissues and altered deposition and degradation during fibrogenesis (Bukong et al. 2016)(Venkatesan et al. 2000), there is a particular need to investigate the effects of versican in regulating multiple collagen behaviors. In this work, I have studied the interaction between collagen and versican both in vitro and in vivo and have identified their binding sites. The role of versican in regulating collagen behaviors at multiple scales (different levels) has been investigated via different approaches covering collagen fibrillogenesis, fibrous network organization, cell-mediated collagen functions and mechanics.

Understanding the mechanism of the collagen/versican interaction is an essential start for evaluating the role of versican in modulating collagen behaviors. This work has confirmed that there is a direct interaction between versican and collagen in vitro and a colocalization of versican and collagen fibers in vivo. The versican/collagen binding sites have for the first time been identified as the versican C-terminal G3 domain and collagen sequences within Toolkit 4, 8, 11 and 18 peptides. Comparing the binding capacities for isolated versican, recombinant V3 isoform and recombinant G1 and G3 domains with a solid phase assay makes it possible to overcome the problem that native isolated versican is contaminated with some decorin and aggrecan, and enabled me to localize the binding site at the C-terminus (G3). Given the impurity of my isolated versican, the actual collagen binding with full length versican might show some differences which could be due to the physical repulsion caused by negatively charged GAGs; the core protein level interaction should remain consistent as my data showed that the positive bindings aligned well for isolated versican, V3 and G3. Evaluating the impact of pH and ionic strength illustrates the importance of charged residues, such as positive tracts including 3182-KYFAHRR-3188, 3306-KTFGKMKPR-3324, 3360-RTYSMKYFK-3368 and 3386-RWSRR-3390 and negative tracts including 3122-DQCELDFDE-3130 and 3163-EQDTETCD-3170 on the G3 domain, in mediating collagen/versican binding. The recent development of the Collagen Toolkit provided me with an approach to easily test various peptides that cover the entire amino acid sequence of type II collagen (which is similar in sequence to type I collagen) and this finding indicates that: the binding sites are likely located at the D1-period and the most commonly observed R-G-Hydrophobic-O motif (O represents hydroxyproline) is crucial for collagen/versican binding. Additionally, the colocalization of versican and collagen fibers using the in vivo IEM assay further supports the direct interaction between collagen and versican and the quantitative findings align well with the previous observation from our lab that versican is a potential collagen regulator during bile duct development (Khandekar et al. 2020).

I used collagen gels, specifically the gelation process and fibrous network structure, as an in vitro model to investigate: (1) collagen gelation, whereby the kinetic curves generated by the in vitro turbidity assay provide information partially representing fibrillogenesis; (2) fiber organization, to the extent that the relative structural features of networks persist after dehydration during SEM. In this work, versican demonstrated the unique (amongst the PGs studied) functions of upregulating collagen gelation (fibrillogenesis) and promoting the formation of a looser meshwork with larger fiber bundles and smaller pores. The behavior of versican in these assays is distinct from that of other matrix PGs including the structurally-similar hyalectan PG aggrecan. Further investigation into fibroblast-mediated collagen fibrillogenesis demonstrated again the unique role of versican in modulating cell derived collagen deposition and organization. The FDM assay also demonstrated an unusual role for versican in fibrillogenesis, as compared to other PGs, via promoting the deposition of collagen-rich matrix with increased fiber alignment mediated by fibroblasts. The collagen plug assay showed how versican, but not the other PGs tested, upregulates long-range force transmission-guided collagen compaction and realignment. The microfabricated engineered microtissue gauges, made it possible to evaluate the impact of ECM proteins on collagenous tissue contraction using less material than required for traditional collagen gel contraction assays. Studying higher level tissue organization, as modeled by the engineered microtissue gauges, showed that contraction of collagenous microtissues is also increased due to versican-mediated regulation of collagen reorganization, but does not occur with other PGs.

Tissue mechanics are dependent on the organization of collagen fibrous networks (Ban et al. 2019). Versican, as a regulator of collagen fiber organization, plays an important and potentially unique role in modulating tissue mechanics. I focused on shear modulus and non-linear rheological behaviors in this work, studying collagenous matrices in vitro and in tissues, specifically liver. Of the matrix PGs studied (including aggrecan and decorin, only the addition of versican (or its V3 isoform) into collagen gels decreased the G’ and attenuated the strain

stiffening behaviors. I believe these changed behaviors are due to decreased network connections, which I observed (by SEM) in collagen/versican co-gels. To study the impact of versican on tissue mechanics, I used enzymatic perfusions targeted at versican and GAGs to make it possible to assess the participation of versican and its CS side chains in tissue mechanics without using complicated animal models (such as versican conditional null mice). The loss of cleaved versican fragments and CS side chains eliminated compression stiffening, and the strain softening behaviors of treated tissues were numerically lower although not statistically different from controls. Importantly, the data suggest that versican and its CS chains also play a role in maintaining tissue plasticity under small deformation (about 2%) via the versican/collagen interaction and an additional undefined CS/collagen interaction.

Overall, this thesis demonstrates the direct binding between collagen and versican, highlights the unique roles of versican in upregulating collagen fibrillogenesis, condensation, alignment, and contraction in contrast to other PGs, and indicates the specific contribution of versican into collagen and tissue mechanics. The distinct regulations of different matrix PGs on collagen structure and mechanics shed light on the importance of evaluating the time-dependent deposition of different PGs quantitatively, which will yield a better understanding of the structural and mechanical complexity of ECM and tissue. Versican, which binds HA via its N-terminal G1 and collagen via its C-terminal G3, could function as a linker between collagen fibers and long HA chains in ECM modulating the organization of this complex fibrous network (Figure 6.1A, B). Unlike SLRPs, which binding collagen monomers and affect fibril formation, versican is likely to participate in higher-level fiber organization given its large molecular weight and formation of HA/versican bio-aggregates. In addition, aggrecan can bind HA via its G1 domain and collagen via its KS domain, which maintains a fixed and relatively close distance between collagen fibers and HA chains (Figure 6.1A). However, the core protein of different versican isoforms can range from 74 kDa to 372 kDa, which might result in dramatically altered distances between collagen

fibers and HA chains in the fibrous network (Figure 6.1A). Negatively-charged CS side chains and HA are likely to preferentially occupy void space (attracting water) and the presence of different isoforms with distinct GAG domains might alter the space filling ability. Thus, different versican isoforms, as distinct linkers (spacers) between collagen and HA, can likely modulate collagen/versican/HA networks differently due to their various length and charge densities. These linkers can further modulate mechanics by regulating network structure including fiber arrangement and hydrated pore space and altering the osmotic pressure from GAG-induced swelling. Although collagen and HA can interact with each other, highly negatively charged versican and HA/versican aggregates could hypothetically inhibit their direct interaction. Therefore, versican, as a linker within a collagen/HA network, almost certainly has an important role in tissue structure and mechanics. For example, I report here that versican-induced cell-mediated collagen realignment is pH sensitive (Figure 4.5G). Decreasing pH, with increasing H+, could neutralize negatively-charged CS to downregulate the charge-mediated physical repulsion between fibers. Meanwhile, the cleavage of versican by ADAMTS-5 could break the link between collagen fibers and HA chains, weakening the network and suppressing tissue stiffening under compression. Given the finding that versican upregulates collagen compaction, alignment and fiber fusion into bundles, it could have a crucial physiological function during fibrogenesis as a cause of the highly condensed and aligned collagen fibers that I observed by SEM and in the collagen plug assay. By decreasing versican expression and increasing its degradation, it might be possible to downregulate collagen deposition, fibrous network condensation and tissue stiffness, which could make it possible to reverse fibrogenesis and fibrosis. Thus, versican, as a unique regulator of collagen behaviors, needs to be further investigated as a modulator for embryonic development, homeostasis, and tissue remodeling and as a therapeutic target for collagen-related fibroproliferative disorders including fibrosis, metastasis and inflammation.

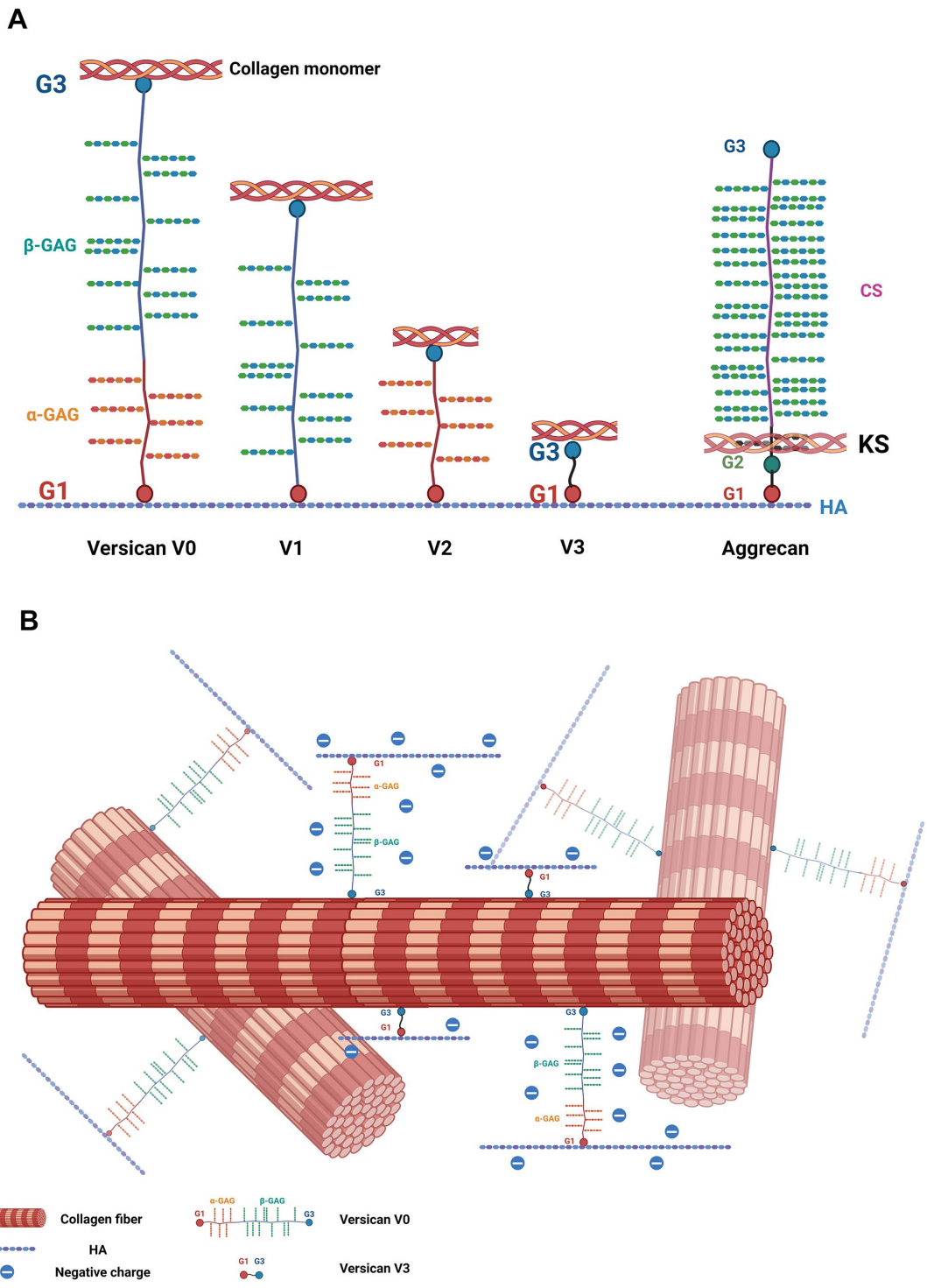
A
G3
Collagen monomer
β-GAG
α-GAG
G1
CS
KS
G2
HA
Versican V0
V1
V2
V3
Aggrecan
B
Collagen fiber
HA
Negative charge
Versican V0
Versican V3

Figure 6.1 Schematic of the interaction between collagen and large PGs and the collagen/versican/HA network. (A) The collagen binding sites on different versican isoforms and aggrecan. (B) Versican could function as a linker between collagen fibers and HA chains in fibrous network. The diameter of collagen fibril/fiber is about 200 nm and the size of isolated versican is 203.4 nm (measured by dynamic light scattering, data not shown here). (Illustrations were created with BioRender.com).

6.2 FUTURE DIRECTIONS

6.2.1 Define the collagen/versican interaction in more detail

In this work, I started using isolated versican and the recombinant V3 isoform (G1 and G3 domains only) to investigate versican/collagen interactions. Binding has been confirmed in both cases and thus I have used recombinant V3, which contains the collagen binding site of versican, to identify the binding sites. Given the similar binding results from isolated versican, V3 and G3, my findings strongly support that G3 is the major collagen binding domain of versican. Notably, however, the collagen binding capacity of the GAG binding domains of versican have not been well studied here. To overcome this limitation, there are several approaches that could be used in future experiments. The first is based on the isolation and purification of different versican isoforms from native tissue. Although versican is generally expressed in most tissues, there is a differential deposition of different isoforms. For example, V1 is the most common isoform in liver (Cattaruzza et al. 2002) while V2 is the major isoform found in bovine brain (Schmalfeldt et al. 1998). Selecting a source tissue with higher expression of certain isoforms combined with long-term ultracentrifugation or size-exclusion chromatography would make it possible to isolate and purify single isoforms according to their abundance and molecular weight. Gene-edited fibroblasts with overexpression of selected versican isoforms could also achieve the production of pure isoforms derived from cell lysate, although versican is a large gene and proper GAG modification could be difficult to achieve (Sheng et al. 2005). Another approach would be to synthesize

recombinant versican fragments and even versican mimetic peptides (as for the synthesis of the Collagen Toolkit) for studying the binding in more detail. Comparing the binding affinity of different versican isoforms and recombinant versican peptides will shed light on the role of the GAG domain, if it has one, in versican/collagen interactions and may uncover other potential collagen binding sites on versican and generate distinct collagen binding models for specific isoforms. GAGs themselves, as collagen regulators, can also mediate collagen/versican interactions via the negative charges and resulting physical repulsion and electrostatic interactions. For example, CS can accelerate in vitro fibrillogenesis and alter fibrous networks by increasing void space which is further correlated with decreased gel stiffness (Stuart and Panitch 2008). In addition, my work indicates that the collagen/versican interaction is pH and ionic strength dependent, highlighting the importance of highly charged motifs in this interaction. Given that the G3 domain of versican contains the collagen binding site, evaluating the binding capacity of recombinant highly charged motifs (such as positive tracts including 3182-KYFAHRR-3188, 3306-KTFGKMKPR-3324, 3360-RTYSMKYFK-3368 and 3386-RWSRR-3390 and negative tracts including 3122-DQCELDFDE-3130 and 3163-EQDTETCD-3170, shown in Figure 2.7) will enable better development of a collagen/versican binding model. The 3D structure/conformation of versican, including the V0-V3 isoforms and the G3 domain, remains unknown and should be solved using X-ray crystallography (Y. Shi 2014) and cryo-EM (Danev, Yanagisawa, and Kikkawa 2019). This requires a pure versican sample but could be beneficial to understanding the structural interactions between collagen and versican (including different isoforms).

6.2.2 Understand the distinct effects of different versican isoforms in altering collagen behaviors

Given the evidence that distinct versican isoforms have diverse or even opposing effects on cell functions (Ricciardelli et al. 2009) and that CS can play a role in collagen fibrillogenesis (Stuart and Panitch 2008)(Moorehead, Prudnikova, and Marcolongo 2019), the V0-V3 isoforms may

have distinct effects on collagen behaviors including fibrillogenesis, fiber organization and mechanics. The investigations described in 6.2.1 would provide more information, especially on the interaction between collagen and versican isoforms, and would provide important information about the importance and feasibility of studying specific isoform-mediated collagen behaviors. After obtaining versican isoforms (as in 6.2.1), the in vitro turbidity assay, FDM and engineered microtissue assays used in this thesis could also be carried out to evaluate the influence of specific isoforms in altering collagen gelation, fibroblast-mediated collagen fibril deposition and organization as well as their role in collagenous tissue contraction. If enough of each versican isoform could be isolated from native tissues or cell lysates, a collagen plug assay and collagen/isoform co-gel rheometry could be carried out and would provide a better understanding of isoform-dependent cell-mediated collagen reorganization and collagen network mechanics. Given the fact that there is a differential versican isoform expression during embryonic development (Snyder et al. 2015)(Landolt et al. 1995) and a tissue specific isoform deposition (Cattaruzza et al. 2002), investigating the isoform-dependent regulation of collagen functions will help to explain the mechanism underlying the spatially and temporally variant expression of different versican isoforms. Thus, certain versican isoforms may be crucial for maintaining the normal functions of certain tissues and the same isoform-dependent pattern could also be taken into consideration when studying versican-related disorders.

6.2.3 Investigate the role of versican in collagen behaviors when forming HA/versican aggregates

Versican, regardless of its different isoforms, has an N-terminal G1 domain that binds HA to form a large bottlebrush like bio-aggregate which can be stabilized by Link proteins (S. Shi et al. 2004). These HA/CSPG aggregates are important structural components of many tissues including articular cartilage and blood vessels. In this thesis, I have learned that there are specific effects of versican, even without binding HA to form bio-aggregates, on the regulation of in vitro collagen

gel stiffness; the presence of HA in collagen/versican co-gels balances the softening from versican via HA-induced network stiffening (Figure 5.6). The mechanical differences suggest that HA/versican aggregates may have specific structural effects on collagen fibrous networks since versican is a linker that binds HA via its G1 domain and collagen via its G3 domain. The presence of HA/versican bio-aggregates could control the distance between collagen fibers and HA chains and fill the void space between fibers, which can further alter the organization of collagen fibrous network. Given the distinct molecular weights and GAG quantities of versican isoforms, HA aggregates bound with different isoforms might have distinct effects on fibrous networks that could also change the mechanics in different ways. To validate this hypothesis, in vitro collagen gels could be manipulated with HA and versican (various isoforms generated from 6.2.1) aggregates and their roles in collagen gelation (fibrillogenesis), fibrous network structure and tissue contraction could be evaluated using the turbidity assay, FDM, SEM and engineered microtissue assays. The amount of isolated isoforms would determine the feasibility of studying the impact of HA/versican aggregates on cell-mediated collagen compaction and realignment using the collagen plug assay; this is also true for using shear rheometry to assess the isoform-dependent effects of these aggregates in the viscoelasticity of collagen gels given the fact that both assays require significant amount of gel solution (1 mL for 3 technical repeats).

6.2.4 Investigate the role of versican in tissue structure and mechanics using mouse models

In this work, in vitro assays including SEM (on collagen gels), FDM and collagen plug assays have been carried out to study the structure of fibrous networks and cell-mediated collagen reorganization, although the structural regulation of the collagen/versican interaction in vivo has not been investigated in detail here. Mouse models with altered versican expression could provide diverse tissue samples to study the role of versican in collagen organization in vivo. There are three published mouse models available to achieve this goal: versican-deficient mice

(Kang et al. 2017), versican knockin mice (versican overexpression) (Islam et al. 2020), and ADAMTS-4 and -5 knockout mice (versican proteolysis is protected) (Demircan et al. 2014). Collagen fibrous networks in liver samples (or other tissues) could be imaged by SHG and versican and HA stained with anti-versican antibodies and HA binding protein (HABP). The organization of the collagen fibrous network in versican-deficient and -overexpressed samples should be compared by analyzing SHG images using CT-FIRE for fiber size, length and orientation quantification. Given the evidence that versican regulates hepatic fibrosis (Bukong et al. 2016), the carbon tetrachloride (CCl_4) method of inducing liver fibrosis could be applied to these mouse models, which have different levels of versican expression, and used to evaluate the effect of versican on collagen network alterations during fibrogenesis as well as recovery. As versican causes upregulation of collagen compaction, alignment and contraction, I predict that increased deposition of versican will worsen fibrosis by condensing and realigning collagen fibers with increased fiber entanglement into bundles.

Livers perfused with ADAMTS-5 and studied with shear rheometry have been used in this work to explore the mechanical functions of versican in native tissues. However, incomplete knowledge of versican proteolysis and the localization of some proteolytic products after prefusion make it difficult to interpret the relationship between versican (as well as its cleaved fragments) and tissue mechanics. Importantly, a recent publication using quantitative proteomics has discovered additional 21 cleavage sites for ADAMTS-1, -4 and -5 degradation (with 9 novel sites for ADAMTS-5) (Martin et al. 2021). Thus, I cannot fully understand the relationship between versican and tissue mechanics based on my findings. In the future, mouse models with versican deficiency or overexpression will shed light on the contribution of versican in modulating tissue mechanics. The relationship can be quantitatively established by evaluating versican content in different mouse models and measuring tissue viscoelasticity as well as non-linear rheological behaviors. Using the CCl_4 liver fibrosis model in these mouse models would help to understand

the role of versican in mediating tissue stiffening during fibroproliferative processes. Nanoindentation on un-aligned and aligned collagen areas with an analysis of versican deposition in corresponding areas could also be used to study the regulation of versican on collagen bridging in vivo and its effect on local ECM stiffening within the highly aligned collagen bundles.

6.2.5 Understand the role of different matrix PGs expression in collagen behaviors

It has been confirmed many times via diverse approaches in this work that distinct matrix PGs, even belonging to the same subfamily and having structural similarities, have different effects on collagen structural and mechanical behaviors. Differential expression and deposition of matrix PGs have been observed in multiple physiological settings including embryonic development and fibrosis. During tendon development, both lumican and fibromodulin mediate fibrillogenesis at the early stage but only fibromodulin plays a dominant role in maturation with an upregulated ratio of fibromodulin to lumican (Ezura et al. 2000). For collagen assembly in cornea, lumican deficiency as well as lumican/biglycan double deficiency leads to corneal opacity with irregular collagen organization and abnormal fiber size while biglycan deficiency has no impact (S. Chen et al. 2014). When studying bile duct development, our group has also found that different matrix PGs have a distinct time course of deposition: lumican deposition decreases over time while decorin remains constant (Khandekar et al. 2020). As for fibrotic disorders, taking liver as an example, lumican and aggrecan show a time-dependent expression but fibromodulin does not (Krull and Gressner 1992). Although both lumican and versican expression has been found to increase during liver fibrosis, lumican deficiency cannot inhibit fibrogenesis while versican deficiency results in decreased fibrogenesis and reduced proliferation (Bukong et al. 2016)(Krishnan et al. 2012). Thus, there is a particular interest in quantitatively investigating the spatial and temporal deposition of different matrix PGs by carrying out western blots on tissue samples harvested at various time points during development or fibrogenesis. After knowing the dynamics of matrix PG

content during a physiological process, the most predominant PG at a crucial time, such as during initiation of fibril assembly into fibers or the development of bridging fibrosis, will be regarded as a regulatory target for future therapeutic research. This quantitative information will also help with understanding the correlation between structure and mechanics of collagen fibrous networks. This thesis has already provided quantitative data on the structure of collagen/PG networks including fiber diameter and length, network connection and pore size. A future collaboration with a computational modeling group which has expertise in theoretical mechanobiology would help build the model to explain the correlation between PG-related structural features and collagen mechanics by using inputs including PG content and structural information and outputs such as G' or even complicated strain stiffening behaviors.

BIBLIOGRAPHY

Abhilash, A. S., Brendon M. Baker, Britta Trappmann, Christopher S. Chen, and Vivek B. Shenoy. 2014. “Remodeling of Fibrous Extracellular Matrices by Contractile Cells: Predictions from Discrete Fiber Network Simulations.” *Biophysical Journal* 107 (8): 1829–40. https://doi.org/10.1016/j.bpj.2014.08.029.

Achilli, Matteo, and Diego Mantovani. 2010. “Tailoring Mechanical Properties of Collagen-Based Scaffolds for Vascular Tissue Engineering: The Effects of PH, Temperature and Ionic Strength on Gelation.” *Polymers* 2 (4): 664–80. https://doi.org/10.3390/polym2040664.

Al-Jamal, Rehab, and Mara S. Ludwig. 2001. “Changes in Proteoglycans and Lung Tissue Mechanics During Excessive Mechanical Ventilation in Rats.” *American Journal of Physiology - Lung Cellular and Molecular Physiology* 281 (5): 1078–87. https://doi.org/10.1152/ajplung.2001.281.5.l1078.

Alberton, Paolo, Hans Christian Dugonitsch, Bastian Hartmann, Ping Li, Zsuzsanna Farkas, Maximilian Michael Saller, Hauke Clausen-Schaumann, and Attila Aszodi. 2019. “Aggrecan Hypomorphism Compromises Articular Cartilage Biomechanical Properties and Is Associated with Increased Incidence of Spontaneous Osteoarthritis.” *International Journal of Molecular Sciences* 20 (5). https://doi.org/10.3390/ijms20051008.

Appunni, Sandeep, Vivek Anand, Madhuram Khandelwal, Nidhi Gupta, Muni Rubens, and Alpana Sharma. 2019. “Small Leucine Rich Proteoglycans (Decorin, Biglycan and Lumican) in Cancer.” *Clinica Chimica Acta* 491 (January): 1–7. https://doi.org/10.1016/j.cca.2019.01.003.

Aspberg, Anders. 2012. “The Different Roles of Aggrecan Interaction Domains.” *Journal of Histochemistry and Cytochemistry* 60 (12): 987–96. https://doi.org/10.1369/0022155412464376.

Balian, Gary, Eva Marie Click, and Paul Bornstein. 1980. “Location of a Collagen-Binding Domain in Fibronectin.” *Journal of Biological Chemistry* 255 (8): 3234–36.

Ban, Ehsan, J. Matthew Franklin, Sungmin Nam, Lucas R. Smith, Hailong Wang, Rebecca G. Wells, Ovijit Chaudhuri, Jan T. Liphardt, and Vivek B. Shenoy. 2018. “Mechanisms of Plastic Deformation in Collagen Networks Induced by Cellular Forces.” *Biophysical Journal* 114 (2): 450–61. https://doi.org/10.1016/j.bpj.2017.11.3739.

Ban, Ehsan, Hailong Wang, J. Matthew Franklin, Jan T. Liphardt, Paul A. Janmey, and Vivek B. Shenoy. 2019. “Strong Triaxial Coupling and Anomalous Poisson Effect in Collagen Networks.” *Proceedings of the National Academy of Sciences of the United States of America* 116 (14): 6790–99. https://doi.org/10.1073/pnas.1815659116.

Banos, Charles C., Amelia H. Thomas, and Catherine K. Kuo. 2008. “Collagen Fibrillogenesis in Tendon Development: Current Models and Regulation of Fibril Assembly.” *Birth Defects Research Part C - Embryo Today: Reviews* 84 (3): 228–44. https://doi.org/10.1002/bdrc.20130.

Baselt, David R., Jean-Paul Revel, and John D. Baldeschwieler. 1993. “Subfibrillar Structure of Type I Collagen Observed by Atomic Force Microscopy.” *Biophysical Journal* 65 (6): 2644–55. https://doi.org/10.1016/S0006-3495(93)81329-8.

Bensadoun, Eric S., Adrian K. Burke, James C. Hogg, and Clive R. Roberts. 1996. “Proteoglycan Deposition in Pulmonary Fibrosis.” *American Journal of Respiratory and Critical Care Medicine* 154 (6): 1819–28. https://doi.org/10.1164/ajrccm.154.6.8970376.

Bierbaum, Susanne, Timothy Douglas, Thomas Hanke, Dieter Scharnweber, Sonja Tippelt, Thomas K. Monsees, and Richard H. W. Funk. 2006. “Collageneous Matrix Coatings on Titanium Implants Modified with Decorin and Chondroitin Sulfate: Characterization and Influence on Osteoblastic Cells.” *Journal of Biomedical Materials Research. Part A* 77A (3): 551–62. https://doi.org/10.1002/jbm.a.

Birk, David E. 2001. “Type V Collagen: Heterotypic Type I/V Collagen Interactions in the Regulation of Fibril Assembly.” *Micron* 32 (3): 223–37.

Birk, David E., and Robert L. Trelstad. 1986. “Extracellular Compartments in Tendon Morphogenesis: Collagen Fibril, Bundle, and Macroaggregate Formation.” *Journal of Cell Biology* 103 (1): 231–40. https://doi.org/10.1083/jcb.103.1.231.

Bittner, Katharina, Claudia Liszio, Petra Blumberg, Elke Schönherr, and Hans Kresse. 1996. “Modulation of Collagen Gel Contraction by Decorin.” *Biochemical Journal* 314 (1): 159–66. https://doi.org/10.1042/bj3140159.

Bode-Lesniewska, Beata, María T. Dours-Zimmermann, Bernhard F. Odermatt, Jakob Briner, Philipp U. Heitz, and Dieter R. Zimmermann. 1996. “Distribution of the Large Aggregating Proteoglycan Versican in Adult Human Tissues.” *Journal of Histochemistry and Cytochemistry* 44 (4): 303–12. https://doi.org/10.1177/44.4.8601689.

Boudaoud, Arezki, Agata Burian, Dorota Borowska-Wykręt, Magalie Uyttewaal, Roman Wrzalik, Dorota Kwiatkowska, and Olivier Hamant. 2014. “FibrilTool, an ImageJ Plug-in to Quantify Fibrillar Structures in Raw Microscopy Images.” *Nature Protocols* 9 (2): 457–63. https://doi.org/10.1038/nprot.2014.024.

Bozec, Laurent, and Michael Horton. 2005. “Topography and Mechanical Properties of Single Molecules of Type I Collagen Using Atomic Force Microscopy.” *Biophysical Journal* 88 (6): 4223–31. https://doi.org/10.1529/biophysj.104.055228.

Brightman, A. O., B. P. Rajwa, J. E. Sturgis, M. E. McCallister, J. P. Robinson, and S. L. Voytik-Harbin. 2000. “Time-Lapse Confocal Reflection Microscopy of Collagen Fibrillogenesis and Extracellular Matrix Assembly In Vitro.” *Biopolymers* 54 (3): 222–34. https://doi.org/10.1002/1097-0282(200009)54:3<222::AID-BIP80>3.0.CO;2-K.

Buehler, Markus J. 2006. “Nature Designs Tough Collagen: Explaining the Nanostructure of Collagen Fibrils.” *Proceedings of the National Academy of Sciences of the United States of*

America 103 (33): 12285–90. https://doi.org/10.1073/pnas.0603216103.

Bukong, Terence N., Sean B. Maurice, Barinder Chahal, David F. Schaeffer, and Paul J. Winwood. 2016. “Versican: A Novel Modulator of Hepatic Fibrosis.” *Laboratory Investigation* 96 (3): 361–74. https://doi.org/10.1038/labinvest.2015.152.

Canty, Elizabeth G., and Karl E. Kadler. 2005. “Procollagen Trafficking, Processing and Fibrillogenesis.” *Journal of Cell Science* 118 (7): 1341–53. https://doi.org/10.1242/jcs.01731.

Carthy, Jon M., Anna J. Meredith, Seti Boroomand, Thomas Abraham, Zongshu Luo, Darryl Knight, and Bruce M. McManus. 2015. “Versican V1 Overexpression Induces a Myofibroblast-like Phenotype in Cultured Fibroblasts.” *PLoS ONE* 10 (7): 1–16. https://doi.org/10.1371/journal.pone.0133056.

Carthy, Jon, Maziar Rahmani, Seti Boroomand, Darryl Knight, and Bruce McManus. 2008. “Versican Induces Fibroblast Contraction of Collagen Gels.” *Matrix Biology* 27 (time 0): 56–57. https://doi.org/10.1016/j.matbio.2008.09.409.

Cattaruzza, Sabrina, Monica Schiappacassi, Åsa Ljungberg-Rose, Paola Spessotto, Daniela Perissinotto, Matthias Mörgelin, Maria Teresa Mucignat, Alfonso Colombatti, and Roberto Perris. 2002. “Distribution of PG-M/Versican Variants in Human Tissues and de Novo Expression of Isoform V3 upon Endothelial Cell Activation, Migration, and Neoangiogenesis in Vitro.” *Journal of Biological Chemistry* 277 (49): 47626–35. https://doi.org/10.1074/jbc.M206521200.

Chakravarti, Shukti, Guiyun Zhang, Inna Chervoneva, Luke Roberts, and David E. Birk. 2006. “Collagen Fibril Assembly during Postnatal Development and Dysfunctional Regulation in the Lumican-Deficient Murine Cornea.” *Developmental Dynamics* 235 (9): 2493–2506. https://doi.org/10.1002/dvdy.20868.

Chen, Dongning, Lucas R. Smith, Gauri Khandekar, Pavan Patel, Christopher K. Yu, Kehan Zhang, Christopher S. Chen, Lin Han, and Rebecca G. Wells. 2020. “Distinct Effects of

Different Matrix Proteoglycans on Collagen Fibrillogenesis and Cell-Mediated Collagen Reorganization." *Scientific Reports* 10 (1): 1–13. https://doi.org/10.1038/s41598-020-76107-0.

Chen, Shoujun, Marian F. Young, Shukti Chakravarti, and David E. Birk. 2014. "Interclass Small Leucine-Rich Repeat Proteoglycan Interactions Regulate Collagen Fibrillogenesis and Corneal Stromal Assembly." *Matrix Biology* 35: 103–11. https://doi.org/10.1016/j.matbio.2014.01.004.

Chen, Yunfeng, Lining Ju, Muaz Rushdi, Chenghao Ge, and Cheng Zhu. 2017. "Receptor-Mediated Cell Mechanosensing." *Molecular Biology of the Cell* 28 (23): 3134–55. https://doi.org/10.1091/mbc.E17-04-0228.

Chockalingam, Priya S., Weilan Zeng, Elisabeth A. Morris, and Carl R. Flannery. 2004. "Release of Hyaluronan and Hyaladherins (Aggrecan G1 Domain and Link Proteins) From Articular Cartilage Exposed to ADAMTS-4 (Aggrecanase 1) or ADAMTS-5 (Aggrecanase 2)." *Arthritis & Rheumatism* 50 (9): 2839–48. https://doi.org/10.1002/art.20496.

Chopra, Anant, Matthew L Kutys, Kehan Zhang, William J Polacheck, Calvin C Sheng, Rebeccah J Luu, Jeroen Eyckmans, et al. 2018. "Force Generation via β-Cardiac Myosin, Titin, and α-Actinin Drives Cardiac Sarcomere Assembly from Cell-Matrix Adhesions." *Developmental Cell* 44 (1): 87–96. https://doi.org/10.1016/j.devcel.2017.12.012.

Chopra, Anant, Erdem Tabdanov, Hersh Patel, Paul A Janmey, and J Yasha Kresh. 2011. "Cardiac Myocyte Remodeling Mediated by N-Cadherin-Dependent Mechanosensing." *Am J Physiol Heart Circ Physiol* 300 (4): 1252–66. https://doi.org/10.1152/ajpheart.00515.2010.

Danev, Radostin, Haruaki Yanagisawa, and Masahide Kikkawa. 2019. "Cryo-Electron Microscopy Methodology: Current Aspects and Future Directions." *Trends in Biochemical Sciences* 44 (10): 837–48. https://doi.org/10.1016/j.tibs.2019.04.008.

Demircan, Kadir, Vehap Topcu, Tomoyuki Takigawa, Sumeyya Akyol, Tomoko Yonezawa, Gulfer

Ozturk, Veli Ugurcu, et al. 2014. “ADAMTS4 and ADAMTS5 Knockout Mice Are Protected from Versican but Not Aggrecan or Brevican Proteolysis During Spinal Cord Injury.” *BioMed Research International* 2014: 693746. https://doi.org/10.1155/2014/693746.

Desmoulière, Alexis, Christine Chaponnier, and Giulio Gabbiani. 2005. “Tissue Repair, Contraction, and the Myofibroblast.” *Wound Repair and Regeneration* 13 (1): 7–12. https://doi.org/10.1111/j.1067-1927.2005.130102.x.

Dewavrin, Jean Yves, Nader Hamzavi, V. P.W. Shim, and Michael Raghunath. 2014. “Tuning the Architecture of Three-Dimensional Collagen Hydrogels by Physiological Macromolecular Crowding.” *Acta Biomaterialia* 10 (10): 4351–59. https://doi.org/10.1016/j.actbio.2014.06.006.

Diamantides, Nicole, Louis Wang, Tylar Pruiksma, Joseph Siemiatkoski, Caroline Dugopolski, Sonya Shortkroff, Stephen Kennedy, and Lawrence J. Bonassar. 2017. “Correlating Rheological Properties and Printability of Collagen Bioinks: The Effects of Riboflavin Photocrosslinking and PH.” *Biofabrication* 9 (3). https://doi.org/10.1088/1758-5090/aa780f.

Doege, Kurt J., and John H. Fessler. 1986. “Folding of Carboxyl Domain and Assembly of Procollagen I.” *Journal of Biological Chemistry* 261 (19): 8924–35. https://doi.org/10.1016/s0021-9258(19)84471-x.

Dours-Zimmermann, Maria T., and Dieter R. Zimmermann. 1994. “A Novel Glycosaminoglycan Attachment Domain Identified in Two Alternative Splice Variants of Human Versican.” *Journal of Biological Chemistry* 269 (52): 32992–98. https://doi.org/10.1016/s0021-9258(20)30089-2.

Dourte, Leann M., Lydia Pathmanathan, Abbas F. Jawad, Renato V. Iozzo, Michael J. Mienaltowski, David E. Birk, and Louis J. Soslowsky. 2012. “Influence of Decorin on the Mechanical, Compositional, and Structural Properties of the Mouse Patellar Tendon.” *Journal of Biomechanical Engineering* 134 (3): 1–8. https://doi.org/10.1115/1.4006200.

Du, William Weidong, Weining Yang, and Albert J. Yee. 2013. “Roles of Versican in Cancer Biology--Tumorigenesis, Progression and Metastasis.” *Histol Histopathol* 28 (6): 701–13. https://doi.org/HH-11-300 [pii].

Durigova, M., P. Soucy, K. Fushimi, H. Nagase, J. S. Mort, and P. J. Roughley. 2008. “Characterization of An ADAMTS-5-Mediated Cleavage Site in Ggrecan in OSM-Stimulated Bovine Cartilage.” *Osteoarthritis and Cartilage* 16 (10): 1245–52. https://doi.org/10.1016/j.joca.2008.02.013.

Dzamba, Bette J., Hong Wu, Rudolf Jaenisch, and Donna M. Peters. 1993. “Fibronectin Binding Site in Type I Collagen Regulates Fibronectin Fibril Formation.” *Journal of Cell Biology* 121 (5): 1165–72. https://doi.org/10.1083/jcb.121.5.1165.

Emsley, Jonas, C. Graham Knight, Richard W. Farndale, Michael J. Barnes, and Robert C. Liddington. 2000. “Structural Basis of Collagen Recognition by Integrin A2β1.” *Cell* 101 (1): 47–56. https://doi.org/10.1016/S0092-8674(00)80622-4.

Ezura, Yoichi, Shukti Chakravarti, Ake Oldberg, Inna Chervoneva, and David E. Birk. 2000. “Differential Expression of Lumican and Fibromodulin Regulate Collagen Fibrillogenesis in Developing Mouse Tendons.” *Journal of Cell Biology* 151 (4): 779–87. https://doi.org/10.1083/jcb.151.4.779.

Farber, Steven, Atul K. Garg, David E. Birk, and Frederick H. Silver. 1986. “Collagen Fibrillogenesis in Vitro: Evidence for Pre-Nucleation and Nucleation Steps.” *International Journal of Biological Macromolecules* 8 (1): 37–42. https://doi.org/10.1016/0141-8130(86)90069-3.

Farndale, Richard W. 2019. “Collagen-Binding Proteins: Insights from the Collagen Toolkits.” *Essays in Biochemistry* 63 (3): 337–48. https://doi.org/10.1042/EBC20180070.

Fleischmajer, Raul, Larry W. Fisher, E. Douglas MacDonald, Lloydstone Jacobs, Jerome S. Perlish, and John D. Termine. 1991. “Decorin Interacts with Fibrillar Collagen of Embryonic

and Adult Human Skin." *Journal of Structural Biology* 106 (1): 82–90. https://doi.org/10.1016/1047-8477(91)90065-5.

Franco-Barraza, Janusz, Dorothy A. Beacham, Michael D. Amatangelo, and Edna Cukierman. 2016. "Preparation of Extracellular Matrices Produced by Cultured and Primary Fibroblasts." *Current Protocols in Cell Biology* 2016: 10.9.1-10.9.34. https://doi.org/10.1002/cpcb.2.

Gelse, K., E. Pöschl, and T. Aigner. 2003. "Collagens - Structure, Function, and Biosynthesis." *Advanced Drug Delivery Reviews* 55 (12): 1531–46. https://doi.org/10.1016/j.addr.2003.08.002.

Georges, Penelope C., Jia-ji Hui, Zoltan Gombos, Margaret E. Mccormick, Andrew Y. Wang, Masayuki Uemura, Rosemarie Mick, Paul A. Janmey, Emma E. Furth, and Rebecca G. Wells. 2007. "Increased Stiffness of the Rat Liver Precedes Matrix Deposition : Implications for Fibrosis." *Am J Physiol Gastrointest Liver Physiol* 293 (6): 1147–54. https://doi.org/10.1152/ajpgi.00032.2007.

Gordon, Marion K., and Rita A. Hahn. 2010. "Collagens." *Cell Tissue Research* 339 (1): 247–57. https://doi.org/10.1038/jid.2014.371.

Gressner, Axel M., and Anette Vasel. 1985. "Developmental Changes of Proteoglycan Synthesis in Rat Liver and Isolated Hepatocytes." *Mechanisms of Ageing and Development* 31 (3): 307–27. https://doi.org/10.1016/0047-6374(85)90097-1.

Griffiths, J. R. 1991. "Are Cancer Cells Acidic?" *British Journal of Cancer* 64 (3): 425–27. https://doi.org/10.1038/bjc.1991.326.

Halász, Krisztina, Anja Kassner, Matthias Mörgelin, and Dick Heinegård. 2007. "COMP Acts as A Catalyst in Collagen Fibrillogenesis." *Journal of Biological Chemistry* 282 (43): 31166–73. https://doi.org/10.1074/jbc.M705735200.

Hall, Matthew S., Farid Alisafaei, Ehsan Ban, Xinzeng Feng, Chung Yuen Hui, Vivek B. Shenoy,

and Mingming Wu. 2016. “Fibrous Nonlinear Elasticity Enables Positive Mechanical Feedback Between Cells and ECMs.” *Proceedings of the National Academy of Sciences of the United States of America* 113 (49): 14043–48. https://doi.org/10.1073/pnas.1613058113.

Han, Weijing, Shaohua Chen, Wei Yuan, Qihui Fan, Jianxiang Tian, Xiaochen Wang, Longqing Chen, et al. 2016. “Oriented Collagen Fibers Direct Tumor Cell Intravasation.” *Proceedings of the National Academy of Sciences of the United States of America* 113 (40): 11208–13. https://doi.org/10.1073/pnas.1610347113.

Harris, J. Robin, Andrei Soliakov, and Richard J. Lewis. 2013. “In Vitro Fibrillogenesis of Collagen Type I in Varying Ionic and PH Conditions.” *Micron* 49: 60–68. https://doi.org/10.1016/j.micron.2013.03.004.

Hedbom, Erik, and Dick Heinegard. 1993. “Binding of Fibromodulin and Decorin to Separate Sites on Fibrillar Collagens.” *Journal of Biological Chemistry* 268 (36): 27307–12.

Hedlund, Håkan, Erik Hedbom, Dick Heinegård, Silwa Mengarelli-Widholm, Finn P. Reinholt, and Olle Svensson. 1999. “Association of the Aggrecan Keratan Sulfate-Rich Region with Collagen in Bovine Articular Cartilage.” *Journal of Biological Chemistry* 274 (9): 5777–81. https://doi.org/10.1074/jbc.274.9.5777.

Herrera, Jeremy, Craig A. Henke, and Peter B. Bitterman. 2018. “Extracellular Matrix as a Driver of Progressive Fibrosis.” *Journal of Clinical Investigation* 128 (1): 45–53. https://doi.org/10.1172/JCI93557.

Hinz, Boris. 2012. “Mechanical Aspects of Lung Fibrosis: A Spotlight on the Myofibroblast.” *Proceedings of the American Thoracic Society* 9 (3): 137–47. https://doi.org/10.1513/pats.201202-017AW.

Hulmes, David J. S., Jean-claude Jesiort, Andrew Millert, and Carmen Berthet-colominast. 1981. “Electron Microscopy Shows Periodic Structure in Collagen Fibril Cross Sections.” *PNAS* 78

(6): 3567–71.

Humphries, Sally M., Yinhui Lu, Elizabeth G. Canty, and Karl E. Kadler. 2008. “Active Negative Control of Collagen Fibrillogenesis in Vivo: Intracellular Cleavage of the Type I Procollagen Propeptides in Tendon Fibroblasts without Intracellular Fibrils.” *Journal of Biological Chemistry* 283 (18): 12129–35. https://doi.org/10.1074/jbc.M708198200.

Iozzo, Renato V., and Liliana Schaefer. 2015. “Proteoglycan Form and Function: A Comprehensive Nomenclature of Proteoglycans.” *Matrix Biology* 42: 11–55. https://doi.org/10.1016/j.matbio.2015.02.003.

Islam, Shamima, Kantinan Chuensirikulchai, Saichit Khummuang, Tanyaporn Keratibumrungpong, Prachya Kongtawelert, Watchara Kasinrerk, Sonoko Hatano, Akiko Nagamachi, Hiroaki Honda, and Hideto Watanabe. 2020. “Accumulation of Versican Facilitates Wound Healing: Implication of Its Initial ADAMTS-Cleavage Site.” *Matrix Biology* 87 (xxxx): 77–93. https://doi.org/10.1016/j.matbio.2019.10.006.

Jansen, Karin A., Albert J. Licup, Abhinav Sharma, Robbie Rens, Fred C. MacKintosh, and Gijsje H. Koenderink. 2018. “The Role of Network Architecture in Collagen Mechanics.” *Biophysical Journal* 114 (11): 2665–78. https://doi.org/10.1016/j.bpj.2018.04.043.

Jester, James V, Mortiz Winkler, Bryan E Jester, Chyong Nien, Dongyul Chai, and Donald J Brown. 2010. “Evaluating Corneal Collagen Organization Using High Resolution Non Linear Optical (NLO) Macroscopy.” *Eye Contact Lens* 36 (5): 260–64. https://doi.org/10.1038/jid.2014.371.

Jiang, Fengzhi, Khaled Khairy, Kate Poole, Jonathon Howard, and Daniel J. Müller. 2004. “Creating Nanoscopic Collagen Matrices Using Atomic Force Microscopy.” *Microscopy Research and Technique* 64 (5–6): 435–40. https://doi.org/10.1002/jemt.20101.

Jokinen, Johanna, Elina Dadu, Petri Nykvist, Jarmo Käpylä, Daniel J. White, Johanna Ivaska, Piia Vehviläinen, et al. 2004. “Integrin-Mediated Cell Adhesion to Type I Collagen Fibrils.”

Journal of Biological Chemistry 279 (30): 31956–63. https://doi.org/10.1074/jbc.M401409200.

Jones, Mark G., Orestis G. Andriotis, James J.W. Roberts, Kerry Lunn, Victoria J. Tear, Lucy Cao, Kjetil Ask, et al. 2018. “Nanoscale Dysregulation of Collagen Structure-Function Disrupts Mechano-Homeostasis and Mediates Pulmonary Fibrosis.” *ELife* 7: 1–24. https://doi.org/10.7554/eLife.36354.

Justus, Calvin R., Lixue Dong, and Li V. Yang. 2013. “Acidic Tumor Microenvironment and PH-Sensing G Protein-Coupled Receptors.” *Frontiers in Physiology* 4 DEC (December): 1–9. https://doi.org/10.3389/fphys.2013.00354.

Kadler, Karl E., Adele Hill, and Elizabeth G. Canty-Laird. 2008. “Collagen Fibrillogenesis: Fibronectin, Integrins, and Minor Collagens as Organizers and Nucleators.” *Current Opinion in Cell Biology* 20 (5): 495–501. https://doi.org/10.1016/j.ceb.2008.06.008.

Kadler, Karl E., David F. Holmes, John A. Trotter, and John A. Chapman. 1996. “Collagen Fibril Formation.” *Biochem. J.* 11: 1–11.

Kalamajski, Sebastian, Dominique Bihan, Arkadiusz Bonna, Kristofer Rubin, and Richard W. Farndale. 2016. “Fibromodulin Interacts with Collagen Cross-Linking Sites and Activates Lysyl Oxidase.” *Journal of Biological Chemistry* 29 (15): 7951–60. https://doi.org/10.1074/jbc.M115.693408.

Kalamajski, Sebastian, and Åke Oldberg. 2007. “Fibromodulin Binds Collagen Type I via Glu-353 and Lys-355 in Leucine-Rich Repeat 11.” *Journal of Biological Chemistry* 282 (37): 26740–45. https://doi.org/10.1074/jbc.M704026200.

Kalamajski, Sebastian, and Åke Oldberg. 2009. “Homologous Sequence in Lumican and Fibromodulin Leucine-Rich Repeat 5-7 Competes for Collagen Binding.” *Journal of Biological Chemistry* 284 (1): 534–39. https://doi.org/10.1074/jbc.M805721200.

Kalamajski, Sebastian, and Åke Oldberg. 2010. “The Role of Small Leucine-Rich Proteoglycans in Collagen Fibrillogenesis.” *Matrix Biology* 29 (4): 248–53. https://doi.org/10.1016/j.matbio.2010.01.001.

Kang, Inkyung, Ingrid A. Harten, Mary Y. Chang, Kathleen R. Braun, Alyssa Sheih, Mary P. Nivison, Pamela Y. Johnson, et al. 2017. “Versican Deficiency Significantly Reduces Lung Inflammatory Response Induced by Polyinosine-Polycytidylic Acid Stimulation.” *Journal of Biological Chemistry* 292 (1): 51–63. https://doi.org/10.1074/jbc.M116.753186.

Keech, M. K. 1961. “The Formation of Fibrils From Collagen Solutions 2. A Mechanism of Collagen-Fibril Formation.” *The Journal of Biophysical and Biochemical Cytology* 9 (1956): 193–209. https://doi.org/10.1083/jcb.9.1.193.

Kelm, Jens M., Nicholas E. Timmins, Catherine J. Brown, Martin Fussenegger, and Lars K. Nielsen. 2003. “Method for Generation of Homogeneous Multicellular Tumor Spheroids Applicable to a Wide Variety of Cell Types.” *Biotechnology and Bioengineering* 83 (2): 173–80. https://doi.org/10.1002/bit.10655.

Kershenobich Stalnikowitz, David, and Alan Bonder Weissbrod. 2003. “Liver Fibrosis and Inflammation. A Review.” *Annals of Hepatology : Official Journal of the Mexican Association of Hepatology* 2 (4): 159–63. https://doi.org/10.1016/s1665-2681(19)32127-1.

Khandekar, Gauri, Jessica Llewellyn, Alyssa Kriegermeier, Orith Waisbourd-Zinman, Nicolette Johnson, Yu Du, Roquibat Giwa, et al. 2020. “Coordinated Development of the Mouse Extrahepatic Bile Duct: Implications for Neonatal Susceptibility to Biliary Injury.” *Journal of Hepatology* 72 (1): 135–45. https://doi.org/10.1016/j.jhep.2019.08.036.

Kiani, Chris, Liwen Chen, Yao Jiong Wu, Albert J. Yee, and Burton B. Yang. 2002. “Structure and Function of Aggrecan.” *Cell Research* 12 (1): 19–32. https://doi.org/10.1038/sj.cr.7290106.

Kim, Jihan, Jingchen Feng, Christopher A.R. Jones, Xiaoming Mao, Leonard M. Sander, Herbert Levine, and Bo Sun. 2017. “Stress-Induced Plasticity of Dynamic Collagen Networks.”

Nature Communications 8 (1): 1–7. https://doi.org/10.1038/s41467-017-01011-7.

Kischel, Philippe, David Waltregny, Bruno Dumont, Andrei Turtoi, Yannick Greffe, Stephanie Kirsch, Edwin De Pauw, and Vincent Castronovo. 2010. “Versican Overexpression in Human Breast Cancer Lesions: Known and New Isoforms for Stromal Tumor Targeting.” *International Journal of Cancer* 126 (3): 640–50. https://doi.org/10.1002/ijc.24812.

Kleinman, Hynda K., Ermona B. McGoodwin, George R. Martin, Robert J. Klebe, Peter P. Fietzek, and David E. Woolley. 1978. “Localization of the Binding Site for Cell Attachment in the A1(I) Chain of Collagen.” *Journal of Biological Chemistry* 253 (16): 5642–46. https://doi.org/10.1016/s0021-9258(17)30315-0.

Knight, C. Graham, Laurence F. Morton, Anthony R. Peachey, Danny S. Tuckwell, Richard W. Farndale, and Michael J. Barnes. 2000. “The Collagen-Binding a-Domains of Integrins A1/B1 and A2/B1 Recognize the Same Specific Amino Acid Sequence, GFOGER, in Native (Triple- Helical) Collagens.” *Journal of Biological Chemistry* 275 (1): 35–40. https://doi.org/10.1074/jbc.275.1.35.

Krishnan, Anuradha, Xia Li, Winstonwhei Yang Kao, Kimberly Viker, Kim Butters, Howard Masuoka, Bruce Knudsen, Gregory Gores, and Michael Charlton. 2012. “Lumican, an Extracellular Matrix Proteoglycan, Is a Novel Requisite for Hepatic Fibrosis.” *Laboratory Investigation* 92 (12): 1712–25. https://doi.org/10.1038/labinvest.2012.121.

Krull, N. B., and A. M. Gressner. 1992. “Differential Expression of Keratan Sulphate Proteoglycans Fibromodulin, Lumican and Aggrecan in Normal and Fibrotic Rat Liver.” *FEBS Letters* 312 (1): 47–52. https://doi.org/10.1016/0014-5793(92)81407-D.

Kurniawan, Nicholas A., Long Hui Wong, and Raj Rajagopalan. 2012. “Early Stiffening and Softening of Collagen: Interplay of Deformation Mechanisms in Biopolymer Networks.” *Biomacromolecules* 13 (3): 691–98. https://doi.org/10.1021/bm2015812.

Landolt, Reto M., Lloyd Vaughan, Kaspar H. Winterhalter, and Dieter R. Zimmermann. 1995.

"Versican Is Selectively Expressed in Embryonic Tissues That Act as Barriers to Neural Crest Cell Migration and Axon Outgrowth." *Development* 121 (8): 2303–12.

Lee, Hsu-Yi, Lin Han, Peter Roughley, Alan J. Grodzinsky, and Christine Ortiz. 2013. "Age-Related Nanostructural and Nanomechanical Changes of Individual Human Cartilage Aggrecan Monomers and Their Glycosaminoglycan Side Chains." *Journal of Structural Biology* 181 (3): 264–73. https://doi.org/10.1016/j.jsb.2012.12.008.

Li, Shaohua, Caroline Van Den Diepstraten, Sudhir J. D'Souza, Bosco M. C. Chan, and J. Geoffrey Pickering. 2003. "Vascular Smooth Muscle Cells Orchestrate the Assembly of Type I Collagen via Alpha2beta1 Integrin, RhoA, and Fibronectin Polymerization." *American Journal of Pathology* 163 (3): 1045–56. https://doi.org/S0002-9440(10)63464-5 [pii].

Li, Yuping, Amran Asadi, Margo R. Monroe, and Elliot P. Douglas. 2009. "PH Effects on Collagen Fibrillogenesis in Vitro: Electrostatic Interactions and Phosphate Binding." *Materials Science and Engineering C* 29 (5): 1643–49. https://doi.org/10.1016/j.msec.2009.01.001.

Lin, Shengmao, and Linxia Gu. 2015. "Influence of Crosslink Density and Stiffness on Mechanical Properties of Type I Collagen Gel." *Materials* 8 (2): 551–60. https://doi.org/10.3390/ma8020551.

Liu, Xiao Jin, Fan Zhi Kong, Ya Hui Wang, Jiang Hong Zheng, Wei Dong Wan, Chen Liang Deng, Guang Yu Mao, et al. 2013. "Lumican Accelerates Wound Healing by Enhancing A2β1 Integrin-Mediated Fibroblast Contractility." *PLoS ONE* 8 (6): 1–9. https://doi.org/10.1371/journal.pone.0067124.

Lohmander, L. Stefan, Mirela Ionescu, Hitu Jugessur, and A. Robin Poole. 1999. "Changes in Joint Cartilage Aggrecan after Knee Injury and in Osteoarthritis." *Arthritis and Rheumatism* 42 (3): 534–44. https://doi.org/10.1002/1529-0131(199904)42:3<534::AID-ANR19>3.0.CO;2-J.

Lu, X. Lux, Daniel D. N. Sun, X. Edward Guo, Faye H. Chen, W. Michael Lai, and Van C. Mow.

2004. “Indentation Determined Mechanoelectrochemical Properties and Fixed Charge Density of Articular Cartilage.” *Annals of Biomedical Engineering* 32 (3): 370–79. https://doi.org/10.1023/B:ABME.0000017534.06921.24.

Ma, Xiaoyue, Maureen E. Schickel, Mark D. Stevenson, Alisha L. Sarang-Sieminski, Keith J. Gooch, Samir N. Ghadiali, and Richard T. Hart. 2013. “Fibers in the Extracellular Matrix Enable Long-Range Stress Transmission between Cells.” *Biophysical Journal* 104 (7): 1410–18. https://doi.org/10.1016/j.bpj.2013.02.017.

Maccarana, Marco, Sebastian Kalamajski, Mads Kongsgaard, S. Peter Magnusson, Åke Oldberg, and Anders Malmström. 2009. “Dermatan Sulfate Epimerase 1-Deficient Mice Have Reduced Content and Changed Distribution of Iduronic Acids in Dermatan Sulfate and an Altered Collagen Structure in Skin.” *Molecular and Cellular Biology* 29 (20): 5517–28. https://doi.org/10.1128/mcb.00430-09.

Maria De Souza, Márcia, Miguel Tolentino, Bárbara C.A. Assis, Ana Cristina De Oliveira Gonzalez, Tânia Maria Correia Silva, and Zilton A. Andrade. 2006. “Pathogenesis of Septal Fibrosis of The Liver. (An Experimental Study with A New Model.).” *Pathology Research and Practice* 202 (12): 883–89. https://doi.org/10.1016/j.prp.2006.07.004.

Martin, Daniel R., Salvatore Santamaria, Christopher D. Koch, Josefin Ahnström, and Suneel S. Apte. 2021. “Identification of Novel ADAMTS1, ADAMTS4 and ADAMTS5 Cleavage Sites in Versican Using a Label-Free Quantitative Proteomics Approach.” *Journal of Proteomics* 249 (August): 104358. https://doi.org/10.1016/j.jprot.2021.104358.

Mathews, M. B., and L. Decker. 1968. “The Effect of Acid Mucopolysaccharides and Acid Mucopolysaccharide-Proteins on Fibril Formation from Collagen Solutions.” *The Biochemical Journal* 109 (4): 517–26. https://doi.org/10.1042/bj1090517.

McDonald, John A., Diane G. Kelley, and Thomas J. Broekelmann. 1982. “Role of Fibronectin in Collagen Deposition: Fab’ to the Gelatin-Binding Domain of Fibronectin Inhibits Both

Fibronectin and Collagen Organization in Fibroblast Extracellular Matrix." *Journal of Cell Biology* 92 (2): 485–92. https://doi.org/10.1083/jcb.92.2.485.

Meek, Keith M., and Craig Boote. 2004. "The Organization of Collagen in the Corneal Stroma." *Experimental Eye Research* 78 (3): 503–12. https://doi.org/10.1016/j.exer.2003.07.003.

Middendorf, Jill M., Caroline Dugopolski, Stephen Kennedy, Eric Blahut, Itai Cohen, and Lawrence J. Bonassar. 2020. "Heterogeneous Matrix Deposition in Human Tissue Engineered Cartilage Changes The Local Shear Modulus and Resistance to Local Construct Buckling." *Journal of Biomechanics* 105: 109760. https://doi.org/10.1016/j.jbiomech.2020.109760.

Moorehead, Carli, Katsiaryna Prudnikova, and Michele Marcolongo. 2019. "The Regulatory Effects of Proteoglycans on Collagen Fibrillogenesis and Morphology Investigated Using Biomimetic Proteoglycans." *Journal of Structural Biology* 206 (2): 204–15. https://doi.org/10.1016/j.jsb.2019.03.005.

Nam, Sungmin, Joanna Lee, Doug G. Brownfield, and Ovijit Chaudhuri. 2016. "Viscoplasticity Enables Mechanical Remodeling of Matrix by Cells." *Biophysical Journal* 111 (10): 2296–2308. https://doi.org/10.1016/j.bpj.2016.10.002.

Öbrink, Björn. 1973. "A Study of the Interactions between Monomeric Tropocollagen and Glycosaminoglycans." *European Journal of Biochemistry* 33 (2): 387–400. https://doi.org/10.1111/j.1432-1033.1973.tb02695.x.

Oosten, Anne S.G. van, Xingyu Chen, Li Kang Chin, Katrina Cruz, Alison E. Patteson, Katarzyna Pogoda, Vivek B. Shenoy, and Paul A. Janmey. 2019. "Emergence of Tissue-like Mechanics from Fibrous Networks Confined by Close-Packed Cells." *Nature* 573 (7772): 96–101. https://doi.org/10.1038/s41586-019-1516-5.

Oosten, Anne S.G. Van, Mahsa Vahabi, Albert J. Licup, Abhinav Sharma, Peter A. Galie, Fred C. MacKintosh, and Paul A. Janmey. 2016. "Uncoupling Shear and Uniaxial Elastic Moduli of

Semiflexible Biopolymer Networks: Compression-Softening and Stretch-Stiffening." *Scientific Reports* 6 (December 2015): 1–9. https://doi.org/10.1038/srep19270.

Orgel, Joseph P.R.O., Aya Eid, Olga Antipova, Jordi Bella, and John E. Scott. 2009. "Decorin Core Protein (Decoron) Shape Complements Collagen Fibril Surface Structure and Mediates Its Binding." *PLoS ONE* 4 (9). https://doi.org/10.1371/journal.pone.0007028.

Owens, Raymond J., and Francisco E. Baralle. 1986. "Mapping the Collagen-Binding Site of Human Fibronectin by Expression in Escherichia Coli." *The EMBO Journal* 5 (11): 2825–30. https://doi.org/10.1002/j.1460-2075.1986.tb04575.x.

Perepelyuk, Maryna, Likang Chin, Xuan Cao, Anne Van Oosten, Vivek B. Shenoy, Paul A. Janmey, and Rebecca G. Wells. 2016. "Normal and Fibrotic Rat Livers Demonstrate Shear Strain Softening and Compression Stiffening: A Model for Soft Tissue Mechanics." *PLoS ONE* 11 (1): 1–18. https://doi.org/10.1371/journal.pone.0146588.

Persikov, Anton V., John A.M. Ramshaw, Alan Kirkpatrick, and Barbara Brodsky. 2005. "Electrostatic Interactions Involving Lysine Make Major Contributions to Collagen Triple-Helix Stability." *Biochemistry* 44 (5): 1414–22. https://doi.org/10.1021/bi048216r.

Piersma, Bram, M.K. Hayward, and Valerie M. Weaver. 2020. "Fibrosis and Cancer: A Strained Relationship." *Biochim Biophys Acta Rev Cancer* 1873 (2): 188356. https://doi.org/10.1016/j.bbcan.2020.188356.Fibrosis.

Plaas, Anna H.K., and John D. Sandy. 1993. "A Cartilage Explant System for Studies on Aggrecan Structure, Biosynthesis and Catabolism in Discrete Zones of the Mammalian Growth Plate." *Matrix* 13 (2): 135–47. https://doi.org/10.1016/S0934-8832(11)80072-7.

Prockop, Darwin J., Kari I. Kivirikko, Leena Tuderman, and Norberto A. Guzman. 1979. "The Biosynthesis of Collagen and Its Disorders." *New England Journal of Medicine* 301 (1): 13–23.

Rada, Jody A, Pamela K. Cornuet, and John R. Hassell. 1993. “Regulation of Corneal Collagen Fibrillogenesis In Vitro by Corneal Proteoglycan (Lumican and Decorin) Core Proteins.” *Experimental Eye Research* 56 (6): 635–48.

Ramachandran, G. N., and R. Chandrasekharan. 1968. “Interchain Hydrogen Bonds via Bound Water Molecules in the Collagen Triple Helix.” *Biopolymers* 6 (250): 1649–58.

Ramade, Alexandre, Wesley R Legant, Catherine Picart, Christopher S Chen, and Thomas Boudou. 2014. *Microfabrication of a Platform to Measure and Manipulate the Mechanics of Engineered Microtissues*. *Micropatterning in Cell Biology Part C*. 1st ed. Vol. 121. Elsevier Inc. https://doi.org/10.1016/B978-0-12-800281-0.00013-0.

Raspanti, Mario, Manuela Viola, Myriam Sonaggere, Maria Enrica Tira, and Ruggero Tenni. 2007. “Collagen Fibril Structure Is Affected by Collagen Concentration and Decorin.” *Biomacromolecules* 8 (7): 2087–91. https://doi.org/10.1021/bm070091t.

Raub, Christopher B., Vinod Suresh, Tatiana Krasieva, Julia Lyubovitsky, Justin D. Mih, Andrew J. Putnam, Bruce J. Tromberg, and Steven C. George. 2007. “Noninvasive Assessment of Collagen Gel Microstructure and Mechanics Using Multiphoton Microscopy.” *Biophysical Journal* 92 (6): 2212–22. https://doi.org/10.1529/biophysj.106.097998.

Ray, Arja, Rachel K. Morford, Nima Ghaderi, David J. Odde, and Paolo P. Provenzano. 2018. “Dynamics of 3D Carcinoma Cell Invasion into Aligned Collagen.” *Integrative Biology (United Kingdom)* 10 (2): 100–112. https://doi.org/10.1039/c7ib00152e.

Reese, Shawn P., Clayton J. Underwood, and Jeffrey A. Weiss. 2013. “Effects of Decorin Proteoglycan on Fibrillogenesis, Ultrastructure, and Mechanics of Type I Collagen Gels.” *Matrix Biology* 32 (7–8): 414–23. https://doi.org/10.1016/j.matbio.2013.04.004.

Ricard-Blum, Sylvie. 2011. “The Collagen Family.” *Cold Spring Harbor Perspectives in Biology* 3 (1): 1–19. https://doi.org/10.1101/cshperspect.a004978.

Ricciardelli, Carmela, Andrew J. Sakko, Miranda P. Ween, Darryl L. Russell, and David J. Horsfall. 2009. “The Biological Role and Regulation of Versican Levels in Cancer.” *Cancer and Metastasis Reviews* 28 (1–2): 233–45. https://doi.org/10.1007/s10555-009-9182-y.

Robins, S. P. 2007. “Biochemistry and Functional Significance of Collagen Cross-Linking.” *Biochemical Society Transactions* 35 (5): 849–52.

Robinson, Paul S., Tung Fu Huang, Elan Kazam, Renato V. Iozzo, David E. Birk, and Louis J. Soslowsky. 2005. “Influence of Decorin and Biglycan on Mechanical Properties of Multiple Tendons in Knockout Mice.” *Journal of Biomechanical Engineering* 127 (1): 181–85. https://doi.org/10.1115/1.1835363.

Roughley, Peter J., and John S. Mort. 2014. “The Role of Aggrecan in Normal and Osteoarthritic Cartilage.” *Journal of Experimental Orthopaedics* 1 (1): 1–11. https://doi.org/10.1186/s40634-014-0008-7.

Sandy, John D., Jennifer Westling, Richard D. Kenagy, M. Luisa Iruela-Arispe, Christie Verscharen, Juan Carlos Rodriguez-Mazaneque, Dieter R. Zimmermann, et al. 2001. “Versican V1 Proteolysis In Human Aorta in Vivo Occurs at the Glu 441-Ala442 Bond, a Site That Is Cleaved by Recombinant ADAMTS-1 and ADAMTS-4.” *Journal of Biological Chemistry* 276 (16): 13372–78. https://doi.org/10.1074/jbc.M009737200.

Schmalfeldt, Michael, María T. Dours-Zimmermann, Kaspar H. Winterhalter, and Dieter R. Zimmermann. 1998. “Versican V2 Is a Major Extracellular Matrix Component of the Mature Bovine Brain.” *Journal of Biological Chemistry* 273 (25): 15758–64. https://doi.org/10.1074/jbc.273.25.15758.

Scott, John E. 1996. “Proteodermatan and Proteokeratan Sulfate (Decorin, Lumican/Fibromodulin) Proteins Are Horseshoe Shaped. Implications for Their Interactions with Collagen.” *Biochemistry* 35 (27): 8795–99. https://doi.org/10.1021/bi960773t.

Shayegan, Marjan, Tuba Altindal, Evan Kiefl, and Nancy R. Forde. 2016. “Intact Telopeptides

Enhance Interactions between Collagens." *Biophysical Journal* 111 (11): 2404–16. https://doi.org/10.1016/j.bpj.2016.10.039.

Shen, Zhilei L., Mohammad Reza Dodge, Harold Kahn, Roberto Ballarini, and Steven J. Eppell. 2008. "Stress-Strain Experiments on Individual Collagen Fibrils." *Biophysical Journal* 95 (8): 3956–63. https://doi.org/10.1529/biophysj.107.124602.

Sheng, Wang, Guizhi Wang, Yelina Wang, Jiyong Liang, Jianping Wen, Peng-Sheng Zheng, Yaojiong Wu, et al. 2005. "The Roles of Versican V1 and V2 Isoforms in Cell Proliferation and Apoptosis." *Mol Biol Cell* 16 (March): 1330–40. https://doi.org/10.1091/mbc.e04-04-0295.

Shi, Shuiliang, Suzanne Grothe, Yiping Zhang, Maureen D. O'Connor-McCourt, A. Robin Poole, Peter J. Roughley, and John S. Mort. 2004. "Link Protein Has Greater Affinity for Versican than Aggrecan." *Journal of Biological Chemistry* 279 (13): 12060–66. https://doi.org/10.1074/jbc.M310091200.

Shi, Yigong. 2014. "A Glimpse of Structural Biology through X-Ray Crystallography." *Cell* 159 (5): 995–1014. https://doi.org/10.1016/j.cell.2014.10.051.

Silver, Frederick H., and David E. Birk. 1983. "Kinetic Analysis of Collagen Fibrillogenesis: I. Use of Turbidity-Time Data." *Topics in Catalysis* 3 (5): 393–405. https://doi.org/10.1016/S0174-173X(83)80020-X.

Snyder, Jessica M., Ida M. Washington, Timothy Birkland, Mary Y. Chang, and Charles W. Frevert. 2015. "Correlation of Versican Expression, Accumulation, and Degradation during Embryonic Development by Quantitative Immunohistochemistry." *Journal of Histochemistry and Cytochemistry* 63 (12): 952–67. https://doi.org/10.1369/0022155415610383.

Speranza, Maria Luisa, Giovanna Valentini, and Alberto Calligaro. 1987. "Influence of Fibronectin on the Fibrillogenesis of Type I and Type III Collagen." *Topics in Catalysis* 7 (2): 115–23. https://doi.org/10.1016/S0174-173X(87)80003-1.

Spreeuwel, A. C. C. van, N. A. M. Bax, A. J. Bastiaens, J. Foolen, S. Loerakker, M. Borochin, D. W. J. Van Der Schaft, C. S. Chen, F. P. T. Baaijens, and C. V. C. Bouten. 2014. “The Influence of Matrix (an)Isotropy on Cardiomyocyte Contraction in Engineered Cardiac Microtissues.” *Integrative Biology (United Kingdom)* 6 (4): 422–29. https://doi.org/10.1039/c3ib40219c.

Stamov, Dimitar R., Anna Müller, Yanusz Wegrowski, Stephane Brezillon, and Clemens M. Franz. 2013. “Quantitative Analysis of Type I Collagen Fibril Regulation by Lumican and Decorin Using AFM.” *Journal of Structural Biology* 183 (3): 394–403. https://doi.org/10.1016/j.jsb.2013.05.022.

Stefanovic, Branko. 2005. “New Insights into Regulation of Type I Collagen Gene Expression.” *Journal of Biological Sciences*. https://doi.org/10.3923/jbs.2005.10.20.

Stuart, Kate, and Alyssa Panitch. 2008. “Influence of Chondroitin Sulfate on Collagen Gel Structure and Mechanical Properties at Physiologically Relevant Levels.” *Biopolymers* 89 (10): 841–51. https://doi.org/10.1002/bip.21024.

Sun, Mei, Shoujun Chen, Sheila M. Adams, Jane B. Florer, Hongshan Liu, Winston W.Y. Kao, Richard J. Wenstrup, and David E. Birk. 2011. “Collagen V Is a Dominant Regulator of Collagen Fibrillogenesis: Dysfunctional Regulation of Structure and Function in a Corneal-Stroma-Specific Col5a1-Null Mouse Model.” *Journal of Cell Science* 124 (23): 4096–4105. https://doi.org/10.1242/jcs.091363.

Suzuki, Masaru, Damian Kayra, W. Mark Elliott, James C. Hogg, and Thomas Abraham. 2012. “Second Harmonic Generation Microscopy Differentiates Collagen Type I and Type III in Diseased Lung Tissues.” *Multiphoton Microscopy in the Biomedical Sciences XII* 8226 (May 2014): 82263F. https://doi.org/10.1117/12.910815.

Svensson, Liz, Ingmar Närlid, and Åke Oldberg. 2000. “Fibromodulin and Lumican Bind to the Same Region on Collagen Type I Fibrils.” *FEBS Letters* 470 (2): 178–82.

https://doi.org/10.1016/S0014-5793(00)01314-4.

Taufalele, Paul V., Jacob A. VanderBurgh, Adam Muñoz, Matthew R. Zanotelli, and Cynthia A. Reinhart-King. 2019. “Fiber Alignment Drives Changes in Architectural and Mechanical Features in Collagen Matrices.” *PLoS ONE* 14 (5): 1–11. https://doi.org/10.1371/journal.pone.0216537.

Tavakoli Nia, Hadi, Lin Han, Iman Soltani Bozchalooi, Peter Roughley, Kamal Youcef-Toumi, Alan J. Grodzinsky, and Christine Ortiz. 2015. “Aggrecan Nanoscale Solid-Fluid Interactions Are a Primary Determinant of Cartilage Dynamic Mechanical Properties.” *ACS Nano* 9 (3): 2614–25. https://doi.org/10.1021/nn5062707.

Theocharis, Achilleas D. 2008. “Versican in Health and Disease.” *Connective Tissue Research* 49 (3–4): 230–34. https://doi.org/10.1080/03008200802147571.

Tian, Zhenhua, Wentao Liu, and Guoying Li. 2016. “The Microstructure and Stability of Collagen Hydrogel Cross-Linked by Glutaraldehyde.” *Polymer Degradation and Stability* 130: 264–70. https://doi.org/10.1016/j.polymdegradstab.2016.06.015.

Vader, David, Alexandre Kabla, David Weitz, and Lakshminarayana Mahadevan. 2009. “Strain-Induced Alignment in Collagen Gels.” *PLoS ONE* 4 (6). https://doi.org/10.1371/journal.pone.0005902.

Valero, Clara, Hippolyte Amaveda, Mario Mora, and Jose Manuel García-Aznar. 2018. “Combined Experimental and Computational Characterization of Crosslinked Collagen-Based Hydrogel.” *PLoS ONE* 13 (4): 1–16. https://doi.org/10.1371/journal.pone.0195820.

Vanamee, Parker, and Keith R. Porter. 1951. “Observations with The Electron Microscope on The Solvation and Reconstitution of Collagen.” *J Exp Med* 94 (3): 255–68.

Venkatesan, Narayanan, Takae Ebihara, Peter J. Roughley, and Mara S. Ludwig. 2000. “Alterations in Large and Small Proteoglycans in Bleomycin-Induced Pulmonary Fibrosis in

Rats." *Am J Respir Crit Care Med* 161 (6): 2066–73. https://doi.org/10.1164/ajrccm.161.6.9909098.

Vogel, Kathryn G., and John A. Trotter. 1987. "The Effect of Proteoglycans on the Morphology of Collagen Fibrils Formed In Vitro." *Topics in Catalysis* 7 (2): 105–14. https://doi.org/10.1016/S0174-173X(87)80002-X.

Vynios, Demitrios H., Nicoletta Papageorgakopoulou, Helen Sazakli, and Constantine P. Tsiganos. 2001. "The Interactions of Cartilage Proteoglycans with Collagens Are Determined by Their Structures." *Biochimie* 83 (9): 899–906. https://doi.org/10.1016/S0300-9084(01)01332-3.

Wallace, Donald G. 1990. "The Relative Contribution of Electrostatic Interactions to Stabilization of Collagen Fibrils." *Biopolymers* 29 (6–7): 1015–26. https://doi.org/10.1002/bip.360290613.

Walter, B. A., C. L. Korecki, D. Purmessur, P. J. Roughley, A. J. Michalek, and J. C. Iatridis. 2011. "Complex Loading Affects Intervertebral Disc Mechanics and Biology." *Osteoarthritis and Cartilage* 19 (8): 1011–18. https://doi.org/10.1016/j.joca.2011.04.005.

Wang, Hailong, A. S. Abhilash, Christopher S. Chen, Rebecca G. Wells, and Vivek B. Shenoy. 2015. "Long-Range Force Transmission in Fibrous Matrices Enabled by Tension-Driven Alignment of Fibers." *Biophysical Journal* 107 (11): 2592–2603. https://doi.org/10.1016/j.bpj.2014.09.044.

Weber, Irene T., Robert W. Harrison, and Renato V. Iozzo. 1996. "Model Structure of Decorin and Implications for Collagen Fibrillogenesis." *Journal of Biological Chemistry* 271 (50): 31767–70. https://doi.org/10.1074/jbc.271.50.31767.

Wells, Rebecca G. 2008. "The Role of Matrix Stiffness in Regulating Cell Behavior." *Hepatology* 47 (4): 1394–1400. https://doi.org/10.1002/hep.22193.

Wen, Jessica W., Abby L. Olsen, Maryna Perepelyuk, and Rebecca G. Wells. 2012. "Isolation of

Rat Portal Fibroblasts by In Situ Liver Perfusion." *Journal of Visualized Experiments*, no. 64: 1–5. https://doi.org/10.3791/3669.

West, Adrian R., Nishat Zaman, Darren J. Cole, Matthew J. Walker, Wesley R. Legant, Thomas Boudou, Christopher S. Chen, et al. 2013. "Development and Characterization of a 3D Multicell Microtissue Culture Model of Airway Smooth Muscle." *American Journal of Physiology - Lung Cellular and Molecular Physiology* 304 (1): 4–16. https://doi.org/10.1152/ajplung.00168.2012.

Westling, Jennifer, Paul E. Gottschall, Vivian P. Thompson, Amber Cockburn, George Perides, Dieter R. Zimmermann, and John D. Sandy. 2004. "ADAMTS4 (Aggrecanase-1) Cleaves Human Brain Versican V2 at Glu 405-Gln406 to Generate Glial Hyaluronate Binding Protein." *Biochemical Journal* 377 (3): 787–95. https://doi.org/10.1042/bj20030896.

Wight, Thomas N. 2002. "Versican: A Versatile Extracellular Matrix Proteoglycan in Cell Biology." *Current Opinion in Cell Biology* 14 (5): 617–23. https://doi.org/10.1016/S0955-0674(02)00375-7.

Wight, Thomas N., Inkyung Kang, and Mervyn J. Merrilees. 2014. "Versican and the Control of Inflammation." *Matrix Biology* 35: 152–61. https://doi.org/10.1016/j.matbio.2014.01.015.

Williams, Rebecca M., Warren R. Zipfel, and Watt W. Webb. 2005. "Interpreting Second-Harmonic Generation Images of Collagen I Fibrils." *Biophysical Journal* 88 (2): 1377–86. https://doi.org/10.1529/biophysj.104.047308.

Wisdom, Katrina M., Kolade Adebowale, Julie Chang, Joanna Y. Lee, Sungmin Nam, Rajiv Desai, Ninna Struck Rossen, et al. 2018. "Matrix Mechanical Plasticity Regulates Cancer Cell Migration through Confining Microenvironments." *Nature Communications* 9 (1). https://doi.org/10.1038/s41467-018-06641-z.

Wood, G. C. 1960. "The Formation of Fibrils from Collagen Solutions 3. Effect of Chondroitin Sulphate and Some Other Naturally Occuring Polyanions on the Rate of Formation."

Biochemical Journal 75 (1): 605–12. https://doi.org/10.1083/jcb.9.1.193.

Wood, G. C., and M. K. Keech. 1960. “The Formation of Fibrils from Collagen Solutions 1. The Effect of Experimental Conditions: Kinetic and Electron-Microscope Studies.” *Biochemical Journal* 75 (3): 588–98. https://doi.org/10.1042/bj0750588.

Wu, Yao Jiong, David P. La Pierre, Jin Wu, Albert J. Yee, and Burton B. Yang. 2005. “The Interaction of Versican with Its Binding Partners.” *Cell Research* 15 (7): 483–94. https://doi.org/10.1038/sj.cr.7290318.

Wu, Yaojiong, Liwen Chen, Peng Sheng Zheng, and Burton B. Yang. 2002. “B1-Integrin-Mediated Glioma Cell Adhesion and Free Radical-Induced Apoptosis Are Regulated by Binding to a C-Terminal Domain of PG-M/Versican.” *Journal of Biological Chemistry* 277 (14): 12294–301. https://doi.org/10.1074/jbc.M110748200.

Xu, Yi, Sivashankarappa Gurusiddappa, Rebecca L. Rich, Rick T. Owens, Douglas R. Keene, Richard Mayne, Agneta Höök, and Magnus Höök. 2000. “Multiple Binding Sites in Collagen Type I for the Integrins A1β1 and A2β1.” *Journal of Biological Chemistry* 275 (50): 38981–89. https://doi.org/10.1074/jbc.M007668200.

Yamagata, M., K. M. Yamada, M. Yoneda, S. Suzuki, and K. Kimata. 1986. “Chondroitin Sulfate Proteoglycan (PG-M-like Proteoglycan) Is Involved in the Binding of Hyaluronic Acid to Cellular Fibronectin.” *Journal of Biological Chemistry* 261 (29): 13526–35.

Yamauchi, Mtsuo, and Marnisa Sricholpech. 2012. “Lysine Post-Translational Modifications of Collagen.” *Essays Biochem* 52: 113–33. https://doi.org/10.1042/bse0520113.Lysine.

Yan, Mingyan, Bafang Li, Xue Zhao, and Song Qin. 2012. “Effect of Concentration, PH and Ionic Strength on The Kinetic Self-Assembly of Acid-Soluble Collagen from Walleye Pollock (Theragra Chalcogramma) Skin.” *Food Hydrocolloids* 29 (1): 199–204. https://doi.org/10.1016/j.foodhyd.2012.02.014.

Yanagishita, Masaki. 1993. “Function of Proteoglycans in the Extracellular Matrix.” *Acta Pathologica Japonica* 43 (6): 283–93. https://doi.org/10.5357/koubyou.64.193.

Yang, Bing L., Yaou Zhang, Liu Cao, and Burton B. Yang. 1999. “Cell Adhesion and Proliferation Mediated through the G1 Domain of Versican.” *Journal of Cellular Biochemistry* 72 (2): 210–20. https://doi.org/10.1002/(SICI)1097-4644(19990201)72:2<210::AID-JCB5>3.0.CO;2-E.

Yang, Ya-li, and Laura J Kaufman. 2009. “Rheology and Confocal Reflectance Microscopy as Probes of Mechanical Properties and Structure during Collagen and Collagen / Hyaluronan Self-Assembly.” *Biophysical Journal* 96 (4): 1566–85. https://doi.org/10.1016/j.bpj.2008.10.063.

Yang, Ya-li, Lindsay M. Leone, and Laura J. Kaufman. 2009. “Elastic Moduli of Collagen Gels Can Be Predicted from Two-Dimensional Confocal Microscopy.” *Biophysical Journal* 97 (7): 2051–60. https://doi.org/10.1016/j.bpj.2009.07.035.

Yang, Ya-li, Charles Sun, Matthew E. Wilhelm, Laura J. Fox, Jieling Zhu, and Laura J. Kaufman. 2011. “Influence of Chondroitin Sulfate and Hyaluronic Acid on Structure, Mechanical Properties, and Glioma Invasion of Collagen I Gels.” *Biomaterials* 32 (31): 7932–40. https://doi.org/10.1016/j.biomaterials.2011.07.018.

Yeung, Tony, Penelope C Georges, Lisa A Flanagan, Beatrice Marg, Miguelina Ortiz, Makoto Funaki, Nastaran Zahir, Wenyu Ming, Valerie Weaver, and Paul A Janmey. 2005. “Effects of Substrate Stiffness on Cell Morphology , Cytoskeletal Structure , and Adhesion.” *Cell Motility and the Cytoskeleton* 60 (1): 24–34. https://doi.org/10.1002/cm.20041.

Zhang, Guiyun, Shoujun Chen, Silvia Goldoni, Bennett W. Calder, Holly C. Simpson, Rick T. Owens, David J. McQuillan, Marian F. Young, Renato V. Iozzo, and David E. Birk. 2009. “Genetic Evidence for the Coordinated Regulation of Collagen Fibrillogenesis in the Cornea by Decorin and Biglycan.” *Journal of Biological Chemistry* 284 (13): 8888–97. https://doi.org/10.1074/jbc.M806590200.

Zhang, Guiyun, Yoichi Ezura, Inna Chervoneva, Paul S. Robinson, David P. Beason, Ehren T. Carine, Louis J. Soslowsky, Renato V. Iozzo, and David E. Birk. 2006. “Decorin Regulates Assembly of Collagen Fibrils and Acquisition of Biomechanical Properties during Tendon Development.” *Journal of Cellular Biochemistry* 98 (6): 1436–49. https://doi.org/10.1002/jcb.20776.

Zhang, Yuntao, Xiuli Mao, Tyler Schwend, Stacy Littlechild, and Gary W. Conrad. 2013. “Resistance of Corneal RFUVA-Cross-Linked Collagens and Small Leucine-Rich Proteoglycans to Degradation by Matrix Metalloproteinases.” *Investigative Ophthalmology and Visual Science* 54 (2): 1014–25. https://doi.org/10.1167/iovs.12-11277.

Zhang, Zhi, Tania M. Garron, Xiao Jian Li, Yan Liu, Xiong Zhang, Ye Yang Li, and Wei Shi Xu. 2009. “Recombinant Human Decorin Inhibits TGF-β 1 -Induced Contraction of Collagen Lattice by Hypertrophic Scar Fibroblasts.” *Burns* 35 (4): 527–37. https://doi.org/10.1016/j.burns.2008.08.021.

Zhao, Ruogang, Thomas Boudou, Wei Gang Wang, Christopher S. Chen, and Daniel H. Reich. 2013. “Decoupling Cell and Matrix Mechanics in Engineered Microtissues Using Magnetically Actuated Microcantilevers.” *Advanced Materials* 25 (12): 1699–1705. https://doi.org/10.1002/adma.201203585.

Zhu, Jieling, and Laura J. Kaufman. 2014. “Collagen I Self-Assembly: Revealing the Developing Structures That Generate Turbidity.” *Biophysical Journal* 106 (8): 1822–31. https://doi.org/10.1016/j.bpj.2014.03.011.